



National Library  
of Canada

Bibliothèque nationale  
du Canada

Acquisitions and  
Bibliographic Services Branch

Direction des acquisitions et  
des services bibliographiques

395 Wellington Street  
Ottawa, Ontario  
K1A 0N4

395, rue Wellington  
Ottawa (Ontario)  
K1A 0N4

Notice - Avis d'usage

Avis - Notice d'usage

## NOTICE

## AVIS

The quality of this microform is heavily dependent upon the quality of the original thesis submitted for microfilming. Every effort has been made to ensure the highest quality of reproduction possible.

La qualité de cette microforme dépend grandement de la qualité de la thèse soumise au microfilmage. Nous avons tout fait pour assurer une qualité supérieure de reproduction.

If pages are missing, contact the university which granted the degree.

S'il manque des pages, veuillez communiquer avec l'université qui a conféré le grade.

Some pages may have indistinct print especially if the original pages were typed with a poor typewriter ribbon or if the university sent us an inferior photocopy.

La qualité d'impression de certaines pages peut laisser à désirer, surtout si les pages originales ont été dactylographiées à l'aide d'un ruban usé ou si l'université nous a fait parvenir une photocopie de qualité inférieure.

Reproduction in full or in part of this microform is governed by the Canadian Copyright Act, R.S.C. 1970, c. C-30, and subsequent amendments.

La reproduction, même partielle, de cette microforme est soumise à la Loi canadienne sur le droit d'auteur, SRC 1970, c. C-30, et ses amendements subséquents.

Canada

**OPTIMUM DESIGN OF BTA TOOLS WITH STAGGERED CUTTERS BY  
PROBABILISTIC APPROACH AND THEIR DYNAMIC STABILITY**

**Ramakrishna Prasad Koganti**

**A Thesis**

**in**

**The Department**

**of**

**Mechanical Engineering**

**Presented in Partial Fulfilment of the Requirements**

**for the Degree of Master of Applied Science at**

**Concordia University**

**Montreal, Quebec, CANADA**

**June 1993**

**© Ramakrishna Prasad Koganti, 1993**



National Library  
of Canada

Bibliothèque nationale  
du Canada

Acquisitions and  
Bibliographic Services Branch

Direction des acquisitions et  
des services bibliographiques

395 Wellington Street  
Ottawa, Ontario  
K1A 0N4

395, rue Wellington  
Ottawa (Ontario)  
K1A 0N4

*Your file - Votre référence*

*Our file - Notre référence*

**The author has granted an irrevocable non-exclusive licence allowing the National Library of Canada to reproduce, loan, distribute or sell copies of his/her thesis by any means and in any form or format, making this thesis available to interested persons.**

**L'auteur a accordé une licence irrévocable et non exclusive permettant à la Bibliothèque nationale du Canada de reproduire, prêter, distribuer ou vendre des copies de sa thèse de quelque manière et sous quelque forme que ce soit pour mettre des exemplaires de cette thèse à la disposition des personnes intéressées.**

**The author retains ownership of the copyright in his/her thesis. Neither the thesis nor substantial extracts from it may be printed or otherwise reproduced without his/her permission.**

**L'auteur conserve la propriété du droit d'auteur qui protège sa thèse. Ni la thèse ni des extraits substantiels de celle-ci ne doivent être imprimés ou autrement reproduits sans son autorisation.**

ISBN 0-315-87309-4

**Canada**

## ABSTRACT

The purpose of this thesis is to provide an analytical formulation of tool cutting force system for a BTA multi-edge cutting tool with staggered cutters and a procedure of optimizing the tool design in such a way that the tool maintains equal guide pad reactions. The objective function for optimization is formulated, so that the cutting force resultant and the pad resultant reactions balance for a stable cutting process. The design of a general BTA head with multiple edges is carried out by considering the following factors:

- Cutting edges are unsymmetrically located on the tool head with respect to tool axis, so that a non zero resultant cutting force is transmitted to the bore-wall at all times by means of guide pads.
- The predetermined pad reactions are chosen in such a way that the cutting force resultant is transmitted to the bore-wall with equal pad reactions. This optimum cutting force resultant exerts adequate pressure onto the bore-wall which in turn guides the tool and prevents the separation of the guide pads from the wall.
- The parameters incorporated in the cutting force equations and pad reactions are not deterministic. Hence, a probabilistic model is used for the objective function in order to consider the variations of the cutting forces during machining process.

To achieve the above stated objectives a multi-variable, nonlinear, stochastic objective function is formulated. Several constraints are taken into consideration such as, angular

locations of the inserts as well as the guide pads to secure the necessary space for them, width of cut of the inserts, pads included angle, and the location of the outer cutter with respect to guide pads. The Chance constrained programming technique has been applied to solve the resulting optimization problem.

The variations in magnitude and direction of the cutting force resultant are calculated by two probabilistic methods known as the Linear Statistical Approach and the Monte Carlo simulation. In order to assess the variations in magnitude of the pad reactions a normal and an uniform distributions are assumed for coefficient of friction at the guide pads.

The static stability of the cutting tool is studied by Pflieger's method. Different boundary conditions are identified at the cutting tool-workpiece contact depending upon the stability conditions at the tool guide pads. Transverse free vibrations of the cutting tool-boring bar system are predicted for different boundary conditions and the first five lateral mode shapes and natural frequencies of the cutting tool-boring bar system are determined, in order to understand the dynamic stability of the process.

*Dedicated To My Parents*

## ACKNOWLEDGEMENTS

The author expresses his sincere gratitude to the thesis supervisors Drs. Vojislav Latinovic and Waiz Ahmed, for their invaluable guidance and continued encouragement throughout the research. The author also wishes to thank Dr. Rao V. Dukkipati from National Research Council of Canada, Ottawa, for his valuable suggestions.

The author wishes to acknowledge the support of National Science and Engineering Research Council Grant No's. RA-20-N277 and RA-20-N144, during the course of this work.

Rama K.P. Koganti

**TABLE OF CONTENTS**

	<b>PAGE</b>
LIST OF FIGURES	x
LIST OF TABLES	xiii
NOMENCLATURE	xiv
CHAPTER 1 INTRODUCTION	1
1.1 Drilling Operations	1
1.2 Historical Background	4
1.3 Literature Survey	5
1.4 Deep-Hole Machining Process	9
1.4.1 Twist drills	10
1.4.2 Spade Drills	12
1.4.3 Boring	14
1.4.4 Gundrilling	14
1.4.5 BTA-Solid Drills	17
1.4.6 BTA-Counter Boring Tools	19
1.4.7 BTA-Trepanning Tools	19
1.4.8 BTA-Multi Edge Tools	20
1.4.9 Ejector Drills	22
1.5 Cutting Force System	24



	<b>PAGE</b>
1.6 Objectives of this Work	26
<b>CHAPTER 2 OPTIMIZATION OF BTA TOOL WITH STAGGERED CUTTERS BY PROBABILISTIC APPROACH</b>	<b>29</b>
2.1 Introduction	29
2.2 Tool Force System Formulation	33
2.3 Design Concept	36
2.4 Tool Optimization	41
2.4.1 Formulation of the Objective Function	42
2.4.2 Constraints Formulation	49
2.5 Optimization Technique	52
2.5.1 Normalization of the Constraint Equations	54
2.5.2 Initial Value of the Penalty Parameter	56
2.5.3 Unconstrained Minimization	57
2.5.4 Convergence Criteria	57
2.5.6 Deviations of the Cutting Forces	58
2.6 Optimum Tool Model	58
2.7 Conclusions	60
<b>CHAPTER 3 ANALYSIS OF CUTTING FORCES AND PAD REACTIONS VARIATIONS</b>	<b>63</b>

	<b>PAGE</b>
3.1 Introduction	63
3.2 Deviation of the Cutting Forces Magnitude and Direction	67
3.2.1 Linear Statistical Approach	69
3.2.2 Monte Carlo Simulation	74
3.3 Variation of Pad Reaction	76
3.4 Conclusions	85
<b>CHAPTER 4 STABILITY ANALYSIS OF CUTTING TOOL-BORING BAR IN DEEP-HOLE MACHINING</b>	<b>87</b>
4.1 Introduction	87
4.2 Static Stability Analysis	90
4.3 Mathematical Modeling of the Cutting Tool - Boring Bar System's Dynamics	93
4.4 Frequency Analysis of the Cutting Tool - Boring Bar	95
4.5 Conclusions	117
<b>CHAPTER 5 SUMMARY, CONCLUSIONS AND RECOMMENDATIONS</b>	<b>113</b>
5.1.1 Summary	113
5.1.1 Mathematical Model and Optimum Tool Design	113
5.1.2 Cutting Forces and Pads' Reactions Variations	114
5.1.3 Free Transverse Vibrations of Cutting Tool-Boring Bar	115

	<b>PAGE</b>
5.2 Conclusions	115
5.3 Recommendations	118
<b>REFERENCES</b>	<b>119</b>
<b>APPENDIX A</b> Listing of Computer Programs, and Printouts of Results	<b>130</b>
<b>APPENDIX B</b> PDF of Resultant Cutting Force Magnitude for Different Replications	<b>154</b>

**LIST OF FIGURES**

<b>FIGURE</b>	<b>PAGE</b>
1.1 The Principle of BTA Machining	3
1.2 Conventional Twist Drill	11
1.3 Spade Drill	13
1.4 Boring Tools Used for Enlarging Existing Holes	15
1.5 Gundrill	16
1.6 Typical BTA Tools	18
1.7 Tool with Staggered Cutters	21
1.8 Ejector Drill	23
1.9 Cutting Force System	25
2.1 Solid Boring Head with Staggered Cutters	31
2.2 Lower and Upper Limits for Location of Staggered Cutters of BTA Tool	38
2.3 Algorithm for Interior Penalty Method	55
2.4 Optimum BTA Tool Model with Staggered Cutters	59
3.1 Tool Cutting Force System	65
3.2 Variations of Resultant Cutting Force and Pad Reactions	68
3.3 PDF of Cutting Force Magnitude in X-Direction for 30000 Replications	78

<b>FIGURE</b>	<b>PAGE</b>
3.4 PDF of Cutting Force Magnitude in Y-Direction for 30000 Replications	79
3.5 PDF of Cutting Force Resultant Magnitude for 30000 Replications	80
3.6 PDF of Resultant Cutting Force Direction for 30000 Replications	81
3.7 PDF of Pad Reaction Magnitude for 30000 Replications	84
4.1 Tool Force System	89
4.2 Model of the Cutting-Tool Boring Bar Assembly at Stable Equilibrium	96
4.3 Model of the Cutting-Tool Boring Bar Assembly at Indifferent Equilibrium	99
4.4 Model of the Cutting-Tool Boring Bar Assembly at Unstable Equilibrium	101
4.5 Mode Shapes of the Cutting Tool - Boring Bar Assembly at Stable Equilibrium	107
4.6 Mode Shapes of the Cutting Tool - Boring Bar Assembly at Indifferent Equilibrium	108
4.7 Mode Shapes of the Cutting Tool - Boring Bar Assembly at Unstable Equilibrium	109
4.8 Lateral Natural Frequencies of the Cutting Tool - Boring Bar Assembly at Different Tool Penetrations in Stable Equilibrium	110
4.9 Lateral Natural Frequencies of the Cutting Tool - Boring Bar Assembly at Different Tool Penetrations in Indifferent Equilibrium	111

<b>FIGURE</b>		<b>PAGE</b>
4.10	Lateral Natural Frequencies of the Cutting Tool - Boring Bar Assembly at Different Tool Penetrations in Unstable Equilibrium	112
B1	PDF of Resultant Cutting Force Magnitude for 1000 Replications	154
B2	PDF of Resultant Cutting Force Magnitude for 5000 Replications	155
B3	PDF of Resultant Cutting Force Magnitude for 10000 Replications	156
B4	PDF of Resultant Cutting Force Magnitude for 15000 Replications	157
B5	PDF of Resultant Cutting Force Magnitude for 20000 Replications	158
B6	PDF of Resultant Cutting Force Magnitude for 25000 Replications	159

**LIST OF TABLES**

<b>TABLE</b>		<b>PAGE</b>
2.1	Optimum Values of the BTA Tool with Staggered Cutters	62
3.1	Mean Values of the Cutting Forces	76
3.2	Deviations of the Cutting Forces	77
4.1	Clamped-Clamped with Intermediate Simple Support	97
4.2	Clamped-Simple with Intermediate Simple Support	98
4.3	Clamped-Free with Intermediate Simple Support	102
4.4	Natural Frequencies for Different Tool Penetrations in Stable Equilibrium	105
4.5	Natural Frequencies for Different Tool Penetrations in Indifferent Equilibrium	105
4.6	Natural Frequencies for Different Tool Penetrations in Unstable Equilibrium	106

## NOMENCLATURE

$A$	undeformed chip cross-sectional area, area of cross-section of the boring bar
$\Lambda_{1,2}$	constants
$b_i$	width of cut of the cutters
$\bar{b}_1$	mean value of width of cut of the outer cutter
$B_{1,2}$	constants
$c$	constant in the interior penalty method
$C, C^*$	amplitude constants
$C_{p,q}$	cutting force for $b = 1$ mm and $s = 1$ mm in the direction $p$ and $q$
$\bar{C}_{p,q}$	mean values of the specific cutting forces in the directions $p$ and $q$
$C_{1,2}$	constants
$d$	diameter of the cutting head
$d_i$	inner diameter of the boring bar
$d_o$	outer diameter of the boring bar
$D_{1,2}$	constants
$E$	Young's modulus of the boring bar
$E(x)$	expected value of the variable $x$
$E(y)$	expected value of the function $y$
$f(X, Y)$	function of design variables and random variables
$F_{p,q}$	cutting force components in the directions $p$ and $q$
$F_{F,R,T}$	cutting force components in the feed, radial, and tangential directions



$F_N$	pad's normal force
$F_P$	pad's resultant force
$\bar{f}$	mean value of the objective function
$\bar{F}_P$	mean value of the pad's resultant force
$F_{X,Y}$	cutting force resultant in the direction X and Y
$\bar{F}_{X,Y}$	mean values of the cutting force components in X and Y directions
$g$	acceleration due to gravity
$g_j(X,Y)$	jth inequality constraint function
$\bar{g}_j$	mean value of the constraint equations
$i$	subscript, number of replications, number of pads
$I$	moment of inertia of the boring bar
$j$	subscript
$k$	subscript, unconstrained minimization number
$K_p$	unit cutting force
$K_{w1,w2}$	positive weighting factors to the stochastic objective function
$K_{w3}$	positive weighting factor in the constraint equation
$K_{1,2}$	positive weighting factors
$L$	total length of the boring bar
$L_1$	length of the boring bar at the left hand side of the pressure head support
$L_2$	length of the boring bar at the right hand side of the pressure head

	support
$m$	number of constraints
$M_h$	holding moment
$M_t$	tilting moment
$M_B$	driving moment
$M_C$	cutting moment
$n$	number of cutting edges, number of random variables, number of decision variables
$n_i$	constant in the equation (2.3)
$p_i$	specified probabilities
$P$	probability of occupance, constant
$P(X, Y)$	imposed penalty function
$Q$	constant
$r$	radius of the cutting head
$r_{ci}$	centre of the chip-mouth circle
$r_i$	radius of chip-mouth
$r_k$	positive penalty parameter
$R_C$	resultant cutting force
$\bar{R}_C$	mean value of the resultant cutting force
$R_S$	total resultant pads reaction
$\bar{R}_S$	mean value of the resultant pads reaction
$R_{X, Y}$	resultant support reactions in X and Y directions

$s$	depth of cut
$S$	degree of stability
$t$	time
$u_i(X,t)$	deflections of left and right hand sides of the boring bar
$V(x_i)$	variance of variable $x_i$
$V(y)$	variance of function $y$
$x_i$	decision variables
$x_l, x_u$	lower and upper limits of the variable $x$
$x_{1,2}$	exponents to the width of cut
$X$	vector of decision variables, length coordinate
$X_i$	independent random variables
$X^*_k$	optimum values in the optimization problem
$X_0$	initial guess in the optimization problem
$y$	function of independent random variables $X_i$
$y_{1,2}$	exponents to the depth of cut
$Y$	vector of random variables
$\bar{Y}$	mean values of random variables
$\alpha$	normal rake angle
$\alpha_{1,2,3}$	constants in the frequency analysis
$\beta_i$	chipmouth angle, boring bar eigen value
$\Delta\beta_i$	cutter pocket angle
$\gamma$	specific weight of the boring bar

$\gamma_k$	pseudo-objective function
$\delta$	pads included angle
$\epsilon$	convergence factor
$\kappa$	approach angle
$\lambda$	resultant cutting force position angle
$\bar{\lambda}$	mean value of the resultant cutting force position angle
$\rho$	friction coefficient angle
$\mu$	coefficient of friction, expected value of the variable $X_i$
$\mu_M$	mean value of the coefficient of friction
$\mu_{x_i}$	mean values of the variables $x_i$
$\xi$	correction factor
$\xi(X)$	dimensionless lateral displacement of the boring bar
$\sigma_{b_1}$	standard deviation of width of cut of the outer cutter
$\sigma_{C_{pi}, C_{qi}}$	standard deviations of specific cutting forces $C_{pi}$ , and $C_{qi}$ respectively
$\sigma_f$	standard deviation of the objective function
$\sigma_{F_p}$	standard deviation of the pads reaction force
$\sigma_{R_c}$	standard deviation of the resultant cutting force magnitude
$\sigma_x$	standard deviation of independent random variable $X$
$\sigma_{F_{X,Y}}$	standard deviation of the cutting forces in $X$ and $Y$ directions
$\sigma_y$	standard deviation of the variable $y$
$\sigma_\lambda$	standard deviation of the resultant cutting force position angle

$\phi_i$	angular location of the cutters with respect to X - axis
$\phi_{L_i, U_i}$	lower and upper limits of the variable $\phi$
$\phi_j(p_j)$	normal variate
$\omega_{ni}$	natural frequencies of the cutting tool - boring bar

## CHAPTER 1

### INTRODUCTION

#### 1.1 DRILLING OPERATIONS

Mechanical components undergo various machining operations depending upon the requirements of the finished product. Among them drilling of holes is frequently required, and one of the drilling operations is deep-hole machining which is known to be the most demanding of all hole making operations. Deep-hole machining tools though not widely used, constitute a very important area in manufacturing technology. The type of hole making operation selected usually depends upon the following hole requirements:

- a) Diameter of the hole
- b) Depth of the hole
- c) Quality of the hole surface
- d) Size, accuracy, parallelism and straightness

The above factors decide the type of drilling process to be chosen. Since making holes with large length to diameter ratios require high standards of size, parallelism, straightness, and surface finish, it has always been a challenge for the machine tool operators. Conventional drilling tools such as twist drills are inadequate for precision drilling, since hole straightness deteriorates when the hole length to diameter ratio

exceeds three. In case of twist drills both radial and tangential cutting forces are theoretically balanced. But in reality due to an uneven grinding and material inhomogeneity these are unbalanced. Drilling operations involve removal of metal from highly inaccessible regions. The deeper the hole to be machined, the lower is the rigidity of the tool, since the rigid tool support is farther away from the cutting edge. This phenomenon tends to make the hole making process a difficult task for holes of high length to diameter ratio.

The BTA tools introduction (Boring and Trepanning Association) overcomes these difficulties, which are normally experienced with conventional drills. This is achieved by using tools in which cutting forces generated at the cutting edges are balanced by the reactions at guiding pads. These supporting pads are mounted on tool periphery in such a way that they guide the tool against the bore-wall being generated. Thus, these tools are self-guided and are capable of producing accurate bores of depth of up to 100 times the diameter of the hole in a single pass. Specially in mass production a very close tolerance and reasonably good surface finish can be maintained, if the components are produced drilling an integral workpiece and cut to the required length after the drilling operation. The principle of BTA deep hole machining is shown in Fig. 1.1 [1]. The machining process utilizes high pressure cooling oil to remove chips, transfer heat, dampen vibration and lubricate the cutting edges and pads [2].

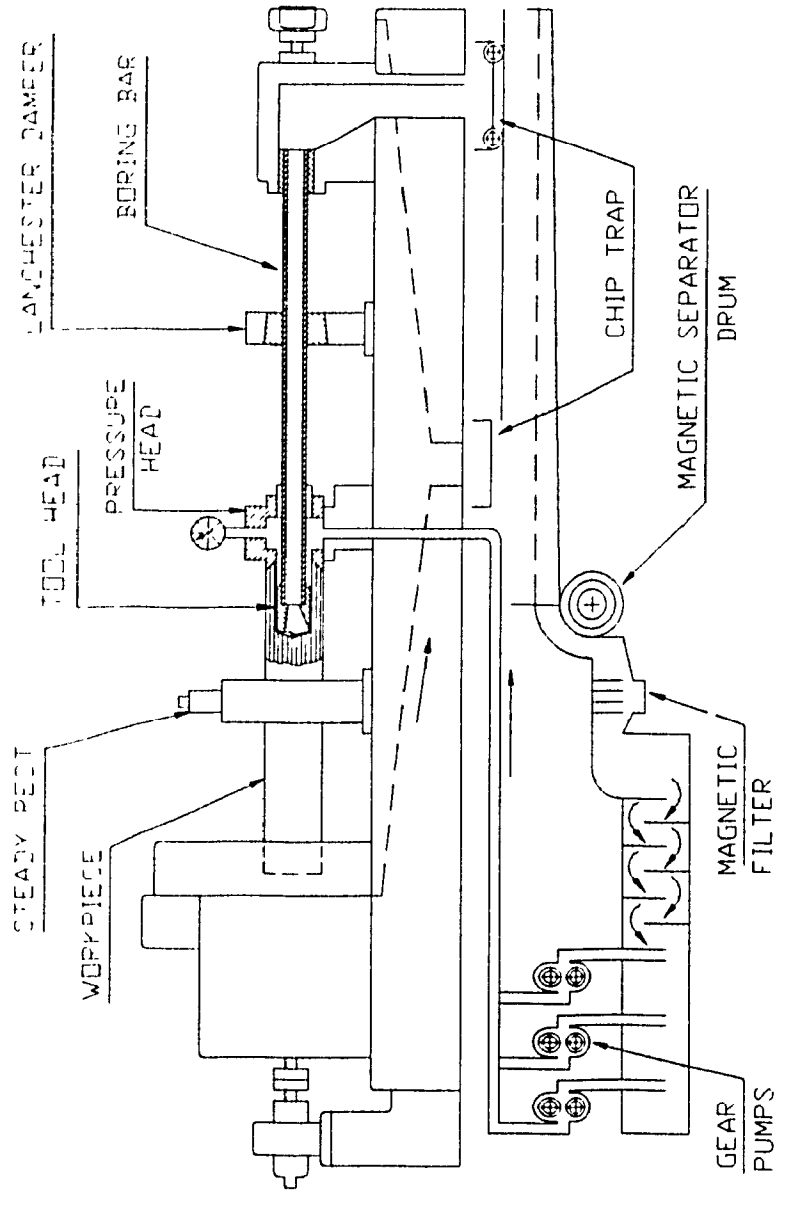


Fig. 1.1 The Principle of BTA Machining



## 1.2 HISTORICAL BACKGROUND

The origin of deep-hole drilling process has been traced to the production of gun barrels during the period from 16<sup>th</sup>-18<sup>th</sup> centuries. The town of Suhl in Germany was known as centre of deep hole drilling during 1500-1750. The technique employed was a water mill driving the spade drill bit as the cutting tool. Two barrels could be drilled simultaneously by two parallel spindles with the feed and thrust produced by the operator. The operator actuated a lever which supplied a certain force amplification. This simple lever enabled him to provide an infinitely variable feed [3]. The first vertical gun boring machine was built by Martiz in 1713. A cutter head mounted on the end of a boring bar was rotated by animal power, and a downward feed was given to the gun barrel. The frame of the machine was built in wood, framed a part of the structure housing.

The first boring machine was produced about 1758 by Vebrugger in collaboration with Ziegler, where the gun was rotated and the feed was given to the boring tool. This was regarded as first generation of machine tool for engineering applications rather than ornamental and artistic use [4]. The cutters used in that machine were spade drills with two cutting edges suitable for drilling a hole in a solid. The other tools employed were counter-boring tools for enlarging and cleaning up existing cast holes.

The first example of drilling machine was made prior to 1782 by Vacuenson, a French

engineer who worked in several fields of engineering and made notable advances in machine-tool design and construction. In 1860, the invention of twist drill in the United States of America, pioneered the important steps in drilling [5]. Morse [6] has first studied the commercial making of twist drill in 1862, at Bridgewater but he did not secure the aid of capital until 1864, when the Morse Twist Drill and Machine Company was founded and its work moved to New Bedford. Introduction of gundrills in 1940's in drilling extended the deep hole drilling process to small bores [7].

### **1.3 LITERATURE SURVEY**

In 1851, a french investigator Cocquillent was first involved into the investigation on Mechanics of cutting process. He studied on various materials such as iron, brass, stone and other materials in drilling operation to find out the work required to remove given volume of material. Several other researchers in the cutting mechanics and chip formation in the past were Joessel, Tresca, and Reuleaux in France, Time, Zvorykin and Briks in Russia, Mallock in England. Taylor in the United States - made his contribution in the area of tool wear and tool life [8].

In November 1885, W.H. Thron presented a paper on "Twist drills" at the XII Annual Meeting of ASME in Boston, which dealt with the early problems of drilling - the introduction of standard drill diameters, shank taper and establishment of optimal helix, cutting and clearance angles. This event was the milestone for the subsequent research

work on drilling and boring which, in turn contributed to a tremendous progress in this area of metal working.

Between 1944-45, Merchant [9,10] formulated the first analytical model of the cutting process. The analysis has been applied in general terms to quite large range of cutting conditions and it encouraged the later researchers to rethink the assumptions on which the model is based.

Several researchers Shaw, Cook, and Smith [11] in 1952, demonstrated the similarities between drilling and conventional turning operations. In 1955, Oxford, Jr. [12] used a quick stop device to freeze the chip formation process. He concluded that the action along the cutting lip is similar to other cutting processes, and the action of the chisel edge produces extrusion by high compressive loads. Further in 1957, Shaw and Oxford, Jr. [13] applied dimensional analysis and they found that the results are in good agreement with the experimental results in terms of torque and thrust in drilling.

Above researchers assumed that cutting operations are steady state process and the resulting cutting force magnitudes and directions are assumed to represent the steady-state means. The fluctuations in cutting forces had been ignored. However, it is essential to know the fluctuations of the cutting forces for accurate dynamic analysis and stability of machine tools. The important parameters such as the machinability, surface texture of a machined workpiece, tool life and power consumption depend upon the magnitude and

variations of the cutting forces.

In 1964, Albercht [14] has proven that the major cutting parameters are dynamic and time dependent, the mean values of which are identical to the steady-state solution of Merchant. In 1969, Williams [15] introduced the dynamic geometry of a twist drill and he made an investigation on the effect of the feed velocity on the cutting geometry of the drill cutting edges.

Other researchers Bickel [16], Kwiatkowski et al [17,18], Peklenik et al [19], Optiz et al [20] have concluded that the cutting forces in metal cutting are stochastic in nature possessing a high degree of randomness. Osman and Sankar [21] have considered the random force variations as stationary and Gaussian signals in their proposed short time acceptance test for machine tools.

Later Margos [22] has conducted some experiments in turning operation and concluded that the cutting forces in turning are stochastic and Gaussian distributed only in the finishing operation. Rakhit et al [23] have verified the results of Margos [22] and they also concluded that the cutting forces in turning operation are Gaussian distributed and they also found that surface texture has direct relation with fluctuations of the cutting forces. Furthermore, Chahil [24] in his experimental investigation on torque and thrust in drilling concluded that these are the random variables, stationary and Gaussian distributed with most of the power concentrated at certain dominant frequencies.

The research on BTA tools started in Germany during the early 1940's and proved that the BTA technique is the most economical method of hole machining with high length to diameter ratio [25-54]. The holes produced with deep-hole machining are of high accuracy of size, parallelism, straightness and surface finish. The method basically consists of a single edge cutting head with two carbide guide pads. The cutting tool is screwed to the boring bar and high pressure coolant removes the chips produced during the machining through the interior of the boring bar. The experts in boring tools have concluded that, this system is optimum for all hole-making and different boring heads have been designed having the distinguished feature of the single-edge cutting tool with carbide pads. This boring machining has become known as the BORING AND TREPANNING ASSOCIATION or BTA method.

The concept of multi edge cutting tool was proposed in 1970's by Latinovic and Osman [49]. This method can be more efficient than single edge cutting in terms of material removal rate. They proposed two types of multi edge cutting tools. Torabi [56] has carried out a comparative study of the commercially available tools and a tool prototype with staggered cutters. The study revealed advantages and some anticipated disadvantages of the newly developed prototype.

Chandrashekhar [50] concluded from his experiments that the statistical properties of torque and thrust in BTA solid boring tools are random in nature and their dynamics can be characterised as a weakly stationary, wide band random process with Gaussian

distribution. The stability analysis of the BTA tools was studied by Pfléghar [32] and Gessesse [1]. Pfléghar [55] has studied the static stability of self-guided tools, by considering the moments of the forces acting about each pad. He identified three types of stability such as stable balance, indifferent balance and unstable balance depending on the reactions on the guide pads. Gessesse [1] has concentrated his investigation on tool static and dynamic stability and identified conditions under which tool enters into unstable region called spiralling.

Considerable investigation in deep hole drilling and boring system has been carried out in the past few decades in analyzing the process, stability of the tool and problems during machining. To achieve a compromise between tool stability and hole quality a thorough understanding of the drilling process, force system involved, variations of the cutting forces as well as pad reaction forces, and dynamic behaviour of the cutting tool-boring bar system is essential. A literature survey is carried out covering various factors and aspects of deep-hole machining in the previous research work prior to the present investigation.

#### **1.4 DEEP-HOLE MACHINING PROCESS**

There are many types of drilling and boring tools which are used in deep-hole manufacturing process. Most of them use a similar principle; they involve a relative speed between the work-piece and the tool, and require a large thrust force for the feed.

In deep-hole machining process the cutting forces generated in a single or multi edge tools are generally unbalanced but supported by guide pads located at the tool periphery. In this section various types of deep-hole drilling tools are discussed, their advantages and disadvantages as well as their applications are discussed. Various drilling processes available are reviewed and a general concept in selecting a particular drilling tool over the others is provided.

#### **1.4.1 TWIST DRILLS**

Drills with helical flutes are called as twist drills and these are the most common drilling tools used in hole making operations. The twist drills are an improvement of spade drills and it has highly complex tool geometry used to produce rough holes. Twist drills consist of two cutting edges on either side along the diameter and chisel edge in the middle as shown in Fig. 1.2. The curly chips which are produced during machining are removed through the twist flute. These can be used with any type of machine tool that can provide relative rotation and axial feed of a tool and/or a workpiece. Even though the twist drills are manufactured to fairly close tolerances, it is not a precision tool. The reasons why twist drills are not suitable in deep-hole drilling operations are (1) Its low torsional strength (2) Chip removal is difficult (3) Heating problems are unavoidable (4) Hole straightness achieved is poor (5) Hole which can be drilled is limited.

The disturbances that might arise from uneven grinding or wear of the drill cutting edges

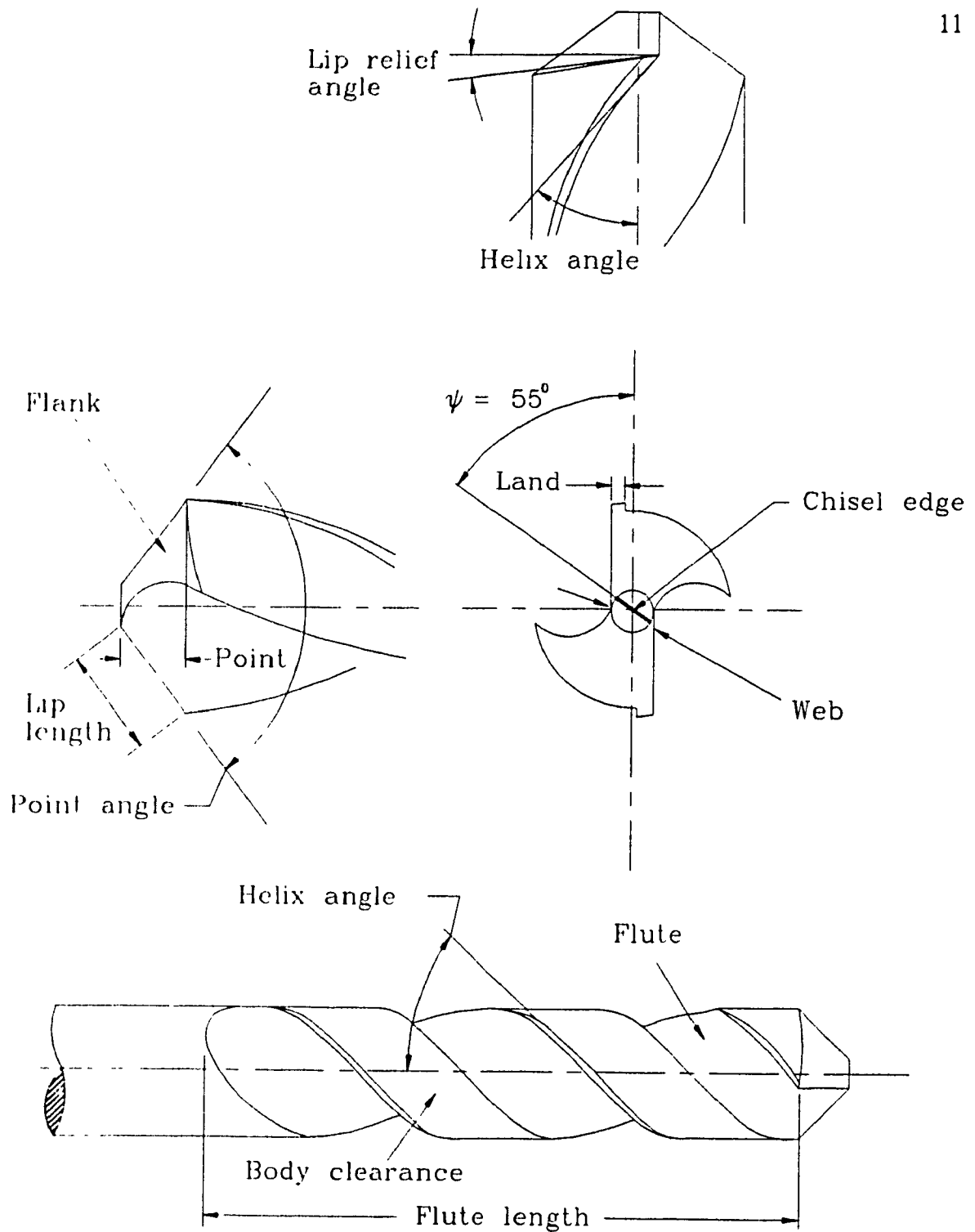


Fig. 1.2 Conventional twist drill



could cause unstable drilling process. The unbalance of the forces can only be controlled by the encastre effect of the drill which might not be sufficient in the case of long drills to prevent considerable run out of the drilled hole. Twist drills are repeatedly withdrawn from the hole for lubrication and swarf removal during machining, which considerably slows down the operation.

#### **1.4.2 SPADE DRILLS**

The spade drill consists of two cutting edges and a shank as shown in Fig. 1.3. The cutting edges are flat blades slightly inclined from the centre towards the periphery on either side. Because of the symmetry of two cutting edges, the forces on the cutting edges theoretically balance each other during machining process.

The narrow chips formed during machining are due to the slots that are provided in the cutting edges. The positive rake angle of the spade drills vary from 5 to 12 degrees. The problems associated with spade drills are chip removal and excessive heating of the cutting edge. The chips that are generated during this process are disposed through two straight flutes in the shank to which the blade is attached by a fastener. The other problem is that the cutting edge gets overheated due to the insufficient cooling by the cutting fluid.

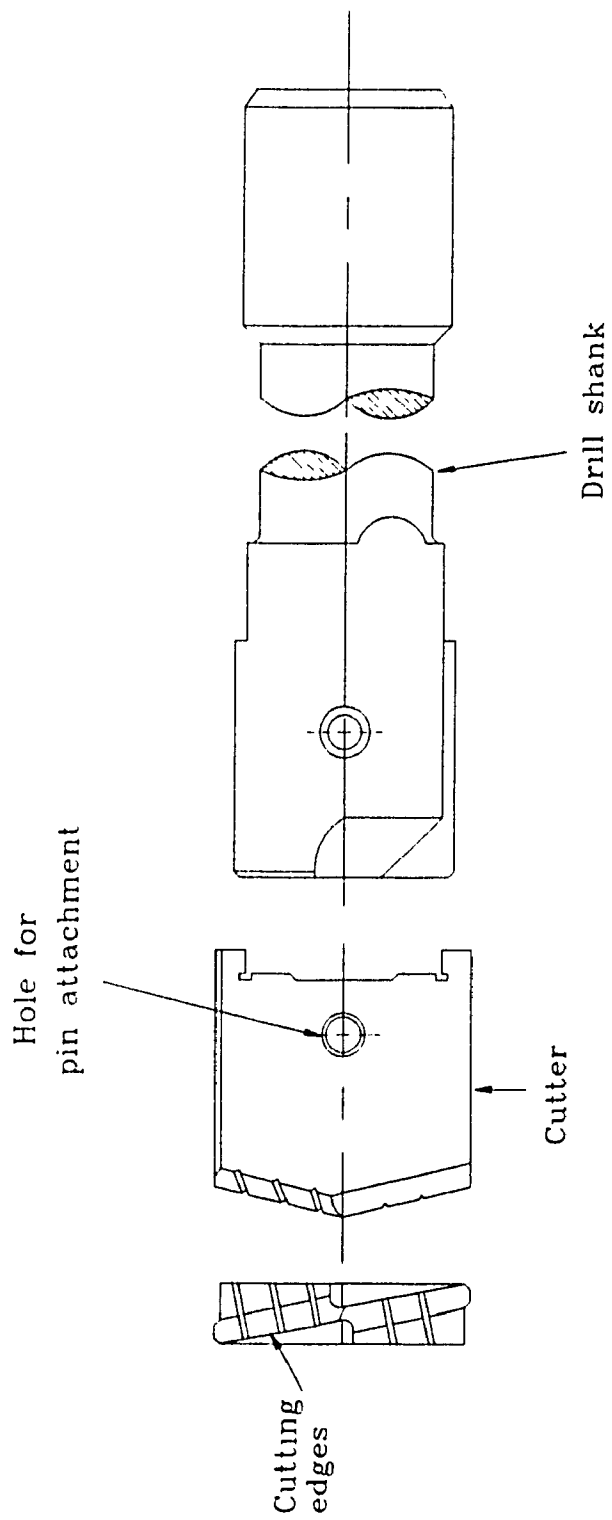


Fig. 1 3 Spade drill

### **1.4.3 BORING**

Generally, boring operation is finishing operation and is mostly used for enlarging and cleaning holes or other circular contours, which requires a previously produced hole. The material removal in this operation is comparatively smaller than drilling in order to achieve a smoother surface finish and closer tolerances. The most commonly used boring tools are shown in Fig. 1.4. In Fig. 1.4(a) the cutting edge is supported by tool post and is fed axially to the rotating work piece. Boring is restricted to shallow holes because the boring bar stiffness is limited by bore size and the length.

The above mentioned limitations can be partly overcome by a boring tool shown in Fig. 1.4(b). In this arrangement the tool is attached to a boring bar and the depth of hole which is dictated by lateral stiffness of the boring bar, can be used increased. The tool can be used for machining holes in heavy objects with unsymmetrical shape by rotating the boring bar with the tool.

### **1.4.4 GUNDRILLING**

The typical gun drill consists of a cutting tip, kidney shaped shank and a driver as shown in Fig. 1.5 [1]. The cutting tip is brazed to the shank and the shank provides an adequate driver to the tool. It also gives required torsional stiffness to allow a reasonable continuous feed during machining [57]. The coolant is pumped through the holes

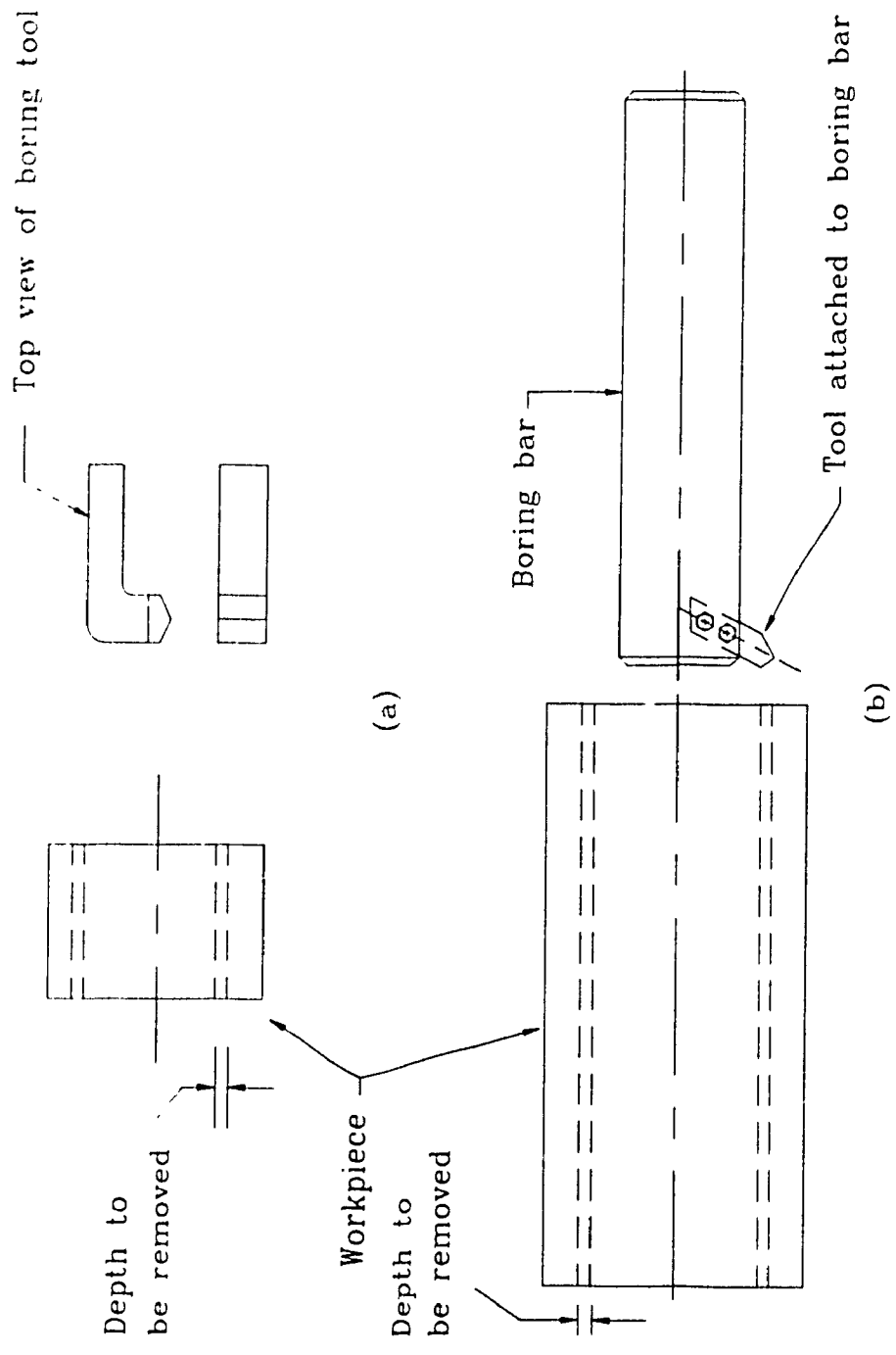


Fig. 1 4 Boring tools used for enlarging existing holes

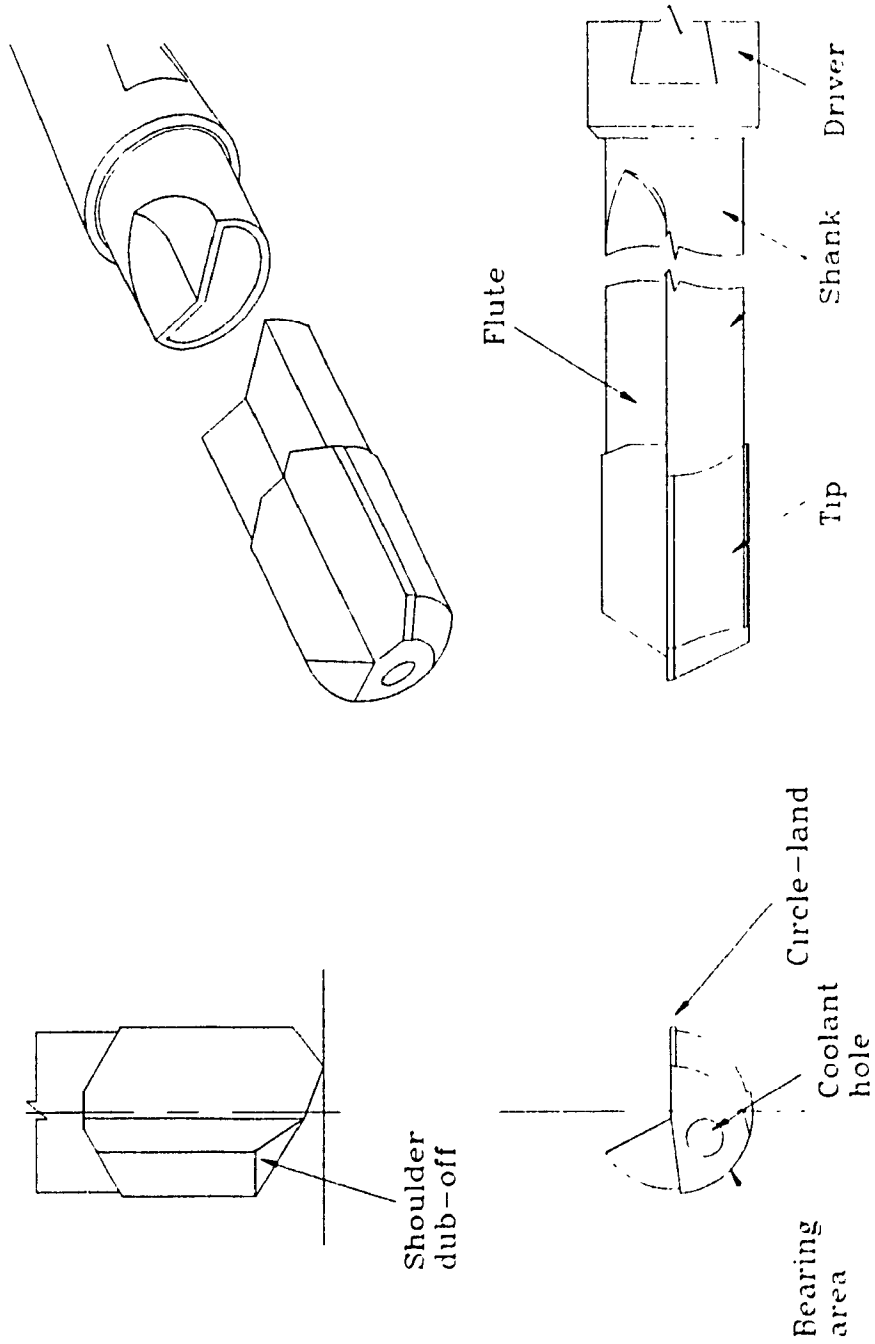
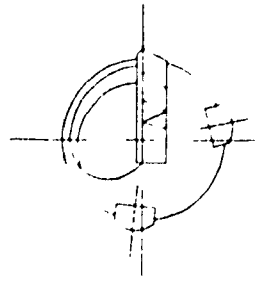
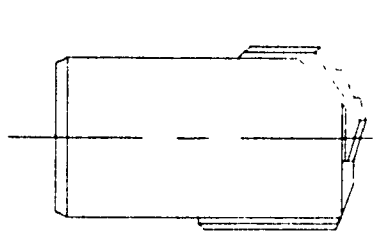


Fig 1 5 Gundrill

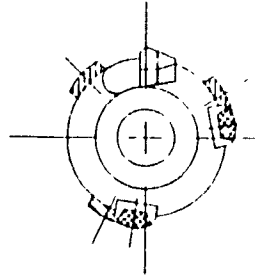
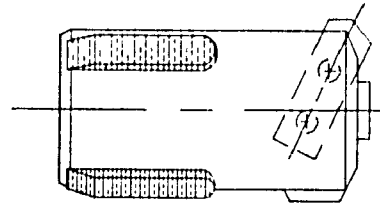
provided in the tip body and flows over the cutting zone and the swarf is carried out through a V-shaped channel in the shank. The kidney shape of the coolant passage is the consequence of a V-channel on the shank for return of the swarf and coolant mixture. The main advantage of the gun drills over other tools is inclusion of guide pads. These guide pads help in balancing the unbalanced forces on the cutter. Since gundrills are self-guided tools, they require an aid during initial cut into a workpiece. This problem is solved by either an accurate pre-machined starting hole in the workpiece or a guiding-bushing placed next to the workpiece in the fluid transfer unit called pressure head.

#### **1.4.5 BTA SOLID DRILLS**

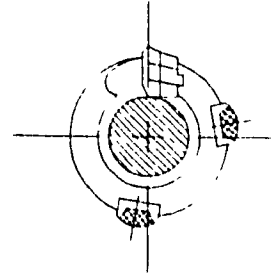
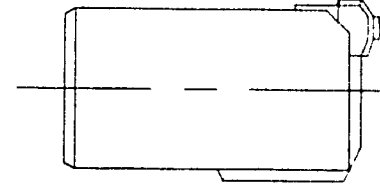
BTA-solid drills are single edge cutting tools and the cutting edge is slightly larger than the radius of the tool as shown in Fig. 1.6 (a) [1]. The pointed cutting edge extends slightly over the centre of rotation in such a way that the zero velocity point falls on the edge. This is a pure end cutting tool, and no extrusion takes place as along the chisel edge in twist drills. The outer and middle cutters are separated by a recess at a specified place and the inner cutting edge is extended so that an edge rather than a point is at the centre line of hole. The recess between the cutting edges causes the chips cut at a limited width. The recess on the rake surface serves as a chip breaker. The chips that are formed during machining are flushed back through the mouth and the throat of the tool and the hole of the boring bar. This forms so called internal chip removal system, where chips are removed through interior of the boring bar and there is no contact of the



a) Solid boring drill



b) Counter-boring drill



c) Trepanning drill

chips and the bore wall, which may cause scratching of the machined and burnished surface.

#### **1.4.6 BTA COUNTER BORING TOOLS**

The BTA counter boring tool is a self guided tool and is shown in Fig. 1.6 (b) [1]. Practically one can machine holes of up to a hundred of the length to diameter ratio. This is mainly used to enlarge an existing hole. Like other BTA tools this tool requires the flow of oil to cool and lubricate the tool-workpiece interface and remove the chips. The guiding pads provided on the periphery of the tool help in giving smooth surface finish by burnishing effect among other functions designated for the BTA tools. Since the operation is used to enlarge holes, the straightness of the resulting hole purely depends on the pre-machined hole especially when referred to major runouts.

#### **1.4.7 BTA TREPANNING TOOLS**

The standard trepanning tools have one cutting edge and two guide pads as shown in Fig. 1.6 (c) [1]. Basically it uses the BTA principle and requires highly pressurised oil to cool the cutting edge and remove chips [58]. In trepanning the cutting takes place only 55-65 % of the diameter, and it leaves a solid core while cutting over a annular area to produce a hole. The trepanning tools are mainly used for making hole size of 60 mm or more. The holes obtained by trepanning are very accurate and straight. If the



machine is properly aligned, the run-out error can be made minimum if the machine is properly aligned.

The major setback in trepanning operation is the handling of the core especially for very large workpieces weighing tens of tons. A special mechanism has to be provided in order to avoid plastic deformation occurring and as a result of the core riding or falling on and touching the finished surface.

#### **1.4.8 BTA MULTI EDGE TOOLS**

Though the cutting action in multi edge cutting tools is not higher than that in the single edge cutting tools, the optimal guiding force at the carbide pads is controlled at predetermined value. In multi-edge cutting tools, the cutting edge is distributed over several overlapping areas of carbide inserts located on either side of the centre. These tools are superior to single edge tools or multi-edge tools with cutters located at  $180^\circ$  to each other [3]. Basically there are two types of these cutting tools, one where the cutters are aligned along a tool diameter and another where the cutters are located on the cutting head such that they form an unsymmetrical configuration. Latinovic and Osman [49] have suggested two types: One the tools with staggered cutters and another one termed tools with unsymmetrical location of cutters.

In tools with staggered arrangement of cutters, the cutters can be combined at will, as

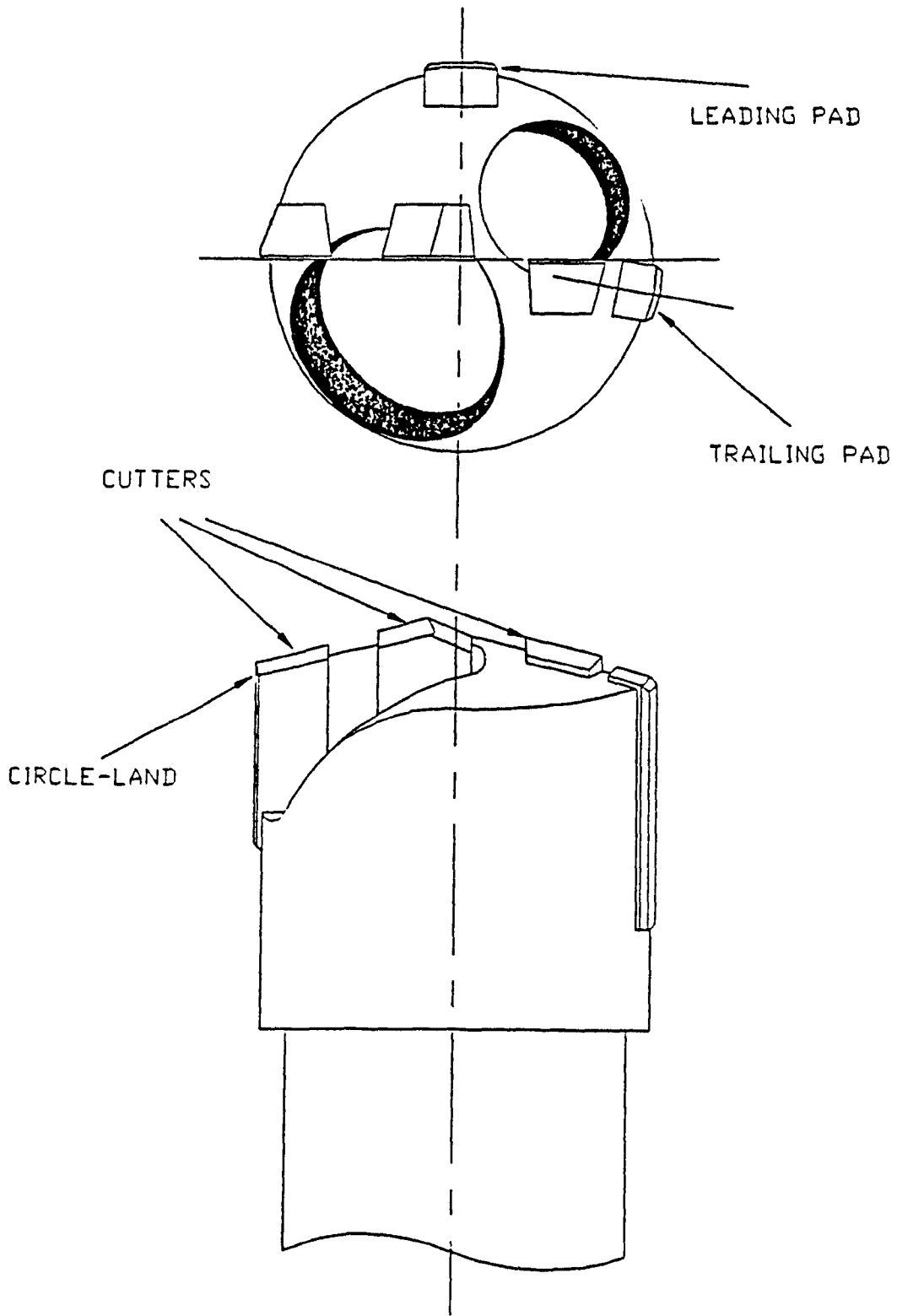


Fig. 17 Tool With Staggered Cutters

far as their approach angles are concerned. Different grades of carbide inserts can be used in this tool, carbide grades with higher grades are used for the outer and middle cutters to meet the requirements of higher hardness and lower grades of carbide grades are used for inner inserts to meet the requirements of lower hardness and higher toughness. The arrangement of inserts on boring head can acquire different configurations based on the sequence in which they cut and these inserts are indexable or brazed to the boring head as shown in Fig. 1.7 [56]. This concept also allows better design flexibility to achieve maximum tool strength by proper location of chipmouths and chipthroats at the cutters.

Another form of multi edge cutting tools are unsymmetrical tools and the basic difference from the tool with staggered cutters is total width of cut covers more than the tool radius. In this arrangement all cutting edges are identically ground to have the same front profile and the chip cross-sectional area depends on the angular spacing between the preceding cutters. The larger the space between the cutters, the thicker the chip and the larger cutting force components are exerted onto the cutting edge.

#### **1.4.9 EJECTOR DRILLS**

Ejector drills use the same principle of BTA tools but eliminates some of its shortcomings. The ejector system consists of a double-tube boring bar in which coolant is supplied to cool the cutting edges through the annular space between inner tube and

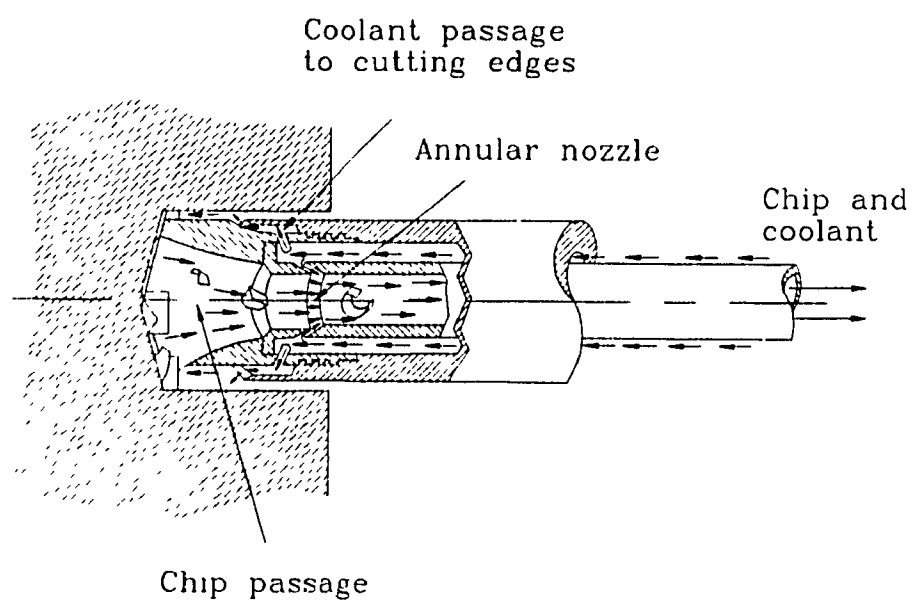


Fig 1 8 Ejector drill

the outer tube and the swarf is flushed out through the inner tube as shown in Fig. 1.8 [1]. The cutting fluid serves both as a coolant and lubrication to the cutting edges and flushes the chips out. The ejector system can be installed both vertically and horizontally with either rotating tool, rotating workpiece and both tool and workpiece rotating in opposite direction.

The ejector drill consists of three cutting edges, two edges are located on one side and the third one at  $180^\circ$  from the other two edges and these edges are distributed over the diameter of the tool. The first cutting edge starts from the periphery of the head cuts through approximately 0.4 of the radius, the second edge cuts through the center approximately 0.4 of the radius and the third one located at  $180^\circ$ , cuts the remainder of the area partially overlapping the area cut by the other two edges. The advantage of arrangement of these cutters gives the tool partially balanced cutting forces, and takes some load off supporting pads.

### **1.5 CUTTING FORCE SYSTEM**

The cutters are located around centre line of the deep hole boring head in such a way that the cutting velocity vector at any point is perpendicular to the cutting edge and hence the operation may be considered as an orthogonal cutting process. In Fig. 1.9 [56] the resultant cutting force  $R$  for orthogonal cutting force can be resolved into 2 main components. The tangential or power contributing component  $F_p = F_t$  parallel to cutting

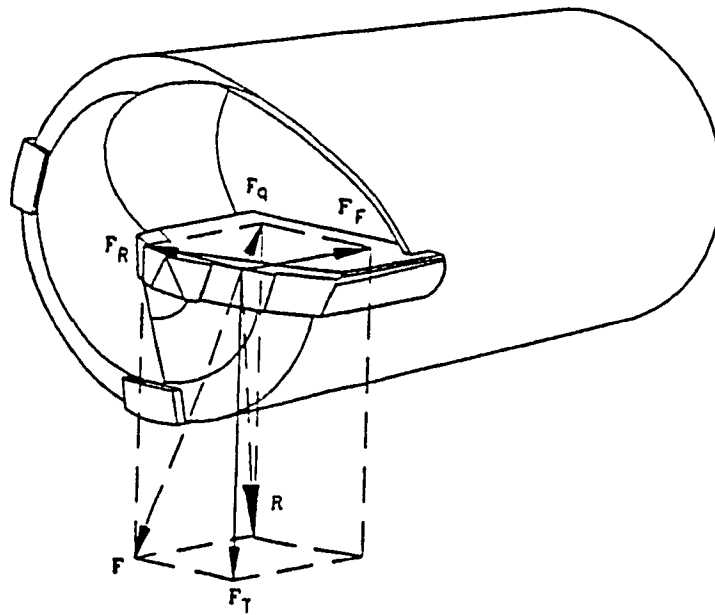


Fig. 1.9 Cutting Force System.

velocity and  $F_q$  perpendicular to cut surface. Further,  $F_q$  is decomposed into two components, the radial component  $F_R$  and the feed component  $F_f$  due to the inclination of cutting edges relative to the radial direction.

## 1.6 OBJECTIVES OF THIS WORK

Several researchers have studied both single and multi-edge cutting tools with conventional design concept of deep hole drilling and boring tools. Normally guide pad reactions in these tools were not controlled nor predicted in the design phase, so they were uneven and the ratio of pad forces on the leading and the trailing pad exceeds two. Cronenjager [59] has considered equal pad forces for the design of deep hole drilling tools and he concluded that they are more stable than previously designed tools. Latinovic et al [32,60,61] have investigated staggered and unsymmetrical multi edge cutting tools applying the same concept of equal guide forces. Torabi [56] has built a prototype of staggered cutting tool with equal pad forces and carried out a comparative study of the prototype and the commercially available single edge and multi edge BTA solid boring tools.

One of the objectives of this work is to provide an analytical formulation of a tool cutting force system and a procedure of optimizing a tool design in such a way that the tool maintains equal guide pad forces. A probabilistic model is used for the objective function in order to consider the variations of the cutting forces during machining

process. In chapter 2, cutting force equations are formulated for deep hole machining with single edge tool. Based on the cutting edge geometry empirical approach is discussed and mathematical expressions for the cutting force components, tangential, radial and feed are given. These equations are used for the design of staggered multi-edge cutting tool. The concept of staggered unsymmetrical multi-edge cutting tool has been discussed. The mathematical formulation for a single cutting tool is used to compute the magnitude of each cutting force component. The objective function is formulated in such a way that the cutting force resultant and the guide pad resultant reactions should balance. Several constraints are to be satisfied in order to meet other requirements from the tool. The method of optimization selected is stochastic optimization of a random objective function with random variables. The nature of the random parameters such as unit cutting forces and width of cut which are incorporated in the objective function are taken from previous research. By this formulation the problem was reduced to a stochastic, nonlinear, and constrained optimization problem, and Interior Penalty method has been used for a selected configuration.

In chapter 3, the variation in magnitude and direction of the cutting force resultant and variations in magnitude of pad reactions during the machining process are predicted using probabilistic methods such as Linear Statistical Approach and Monte Carlo simulation. Since there is no information on the nature of the friction coefficient's variations, the variations in the magnitude of pad reactions are predicted by assuming two distributions for coefficient of friction; a worst case - uniform distribution and most suitable - normal



distribution. The results, however show no significant difference in pad reactions variations because of a small effect of the coefficient of friction on the magnitude of pad reactions.

Another objective of this thesis is to study the stability of the deep-hole machining process. In chapter 4, the stability analysis of the tool is studied by Pfléghar method. Different end conditions of the cutting tool-workpiece interaction are studied depending on the degree of stability at the guide pads during machining process. Free lateral natural frequencies of the cutting tool-boring bar were found for different end conditions.

In chapter 5, summary and conclusions are given and some recommendations for future work are made.

## CHAPTER 2

### OPTIMIZATION OF BTA TOOL WITH STAGGERED CUTTERS BY PROBABILISTIC APPROACH

#### 2.1 INTRODUCTION

The concept of staggered multi edge BTA solid cutting tools with cutters unsymmetrically located on the cutting head was proposed by Latinovic and Osman [60] and Stockert [62]. They designed tools based on equal forces on the supporting pads but no comparative study was conducted with a prototype and commercially available tools. The staggered name comes because of the "zigzag" arrangement of cutters where each cutter cuts its circular zone, partly overlapping with each other. In most applications, these staggered tools are superior to conventional single edge tools or multi edge tools with cutters located at 180 degrees to each other. The basic advantage over the single edge cutting tools is that the cutting forces are controlled, because some of the load is taken off at the supporting pads and the optimum guiding force at the supporting pads is controlled with a predetermined value [3].

In tools with staggered arrangement of cutters these can be combined at will, as far as their approach angles  $\kappa$  are concerned, or use of standard carbide or trepanning inserts. Besides that, different grades of carbide inserts can be used in this type of tool. Carbide grades with higher hardness are used for the outer and middle cutters and grades of

carbide with lower hardness, but higher toughness are used for inner cutters to meet the requirements for higher hardness or higher toughness respectively. Chip removal is facilitated in these tools because of a convenient location of chip-mouths at each cutter. During machining process of heavy cuts and large holes the single edge tools transmit large resultant force to the bore wall through the guide pads; this could cause in undue rubbing and wear of the pads. Another advantage is that the arrangement of inserts on tool head can acquire different configurations based on the sequence in which they cut [56]. This concept allows better design flexibility to achieve maximum tool strength by proper location of chip-mouths and chip-throats. In rotated tools the concept contributes to a better mass balance of the cutting head.

Although tool with staggered cutters is a multi-edge unsymmetrical tool, it does not take full advantage of multi-edge cutting principle since the length of all cutting edges covers only one tool radius and hence it is equivalent to a single-edge tool in terms of metal removal rate. It may allow a slightly higher feed rate or an extended tool life, compared to single-edge tool because of the possibility of combining carbide grades. The cutting force system, acting upon a multi-edge tool with staggered cutters during the machining process, illustrated in Fig. 2.1, implies that boring bar elastic effects are negligible. It can be seen that the boring bar with the cutting head can be considered as cantilever beam clamped at one end and loaded by the cutting force resultant at the other end. This resultant cutting force will be transmitted to the supporting pads if the so-called encastre' effect of boring bar is neglected. However, this encastre' effect is influenced by the

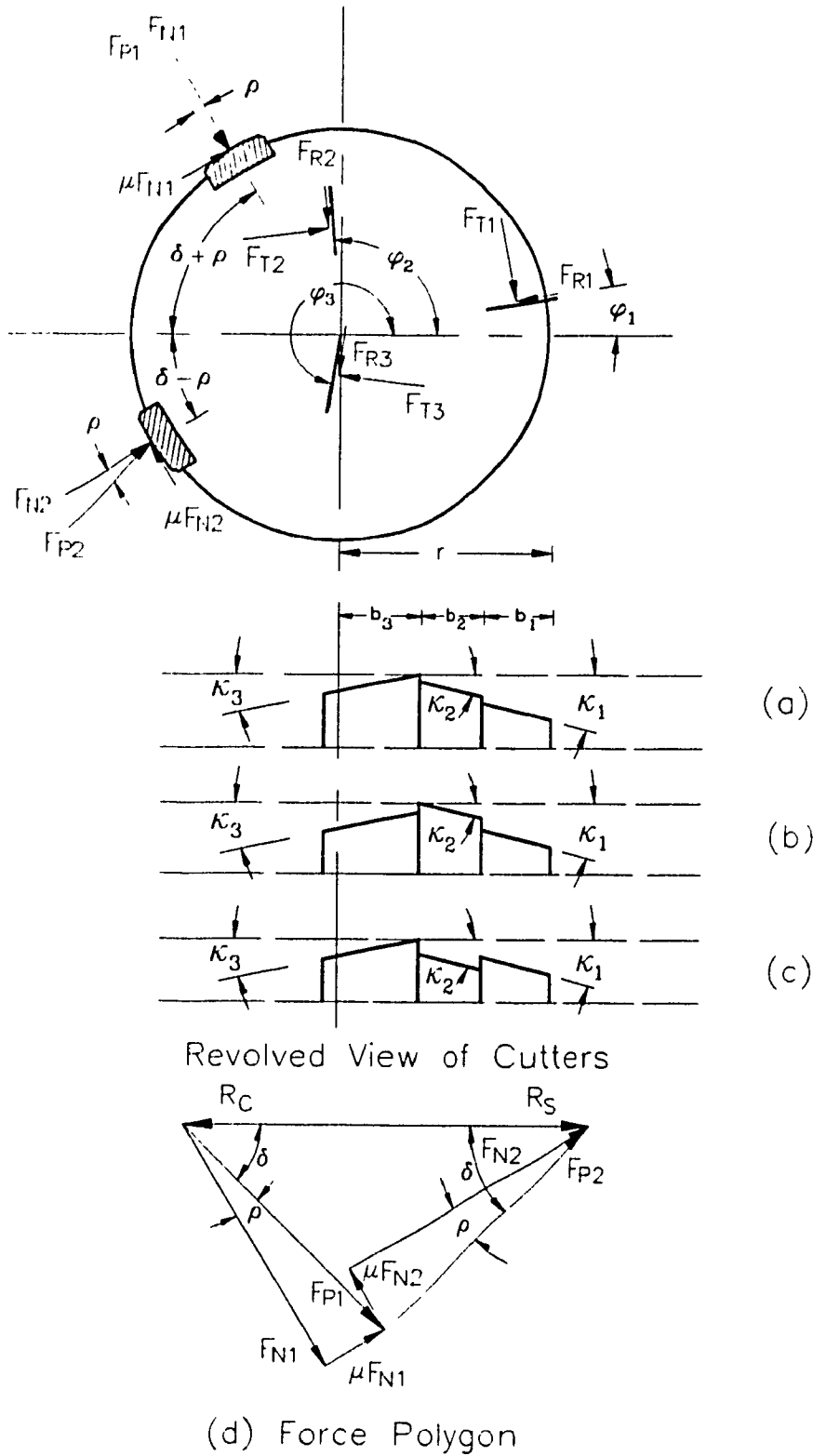


Fig. 2.1 Solid Boring Head with Staggered Cutters

amount of clearance and oil-film thickness between the guide pads of the cutting tool and the machined bore wall. This clearance is an infinitesimal quantity in the case of thin film lubrication and hence the elastic effects can be ignored.

Torabi and Latinovic [51] built a prototype tool with staggered cutters 2 inches in size and tested at various cutting conditions. They compared the results with the prototype and the two commercially available BTA tools of the same size and concluded that the prototype performed better in terms of hole run-out relative to both BTA tools and in terms of hole size error it performed better than BTA multi-edge tool with disposable inserts. The prototype showed to be inferior to the two commercially available tools in terms of surface finish and hole roundness. They concluded in their simulation on BTA-multi edge commercial tool pad's reaction that the force acting on the leading pad is four times higher than that on the trailing pad and the magnitude of reaction force of second pad may approach comparatively small values. This in turn gives low stability to BTA multi-edge tool during the process. The resultant cutting force and pads reactions of BTA solid boring tool are much higher than that of the prototype and the BTA-multi edge tool. Its leading pad mean force is more than two times that of the trailing pad. Sakuma et al [63] compared the performance of BTA solid boring tool and BTA multi edge cutting tools with disposable inserts for quality of the drilled hole and found that the BTA - multi edge tool produced hole with less run-out.

## 2.2 TOOL FORCE SYSTEM FORMULATION

In order to formulate an analytical model of the cutting process in deep hole machining, it is necessary to determine the magnitude and direction of the cutting forces. The resultant cutting force depends on the steady state and variation of the cutting force components. The steady state components can be calculated using two approaches where the limits of variable components are found either from the previous research work or from experiments. The two ways of calculation of the steady state components of cutting forces are either by analytical or empirical method. In the analytical approach the cutting force equations are obtained based on the shear deformation in the cutting zone. In the empirical method the steady state cutting force components are found from the mathematical relationship based on the experimental measurements.

Chandrashekar [50] used the first approach to evaluate cutting forces by assuming the thin shear plane model in deformation zone. Latinovic [3] and Torabi [56] combined the approaches in their work, based on work by Kronenberg [64]. In this approach the so called elementary and extended cutting force laws based on unit cutting force concept in metal cutting is exploited. The same empirical method is used for the design of BTA tool with staggered cutters in this work.

According to Kronenberg [64] the main cutting force or tangential cutting force  $F_T$  can be evaluated from the so-called elementary cutting force law

$$F_T = A K_p \quad (2.1)$$

where

A represents the uncut chip cross sectional area

$K_p$  unit cutting force

Kronenberg concluded from his experiments that unit cutting force decreases with the increase of uncut chip cross-sectional area, but on log-log grid they are linearly related.

This unit cutting force is also function of width of cut and feed rate and given as follows

$$K_p = C_p f(A) = C_p f(b,s) \quad (2.2)$$

where  $C_p$  represents the specific cutting force

b width of cut

s uncut chip thickness

The specific cutting force  $C_p$  is the cutting force for  $b = 1$  mm and  $s = 1$  mm. This specific cutting force represents a very important material constant and plays vital role in cutting mechanics. Since the chip cross-sectional area of  $1 \text{ mm}^2$  represents a unit well within practically encountered chip cross-sectional areas and it is widely accepted in the practice of metal cutting.

It is to be noted from equations (2.1) and (2.2), the unit cutting force  $K_p$  is not a constant but a function of  $b$  and  $s$ . Kronenberg also showed that  $K_p$  is linearly affected by width of cut  $b$  and that  $s$  non linearly affects  $K_p$ , thus it can be written as

$$K_p = C_p s^{n_1} \quad (2.3)$$

by from equations (2.1) and (2.3) the tangential cutting force can be written as

$$F_T = C_p b s^{1-n_1} \quad (2.4)$$

or equation (2.4) can be written as

$$F_T = C_p b^{x_1} s^{y_1} \quad (2.5)$$

Based on the cutting mechanics of orthogonal cutting introduced by Merchant [9], Latinovic [3] determined the cutting force perpendicular to cut surface (thrust component) in terms of feed and depth of cut in an empirical form:

$$F_q = C_q b^{x_2} s^{y_2} \quad (2.6)$$

Knowing  $F_q$  the feed and radial forces can be determined by using the approach angle of cutting edge  $\kappa$ ,

$$F_R = F_q \sin \kappa \quad (2.7)$$

$$F_F = F_q \cos \kappa \quad (2.8)$$

The specific cutting forces  $C_p$  and  $C_q$  can be determined from the experimental results, but due to lack of such information in deep hole drilling process, the data established for turning operation is used. Such data can be found in the VDF machine tool catalogue [65]. It has been found that the tangential cutting force during deep hole machining



process is almost 10 % smaller than that of turning operation [66]. Latinovic [3] collected the values of the constants and exponents in the expressions (2.5) and (2.6) given for the cutting forces of the cutters with zero rake angle. For the tangential force the data for the exponents  $x_1$  and  $y_1$  are identical for different steel materials and were approximated by 1.0 and 0.78 respectively. The average values of the exponents  $x_2$  and  $y_2$  in the radial and feed force were taken at 1.0 and 0.65 respectively.

### **2.3 DESIGN CONCEPT**

The design procedure includes mathematical modeling of cutting force components during machining process, formulation of necessary angles as well as areas necessary for the cutters and guide pads and optimization of certain design parameters. Torabi [56] and Latinovic and Osman [60] built prototype tools with staggered cutters and tested them. The comparison of a prototype of same size as an existing BTA multi-edge tool of a major tool manufacturer was carried out by Torabi [56]. The variation range of the cutting force resultant magnitude as well as its direction and pad reactions were compared to the commercial tool by simulating these variables using the Monte Carlo simulation technique.

The stochastic or probabilistic programming deals with situations where some or all of the parameters of the optimization problem are described by stochastic variables rather than by deterministic quantities. The sources of random variables depend on the nature

of the problem. For example in cutting tool design, the random variables are the specific cutting forces which originate from material failure in shear, machining tolerances, width of cut, feed rate, speed rate, and coefficient of friction etc. These vary about their mean values during machining process. A tool model shown in Fig. 2.1 is the general model of a tool with staggered cutters selected to be optimized and an optimal tool design with its design parameters obtained. The optimization objective selected is a tool layout which will maintain equal total pad reactions.

The angular locations of the cutting edges  $\phi_i$  are specified by the limiting conditions that a cutter location should not conflict with locations of the two adjacent cutters. If the space between the two adjacent cutters is sufficient, these cutters can be moved towards each other. If the space between the cutters is not sufficient the cutters cannot be moved any more towards each other. This also could affect the strength of the head. Fig. 2.2 shows the three arbitrary cutters and two guide pads located on a solid boring tool. Latinovic et al [61] defined an expression for angular location of unsymmetrical multi-edge cutting tool which gives a suitable shape of the chip mouth. The angular space for each mouth is analytically prescribed by  $2\beta$  and angular space of cutting edge by  $\Delta\beta$ . The space requirement dictates the lower and upper limit of the possible requirement of the possible angular location of each cutter given by

$$\phi_{Li} = \phi_{i-1} + \alpha\beta_{i-1} + \Delta\beta_i \quad (2.9)$$

$$\phi_{Ui} = \phi_{i+1} - \alpha\beta_i + \Delta\beta_{i+1} \quad (2.10)$$

where  $i = 1, \dots, n$ ; where  $n$  is number of cutters

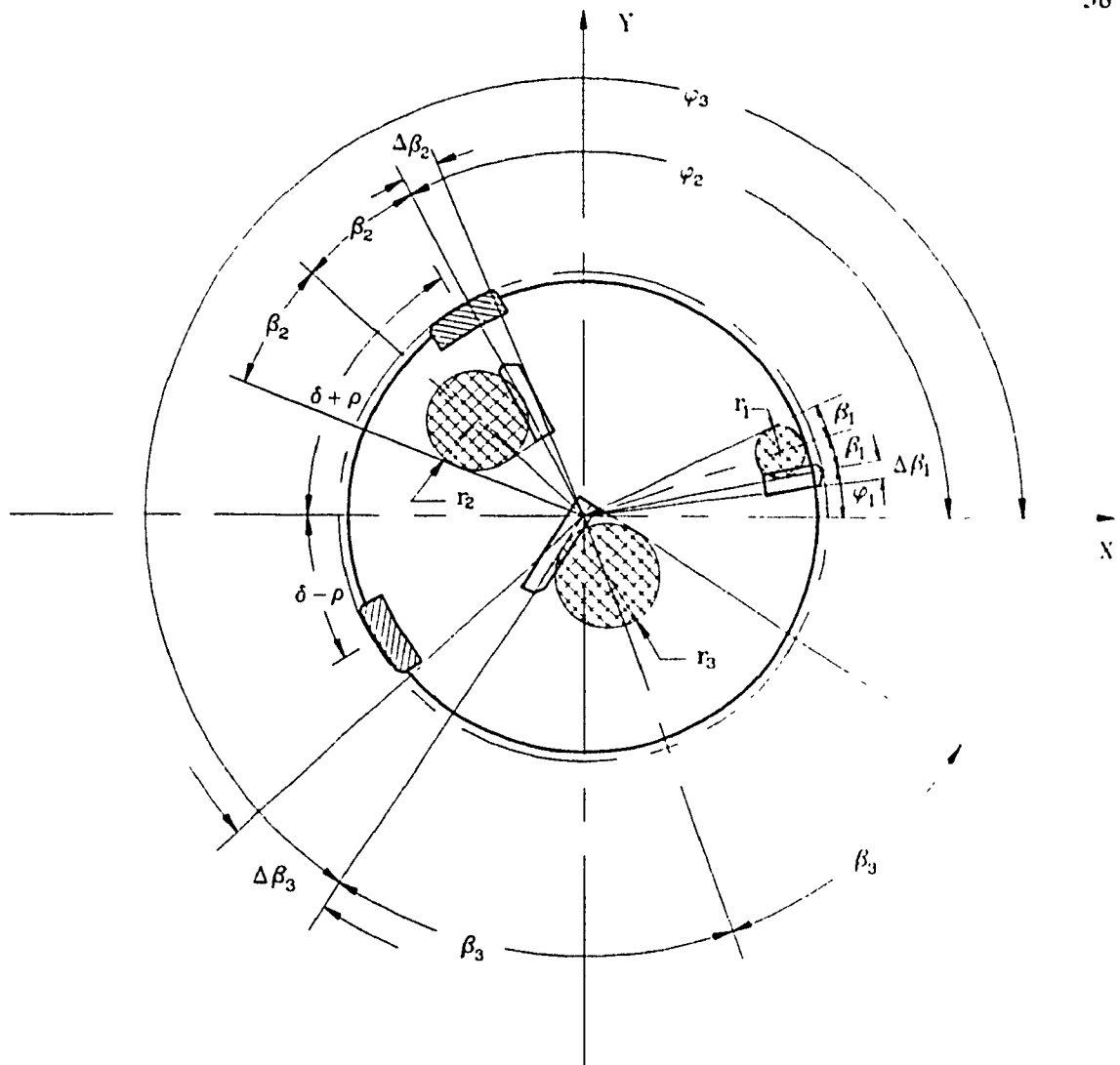


Fig. 2.2 Lower and Upper Limits for Location of Staggered Cutters of BTA Tool

In equations (2.9) and (2.10), the subscripts must be updated by resetting  $i$  to possible value by logic: if  $i = 0$  then  $i = n$ , and if  $i = n+1$  then  $i = 1$ . Values of constants  $\alpha$  and  $\Delta$  depend on space needed above the cutting edge for chip-mouth and space needed below the cutting edge for cutter pocket. In order to meet the space requirement, the best values of  $\alpha$  and  $\Delta$  are recommended as follows [3]

$$\alpha = 0 \text{ and } \Delta = 0.1 - 0.2 \quad \text{for solid boring head}$$

$$\alpha = 1.5 \text{ and } \Delta = 1.5 \quad \text{for trepanning head}$$

The chip-mouth angle  $2\beta$  can be found out by knowing the chip-mouth radius  $r_i$ . The expression for the chip-mouth radius can be written as a function of cutting width and tool diameter as follows [61]

$$r_i = \xi b_i - d + \sqrt{d^2 - \xi d b_i} \quad (2.11)$$

where  $d$  - diameter of the tool head

$b_i$  - represents the width of the cut

$\xi$  - defines the location of the chip-mouth circle w.r.t cutting edge for the best fit of the chip-mouth shape; its value should be between 1.1 - 1.2

The location of the centre of the chip-mouth circle can be written as

$$r_{ci} = r - r_i \quad (2.12)$$

where  $r$  is the radius of cutting head and the expression for chip-throat angle  $\beta_i$  can be expressed as

$$\beta_i = \sin^{-1} (r_i/r_{ci}) \quad i = 1,..,n \quad (2.13)$$

In the present work the general tool layout to be optimized is shown in Fig. 2.1. It consists of 3 inserts and 2 guide pads which are standard components of a major tool manufacturer and used in the previously built model [56]. The sequence of insert cuts into workpiece can be preselected. However the insert angular location is to be found from the optimality criterion which is an equal force acting on each guide pad. The novelty is that the tool configuration is affected by the optimality condition applied. In present tool design the designer does not have control over the pad forces and these are generally unequal, the leading pad force being frequently higher than the trailing pad force.

In order to maintain tool stability and acceptable hole quality the resultant cutting force should be balanced by the resultant pad reaction throughout the machining process. For tool stability the reactions on the pads should always be equal. Due to variation in the friction coefficient at the pads, the total pad force varies slightly. The limits for included angle between the pads can vary but have been found best from practical point of view between  $90^\circ$  and  $110^\circ$ . Commonly in deep-hole drilling practice the maximum pads included angle of  $98^\circ$  is usually recommended. The outer cutter which controls the hole size should be placed nearly opposite to one pad such that hole size control by the outer cutter is maintained by pressure variation at that pad.

In tools with staggered cutters, the total width of cut covers the tool radius and the cutters can be arranged on tool head in different configurations [56]. In any of the three arrangements shown in Fig. 2.1, the width of one of the cutters is fixed, and the width of other two cutters vary in such a way that the required conditions for equal pad force to be satisfied. Thus, by knowing the tool radius equal to the total width of cut, only one of the cutters width can be taken as design variable. However, the outer cutter which controls the hole quality should be placed opposite to one of the guide pads is considered as design parameter. The design parameters in this problem are angular locations of the three cutters, pads included angle and the width of cut of the outer cutter. Hence the number of design variables is five.

#### **2.4. TOOL OPTIMIZATION**

The basic cutting force equations are formulated based on the cutting tool layout shown in Fig. 2.1. The objective is a layout which will balance cutting forces and two equal pad reactions. The objective function has to be formulated to minimize the difference between the cutting force resultant and pads reactions resultant. The location of cutting edges, pads included angle and width of cut of the outer and inner cutters are designated as design variables. Geometrical constraints are imposed on the decision variables such as the lower and upper limits of the angular locations of the cutters, limits of the pads included angle, the allowable limits for the width of cut of the outer cutter and in order to get acceptable hole size control the allowable limits for angular location of the outer

and inner cutters near opposite to one of the guide pads. Additional constraints can be added depending upon the requirements for the cutting tool stability and hole quality. Once the procedure yields the optimum parameters the cutting force variations can be calculated by knowing the variations of the random parameters which are incorporated in the cutting force equations by using the linear statistical approach or the Monte Carlo simulation. The objective function formulation, the constraints equations, variations of the cutting forces and optimization technique are discussed in the following section.

#### 2.4.1 FORMULATION OF THE OBJECTIVE FUNCTION

The objective of this analysis is to achieve the equal predetermined values of pads reactions. For convenience forces in X and Y directions calculated from resultant cutting force components should be always balanced by the resultant of the support reactions. In order to achieve the resultant cutting force to be horizontal, i.e., the magnitude of the cutting force in X-direction  $F_x$  must be equal to the magnitude of the cutting force resultant, the cutting force in Y-direction  $F_y$  must be zero during optimization program. Hence the pad reaction components in Y-direction can be taken as zero in the objective function. The resultant cutting force components in X and Y directions  $F_x$  and  $F_y$  for the tool shown in Fig. (2.1) can be written as

$$F_x = \sum_{i=1}^n (F_{Ri} \cos \phi_i - F_{Ti} \sin \phi_i) \quad (2.14)$$

$$F_Y = \sum_{i=1}^n (F_{R_i} \sin \phi_i + F_{T_i} \cos \phi_i) \quad (2.15)$$

where  $F_{R_i}$  and  $F_{T_i}$  are given by equations (2.5) and (2.7) respectively and  $n$  is no. of cutters. According to Fig. 2.1(d), the predetermined pad force  $F_p$  is chosen such a way that the total support reaction  $R_s$  is balanced by the resultant cutting force  $R_c$ . Since the resultant of support reaction is assumed horizontal, the pads resultant force in Y-direction  $R_Y$  is also zero and both pads total reactions are equal i.e.,  $F_{P1} = F_{P2} = F_p$ , the total support reaction  $R_s$  which is opposite to the cutting force resultant can be written as

$$R_s = R_x = 2 F_p \cos \delta \quad (2.16)$$

From equation (2.16) it can be concluded that the resultant of support reactions  $R_s$  acts always in X-direction and should be balanced by the resultant cutting force  $R_c$ . Therefore the objective is to minimize the difference between the cutting force resultant in X-direction  $F_x$  and pads reaction force  $R_x$  as well as cutting force in Y-direction  $F_Y$  and pads reaction force  $R_Y$  which is for convenience selected to be zero. The objective function then can be written as

$$f(\phi_i, b_i, \delta) = K_1 | F_x - R_x | + K_2 | F_Y | \quad i=1,2,3 \quad (2.17)$$

Where  $K_1$  and  $K_2$  are positive weighting factors and different values can be given during optimization programming depending which condition should be met closer. In this



work, the specific cutting forces and width of cut of the outer cutter which are incorporated in equations (2.5) and (2.6) are considered as random parameters. Since there is no information available on variations of feed rate, and on friction coefficient's distribution at the guide pads, their significance at this stage is considered to be neglected and they are treated as deterministic values. These random parameters vary about their respective mean values during the machining process. The specific cutting forces  $C_p$  and  $C_q$  purely depend upon the workpiece material shear strength and their variation influences the radial and tangential components. The variations in width of cut is controlled by the manufacturing tolerance of the carbide insert. Since the specific cutting forces and the width of cut are incorporated in the cutting force equations, and their variations could effect static stability of the cutting tool, through the variation of the pad reactions.

For tool guidance, stability and accuracy of the hole size, the range of cutting forces variation in magnitude should be known prior to the tool design in order to predict variations in the cutting force resultant. Latinovic [3] found out the variation range of resultant cutting force vector by using the Limit Method. Torabi [56] applied the technique of Monte Carlo simulation to find the range of change of resultant cutting force and pad reactions variations.

In metal cutting operations such as turning and drilling results have proven that the cutting forces are random and Gaussian distributed [22-24]. Several researchers such as

Greuner [25] and Griffiths [30] have measured the cutting force components by using a strain gauge transducer. Chandrashekhar [50], Stockert [67], and Weber [68] have used a piezo-electric dynamometer. However, some of the measurements have been concerned only with the mean values of the cutting force components, other have been conducted to determine the range of change of the cutting force components [25, 50, 68]. Chandrashekhar [50] found from his experiments that the cutting force components in deep-hole machining are Gaussian distributed, and the cutting process has been identified as stationary and ergodic in a weak sense. The specific cutting forces  $C_p$  and  $C_q$  incorporated in tangential and radial cutting force equations (2.4) and (2.7) and the width of cut  $b$  vary about their mean values during machining process. The specific cutting forces  $C_p$  and  $C_q$  vary because of they are directly related to the material failure in shear of the workpiece and the width of cut  $b$  vary because of machining tolerance of the cutters. Based on these assumptions all random variables  $C_p$ ,  $C_q$  and  $b$  are assumed to independent and un-correlated and follow normal distribution. The variation of the specific cutting forces can be taken as  $\pm 10\%$ , since the variation of the radial and tangential forces in the deep hole machining process are reported to be  $\pm 10\%$  [69]. The variation for width of cut  $b$  can be assumed 1%. No information is available on variation and distribution of feed rate  $s$  and distribution of friction coefficient  $\mu$  at the guide pads and they are considered to be deterministic parameters at this stage of investigation.

By assuming all the random variables are independent and un-correlated and follow

normal distribution, . stochastic nonlinear problem can be formulated in standard form as

$$\text{Find } X = \{x_1 \ x_2 \ \dots \ x_n\}^T \text{ which minimizes } f(X, Y) \quad (2.18)$$

$$\text{subject to } P(g_j(X, Y) \leq 0) \geq p_j, \quad j = 1, \dots, m \quad (2.19)$$

Where  $X$  - vector of decision variables =  $\{\phi, \delta, b_1\}^T$ ,  $Y$  - vector of random parameters =  $\{C_{p_i}, C_{q_i}, b_i\}^T$  and  $i=1,2,3$ . Equations (2.19) denote that the probability of realizing  $g_j(X, Y)$  less than or equal to zero must be greater than or equal to the specified probability  $p_j$ . It is to be noted that, in this analysis only decision variable  $b_1$  is considered as random variable.

The stochastic problem given by equations (2.18) and (2.19) can be converted into an equivalent deterministic nonlinear programming problem by applying the chance constrained programming technique. This technique was originally developed by Charnes and Cooper [70] and has been adopted and applied to solve structural engineering problems [71-74]. The advantage of this chance constrained programming technique is that it can be used to solve problems involving chance constraints, that is, constraints having finite probability of being violated. This method permits the constraints to be violated by a specified (small) probability.

The objective function given by equation (2.18) can be expanded into Taylor's series

about the mean value of  $\bar{Y}$  and by neglecting higher order terms, the new stochastic objective function for the purpose of optimization can be obtained as [71]

$$f(X,Y) = K_{w1} \bar{f} + K_{w2} \sigma_f \quad (2.20)$$

Where  $K_{w1} \geq 0$  and  $K_{w2} \geq 0$  and their numerical values indicate the relative importance of  $\bar{f}$  and  $\sigma_f$  for optimization. The mean  $\bar{f}$  and standard deviation  $\sigma_f$  are given by

$$\bar{f} = K_1 |\bar{F}_X - \bar{R}_S| + K_2 |\bar{F}_Y| \quad (2.21)$$

$$\sigma_f = \left( \sum_{i=1}^3 \left( \frac{\partial f}{\partial C_{pi}} \right)^2 \sigma_{C_{pi}}^2 + \sum_{i=1}^3 \left( \frac{\partial f}{\partial C_{qi}} \right)^2 \sigma_{C_{qi}}^2 + \left( \frac{\partial f}{\partial b_1} \right)^2 \sigma_{b_1}^2 \right)^{1/2} \quad (2.22)$$

Where the cutting components  $F_X$  and  $F_Y$  can be written in terms of the random variables  $C_{pi}$ ,  $C_{qi}$  and  $b_1$  from equations (2.14) and (2.15) about their mean values as

$$\bar{F}_X = \sum_{i=1}^3 \left( \bar{C}_{qi} b_i^{x_2} S_i^{y_2} \sin \kappa_i \cos \phi_i - \bar{C}_{pi} b_i^{x_1} S_i^{y_1} \sin \phi_i \right) \quad (2.23)$$

$$\bar{F}_Y = \sum_{i=1}^3 \left( \bar{C}_{qi} b_i^{x_2 y_2} \sin \kappa_i \sin \phi_i + \bar{C}_{pi} b_i^{x_1 y_1} \cos \phi_i \right) \quad (2.24)$$

and

$$\frac{\partial f}{\partial C_{pi}} \Big|_{\bar{Y}} = \sum_{i=1}^3 \left( K_1 | -b_i^{x_1 y_1} \sin \phi_i | + K_2 | b_i^{x_1 y_1} \cos \phi_i | \right) \quad (2.25)$$

$$\frac{\partial f}{\partial C_{qi}} \Big|_{\bar{Y}} = \sum_{i=1}^3 \left( K_1 | b_i^{x_2 y_2} \sin \kappa_i \cos \phi_i | + K_2 | b_i^{x_2 y_2} \sin \kappa_i \sin \phi_i | \right) \quad (2.26)$$

$$\begin{aligned} \frac{\partial f}{\partial b_1} \Big|_{\bar{Y}} = & |K_1 (\bar{C}_{q1} s_1^{y_2} \sin \kappa_1 \cos \phi_1 - \bar{C}_{p1} s_1^{y_1} \sin \phi_1)| \\ & + |K_2 (\bar{C}_{q1} s_1^{y_2} \sin \kappa_1 \sin \phi_1 + \bar{C}_{p1} s_1^{y_1} \cos \phi_1)| \end{aligned} \quad (2.27)$$

where  $x_1 b_i^{x_1-1}$  doesn't show because  $x_1$  is commonly 1, then  $x_1 b_i^0 = 1$

and  $i = 1, 2, 3$

If  $K_{w2} = 0$ , it means that the expected value of  $f$  is to be minimized and effect of standard deviation is ignored and if  $K_{w1} = 0$ , means that we are interested only in the

standard deviation of  $f$  rather than the mean of  $f$ . In the same way if  $K_{w1} = K_{w2} = 1$ , indicates that equal importance is given to the mean and standard deviation of  $f$ .

Another way of solving the standard deviation of  $f$  is to minimize  $\bar{f}$  subject to the

constraint  $\sigma_f \leq K_{w3} \bar{f}$  where  $K_{w3}$  is a positive weighting factor, along with the other

constraints [71].

#### 2.4.2 CONSTRAINTS FORMULATION

Similarly by neglecting higher order terms, the constraint equations formulated in stochastic form in equation (2.19) can be written in deterministic form as [71],

$$\bar{g}_j - \phi_j(p_j) \left[ \left( \sum_{i=1}^3 \frac{\partial g_j}{\partial C_{pi}} \Big|_{\bar{y}} \right)^2 \sigma_{C_{pi}}^2 + \left( \sum_{j=1,2,\dots,m} \frac{\partial g_j}{\partial C_{qi}} \Big|_{\bar{y}} \right)^2 \sigma_{C_{qi}}^2 + \left( \frac{\partial g_j}{\partial b_1} \Big|_{\bar{y}} \right)^2 \sigma_{b_1}^2 \right]^{1/2} \leq 0 \quad (2.28)$$

Since only one decision variable  $b_1$  is probabilistic and other random parameters are not included in the constraints, equation (2.28) can be simplified as

$$\bar{g}_j - \phi_j(p_j) \left[ \left( \frac{\partial g_j}{\partial b_1} \Big|_{\bar{y}} \right)^2 \sigma_{b_1}^2 \right]^{1/2} \leq 0 \quad (2.29)$$

To produce acceptable hole quality, and to maintain stability of the cutting tool the constraint equations should be written for size of the cutters, partition of the cutters, included angle of the guide pads, and the condition that the outer cutter which maintains the hole size should be near opposite to a guide pad. These equations should be satisfied throughout the optimization process and should be written in an appropriate form depending upon the optimization algorithm adopted.

By fixing the width of cut of the middle cutter  $b_2$ , and varying the width of cut  $b_1$  independently, the minimum and maximum width of cuts of the outer cutter  $b_1$  can be limited to:

$$6.0 \leq b_1 \leq 8.0 \quad (2.30)$$

Since the decision variable  $b_1$  is probabilistic and the constraint equation (2.30) contains also probabilistic quantity the following can be written

$$P(g_1 = 6 - b_1 \leq 0) \geq p_1 \quad (2.31)$$

$$P(g_2 = b_1 - 8 \leq 0) \geq p_2 \quad (2.32)$$

Equations (2.31) and (2.32) can be written in deterministic form as

$$6 - \bar{b}_1 - \phi_1(p_1) \left[ \left[ \frac{\partial g_1}{\partial b_1} \right]^2 \sigma_{b_1}^2 \right]^{1/2} \leq 0 \quad (2.33)$$

$$\bar{b}_1 - 8 - \phi_2(p_2) \left[ \left[ \frac{\partial g_2}{\partial b_1} \right]^2 \sigma_{b_1}^2 \right]^{1/2} \leq 0 \quad (2.34)$$

Where  $p_1$  and  $p_2$  are specified probabilities and  $\phi_1(p_1)$  and  $\phi_2(p_2)$  are the corresponding standard normal variates. The probabilities given in equations (2.31) and (2.32) is 99% and the corresponding standard normal variates from standard normal distribution table is 2.33.

The lower and upper boundaries of the cutters required space for the chip-mouths can be found by using the equations (2.9) and (2.10) can be written in generalized form as follows:

$$\phi_{i-1} + \alpha\beta_{i-1} + \Delta\beta_i \leq \phi_i \leq \phi_{i+1} - \alpha\beta_i + \Delta\beta_{i+1} \quad (2.35)$$

where  $i = 1, 2, \dots, n$ ;  $n$  is number of cutters

The explanation regarding the subscripts have been given in the design concept section. The pads included angle  $\delta$  is very important for tool guidance and stability and burnishing action. The larger the included angle the larger the resultant support reactions force  $R_s$  and vice versa. The resultant support reactions should always bisect the included angle of the pads and the constraint equation for minimum and maximum included angle of the guide pads is recommended to be



$$90^\circ \leq 2\delta \leq 110^\circ \quad (2.36)$$

The constraint equations for the outer cutter which controls the hole size should be near opposite to one of the guide pads is expressed in the following conditions

$$\text{If} \quad | \delta - \rho - \phi_1 | \leq | \delta + \rho + \phi_1 |$$

$$\text{Then} \quad | \delta - \rho - \phi_1 | \leq 20^\circ \quad (2.37)$$

$$\text{otherwise} \quad | \delta + \rho + \phi_1 | \leq 20^\circ \quad (2.38)$$

Thus the stochastic optimization problem given by equations (2.18) and (2.19) has been converted into an equivalent deterministic nonlinear programming form as: minimize  $f(X, Y)$  given by equation (2.18) subject to the constraints given by (2.33) to (2.38). This is a multi-variable, nonlinear and constrained with non equality constraints problem and can be solved by using any nonlinear programming techniques.

## 2.5 OPTIMIZATION TECHNIQUE

The optimization technique used to minimize the stochastic objective function given by equation (2.20), subject to constraints (2.33) to (2.38) is called Interior penalty method. Interior penalty method transforms the constrained problem into unconstrained problem such that numerical solution is sought by *sequential unconstrained minimization techniques* (SUMT) [75].

If the constrained optimization problem is of the form

Find  $X$  which minimizes  $f(X, Y)$  subject to

$$g_j(X, Y) \leq 0 \quad (2.39)$$

The general approach is to minimize the objective function as an unconstrained function but to provide some penalty to limit constraint violations. This problem can be converted into an unconstrained minimization problem by constructing a pseudo-objective function of the form

$$\gamma_k = \gamma(X, Y, r_k) = f(X, Y) + r_k P(X, Y) \quad (2.40)$$

where

$f(X, Y)$	represents the original objective function
$P(X, Y)$	represents an imposed penalty function
$r_k$	represents a positive penalty parameter

The penalty parameter  $r_k$  is held constant for a complete unconstrained minimization. The subscript  $k$  represents an unconstrained minimization number. If the unconstrained function of the pseudo-objective function  $\gamma$  is repeated for a sequence of values of the penalty parameter  $r_k$  ( $k=1, 2, \dots$ ), the solution may be brought to converge to that of the original problem stated in equation (2.39). Because of this reason the penalty function methods are called as *sequential unconstrained minimization techniques* (SUMT). In the interior penalty method the penalty function can be written as

$$P(X, Y) = \sum_{i=1}^m -\frac{1}{g_i(X, Y)} \quad (2.41)$$

and

$$P(X, Y) = \sum_{i=1}^m -\log[-g_i(X, Y)] \quad (2.42)$$

The penalty term  $r_k$  plays vital role and is chosen such that its value is small at points away from the constraint boundaries and tends to infinity as the constraint boundaries are approached. Hence the value of the pseudo-objective function  $\gamma$  also blows up as the constraint boundaries are approached. The algorithm for the interior penalty function method is shown in the Fig. 2.3. The basic steps to be followed while formulating any interior penalty method are:

### 2.5.1 NORMALIZATION OF THE CONSTRAINT EQUATIONS

In order to improve the conditioning of the optimization problem the constraints should be normalized while formulating the problem. It is advisable to normalize the constraints so that they vary between -1 and 0 as far as possible. Problem of a type having lower and upper bounds can be normalized as follows:

$$x_l \leq x \leq x_u \quad (2.43)$$

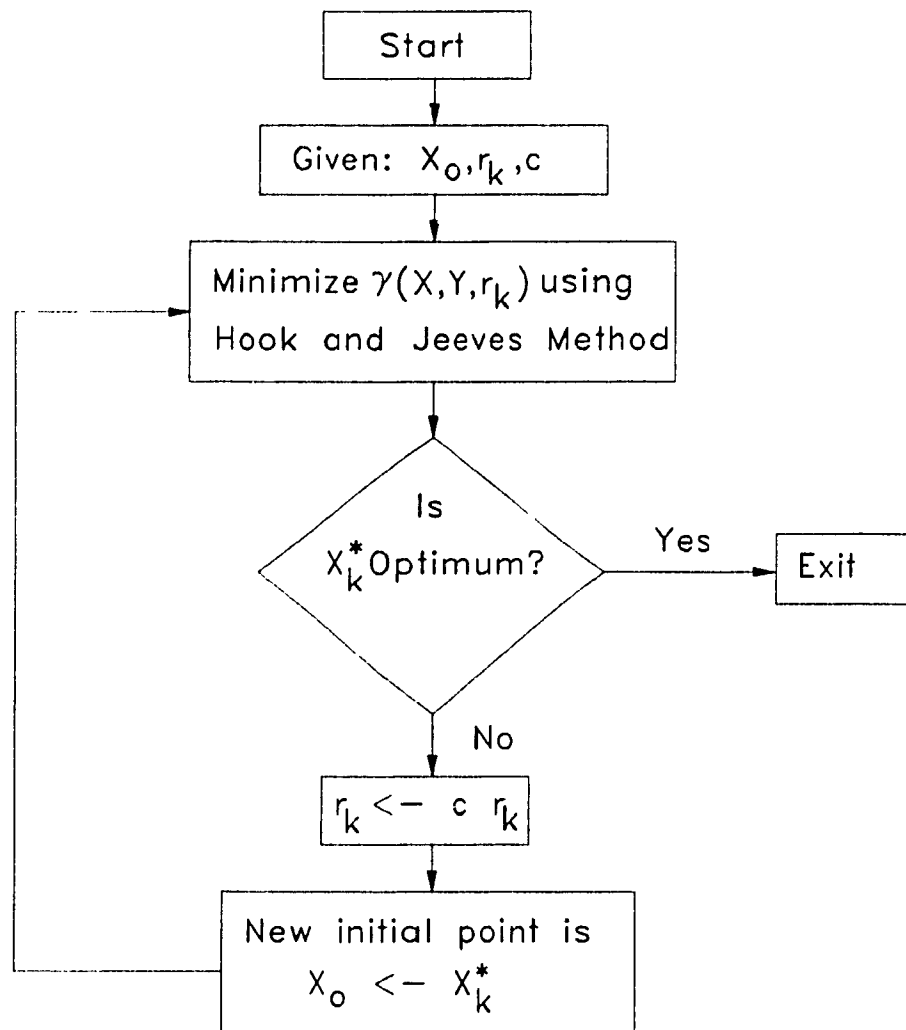


Fig. 2.3 Algorithm for Interior Penalty Method

$$g_1(X) = (x_j/x) - 1 \leq 0 \quad (2.44)$$

$$g_2(X) = (x/x_u) - 1 \leq 0 \quad (2.45)$$

If the constraints are not normalized the problem can still be solved by defining different penalty parameters to each individual constraint equation.

### 2.5.2 INITIAL VALUE OF THE PENALTY PARAMETER

The initial value of penalty parameter  $r_1$  and decreasing value have to be chosen such that the optimum value of penalty function can be achieved. Thus, for any feasible starting point  $X_0$ , the value of  $r_1$  can be taken as

$$r_1 = 0.1 \text{ to } 1 \frac{f(X_0, Y)}{[P(X_0, Y)]} \quad (2.46)$$

After unconstrained minimization the subsequent values of the penalty parameter  $r_k$  have to be chosen such that

$$r_{k+1} \leq r_k \quad (2.47)$$

For convenience, the values of  $r_k$  are chosen according to the relation

$$r_{k+1} = c r_k \quad (2.48)$$

where  $c$  is constant and its value can be taken 0.1, 0.2 or 0.5, etc.

### 2.5.3 UNCONSTRAINED MINIMIZATION

For unconstrained minimization of the pseudo-objective function, Hooke and Jeeves method has been used. Basically the algorithm consists of two major phases, and exploratory search, around the base point and a pattern search in a direction selected for minimization. In the exploratory move one variable is changed at the time and it is sought to produce a sequence of improved approximations towards the minimum of the function. The same procedure is repeated for other variables until last point for first set of exploratory search is found. After the successful exploratory search, a pattern search at the direction of a vector which joins the base point and the point found from last exploratory search is attempted. The process can be terminated if the change in each variable is less than some specified tolerance.

### 2.5.4 CONVERGENCE CRITERIA

The minimization of the unconstrained function can be terminated whenever the relative difference between the values of the objective function obtained at the end of any two consecutive searches falls below a small number  $\epsilon$ .

$$\left| \frac{f(X_k^*, Y) - f(X_{k-1}^*, Y)}{f(X_k^*, Y)} \right| \leq \epsilon \quad (2.49)$$

### 2.5.6 DEVIATIONS OF THE CUTTING FORCES

The variations of the resultant cutting force magnitude and direction can be found by using Linear Statistical Approach or Monte Carlo simulation with the optimum parameters obtained from the stochastic programming. The determination of the cutting forces variations, however, will be discussed in the next chapter.

### 2.6 OPTIMUM TOOL MODEL

The interior penalty method minimizes the objective function given by equation (2.20) subject to the constraints given by equations (2.32) to (2.38). The results of the optimization are given in the Table 2.1 and the optimum tool model is shown in Fig. 2.4. The problem is solved for different configurations of the cutting tool given in Fig. 2.1 and the feasible configuration is the one in which inner cutter cuts into the workpiece first as shown in Fig. 2.1(c). The magnitude for assumed horizontal direction of the resultant support reaction is equal to the resultant cutting force. This shows that the resultant cutting force vector which is horizontal will always be balanced by the resultant supports reaction and it will bisect the pads included angle. Holes of a controlled hole size can be obtained because the outer cutter is located opposite to the trailing pad. Since the width of cut of the middle cutter  $b_2$  is constant and equal 8 mm, the width of the centre cutter  $b_3$  can be calculated according to the configuration shown in Fig. 2.1(c) as 10.923 mm. The data taken for stochastic programming are given as follows:

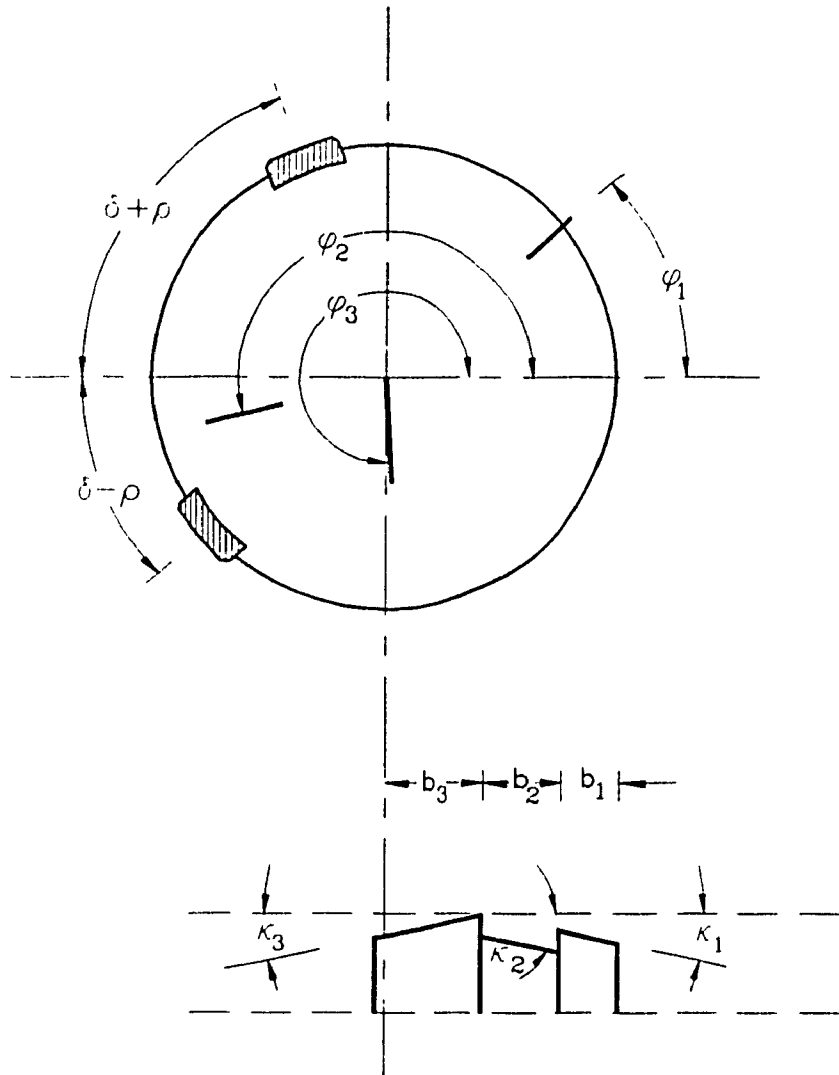


Fig. 2.4 Optimum BTA Tool Model With Staggered Cutters



- The specific cutting forces (random parameters) for the workpiece material DIN-C60 a steel similar to SAE-P255 are [3],  $C_p = 1.730 \text{ kN/mm}^2$  and  $C_q = 1.130 \text{ kN/mm}^2$
- The exponents of the tangential and radial cutting force components are:  
 $x_1 = 1.0$ ;  $x_2 = 1.0$ ;  $y_1 = 0.8$ ;  $y_2 = 0.65$
- The approach angle of the cutters are  $\kappa_1 = 12^\circ$ ,  $\kappa_2 = 12^\circ$ , and  $\kappa_3 = -12^\circ$
- The feed per revolution  $s$  is  $0.17 \text{ mm}$

## 2.7 CONCLUSIONS

Optimum values of the BTA multi-edge tool with staggered cutters are found by using stochastic optimization. The predetermined pad force is chosen in the optimization program in such a way that the optimum resultant cutting force transmits to the bore-wall through the guide pads with equal pad forces and the cutting force resultant vector is always balanced by the resultant support reaction vector. Equal pad forces criterion is achieved by obtaining the magnitude of the cutting force in Y-direction is zero and the magnitude of the cutting force in X-direction is equal to the magnitude of the resultant cutting force. Since the magnitude in X-direction is horizontal to the left, the resultant cutting force is transmitted to the bore-wall with equal pad forces to the right at equal angles  $(180^\circ - \delta)$  and  $(180^\circ + \delta)$ . Constraints are provided in such a way that, the outer cutter which controls the hole size is located approximately opposite to a guiding pad and enough space is provided for the chip-mouths and chip-throats at the cutters. The first

step is finding the mean value of the objective function as the difference of the cutting force resultant and resultant supports reaction which should be equal to zero. However the standard deviation of the objective function is also considered in order to account for the variations of the cutting forces, which vary about their mean values. Initially the objective function is minimized to zero. The contribution of standard deviation to the objective function is ignored by taking  $K_{w2} = 0$ . In the second attempt equal importance is given to the contribution of the mean and standard deviation of the objective function by taking  $K_{w1} = K_{w2} = 1$ . The consideration of the standard deviation of the objective function along with the mean value of the objective function has not yielded any significant difference in the optimum configuration which can be seen in Table 2.1. The results indicate that the objective function value is insignificantly higher in the case of probabilistic case compared to that of the deterministic case. The increase in the objective function value is due to the uncertainties in the random variables. However in both the cases the problem is converging to the same optimum set of parameters. The results indicate that the model can handle the variations during machining process due to the variations of the unit cutting forces and width of cut of the outer cutter, parameters which exhibit high degree of randomness. The main gain is that the optimization process yields the mean value and the standard deviation of the objective function for a set of optimum design parameters of the tool in a single step rather than in two steps; first the optimum mean cutting force resultant through the deterministic optimization and second the standard deviation of the resultant cutting force through the Linear Statistical Approach or Monte Carlo simulation.

Table 2.1 Optimum values of the BTA tool with staggered cutters

Number of cutters	3	
$K_{w1}$	1	1
$K_{w2}$	0	1
Location of the outer cutter $\phi_1$ [deg]	41.8282	41.8296
Location of the middle cutter $\phi_2$ [deg]	196.1391	196.1433
Location of the inner cutter $\phi_3$ [deg]	272.9135	272.9134
Width of cut of the outer cutter $b_1$ [mm]	6.4761	6.4761
Location of pads $\delta$ [deg]	55.0	55.0
Resultant cutting force magnitude $R_C$ [kN]	3.4414	3.4416
Resultant cutting force direction $\lambda$ [deg]	1.6076E-04	1.7862E-04
Resultant pads support reaction $R_s$ [kN]	3.4416	3.4416
Resultant cutting force in X-direction $F_x$ [kN]	3.4414	3.4416
Resultant cutting force in Y-direction $F_y$ [kN]	9.6556E-06	1.0723E-05
Mean of the objective function $f$ [kN]	6.5446E-05	1.1223E-04
Standard deviation of the objective function $\sigma_f$ [kN]	0.0	0.2540

## CHAPTER 3

### ANALYSIS OF CUTTING FORCES AND PAD REACTIONS VARIATIONS

#### 3.1 INTRODUCTION

The cutting forces in any machining process are dynamic in nature with random characteristics. The random parameters incorporated into equations of cutting force components, such as radial and tangential forces vary about their mean values during machining process. Very few results on the variations of amplitude of cutting force components from mean value have been reported. The variations of radial and tangential cutting forces effect the magnitude and direction of resultant cutting force. There are variations in the pad reactions due to variation of coefficient of friction at the guide pads during machining process. In order to assess the tool for its stability the variation ranges of the resultant cutting force magnitude and direction have to be studied.

It has already explained in chapter 2, that the assumed horizontal resultant support reaction balances the resultant cutting force. But the radial and tangential cutting forces vary in magnitude from their mean values because of variations in specific cutting forces, width of cut, and feed rate. For a stable drilling of a given workpiece material with a given tool, the magnitude and direction variations of resultant cutting force need to be within certain limits. The minimum resultant cutting force should be such that sufficient pressure is exerted between the pads and the bore wall in order to secure a proper self-

guidance and burnishing action. The varying burnishing action could produce bad hole quality; hence for that reason the variations of the cutting forces and pad reactions need to be minimum. The state of resultant pads reaction and resultant cutting force during machining process are shown in Fig. 3.1.

In metal cutting processes especially in drilling and turning operation, it has been proven that the cutting forces are random and Gaussian distributed [22-24]. Greuner [25] and Griffiths [30] measured cutting forces by using a strain gauge force transducer and while Chandrashekhar [50], Stockert [67], and Weber [68] used piezo electric dynamometers for the same measurement. While, some of these measurements have been concerned only with the mean values of the components, most of them have been conducted to determine the range of change of the cutting force components [25,50,68]. Chandrashekhar et al [76] concluded from his experiments that the cutting force components in deep-hole machining are Gaussian distributed, and the cutting process has been identified as piecewise stationary and ergodic in a weak sense. Some of the results on the variation of the cutting force components have been recorded during the machining process and reported are used as a base for assessment of tool stability.

1. According to Greuner. B., [25], the fluctuation range of the tangential, radial and feed components had been measured at  $\pm 8\%$ ,  $\pm 21.5\%$  and  $\pm 2\%$  respectively and the variation in boring torque had been reported  $\pm 14\%$ .
2. Cronjager [77] has reported the variation in the magnitude of radial and

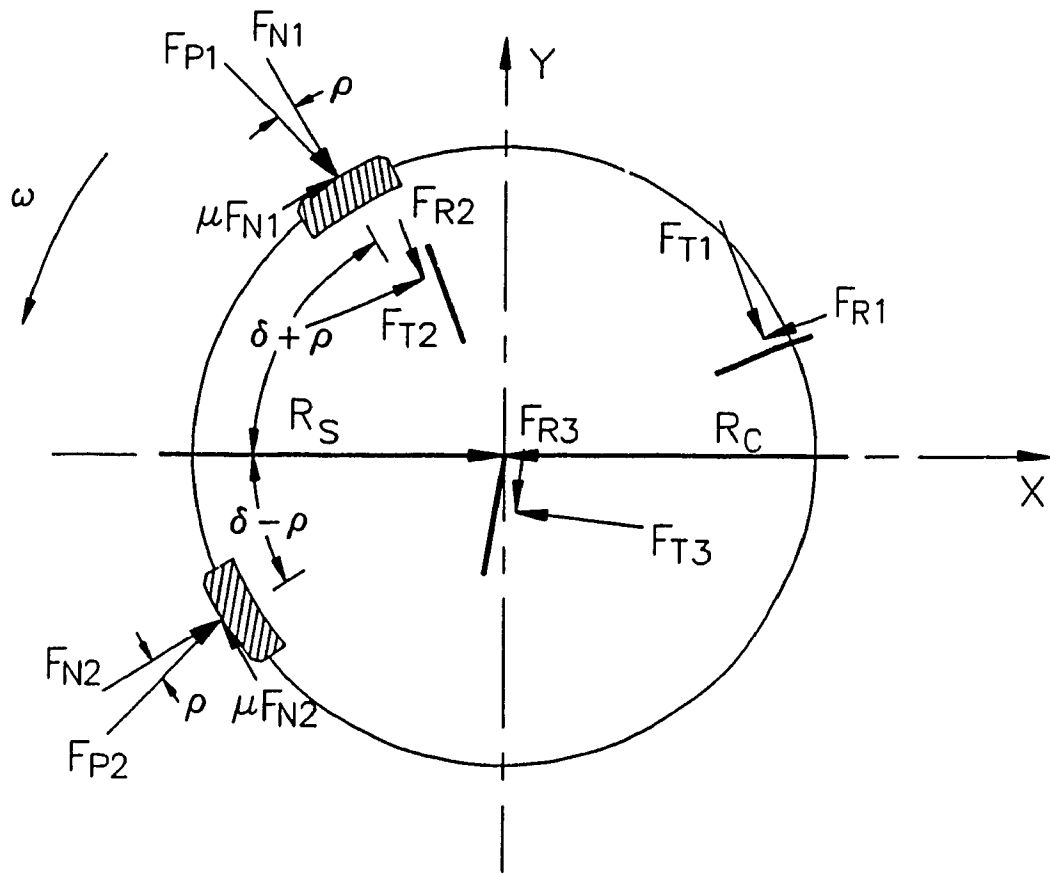


Fig. 3.1 Tool Cutting Force System

tangential components  $\pm 10\%$ .

3. Weber [78] had found that the fluctuation of tangential force in BTA drilling  $\pm 10\%$  with respect to its mean value.
4. Stockert [62] has reported that the variation range for ratio of radial to tangential force component had been found in the range of 0.1-0.2 for a BTA tool of 50.0 mm in diameter.

Based on these reports, the variations of the cutting forces can be found by any analytical methods. Latinovic [3] used the limit method for the worst case to find out the deviations of the cutting force resultant magnitude and direction which are conservative results. Later he has proposed an improved approach using the Monte Carlo simulation which yields a high confidence level provided a large number of replications is used [60]. Torabi [56] used Monte Carlo simulation for three types of BTA cutting tools to find out the variations of resultant cutting force magnitude and direction and variation of magnitude of the guide pads normal forces for purpose of comparison.

In any probabilistic approach the variations of the random parameters which are incorporated into the cutting force equations should be known in order to find the variations of the cutting forces. As it was discussed earlier, the random parameters which vary during machining process are specific cutting forces which originate from the workpiece material, the manufacturing tolerances of the cutters, feed rate, cutting speed and coefficient of friction at the guide pads. Since there is no information available on

the friction coefficient's distribution between the guide pads and the workpiece, the variations of the pad reaction  $F_p$  are assessed by assuming either the worst case an uniform distribution or the general case normal distribution. The variations of the resultant cutting force  $R_c$  which is a function of random parameters such as specific cutting forces and width of cut and the variations of the pad reaction magnitude  $F_p$  which is a function of coefficient of friction is as shown in Fig. 3.2. The variations of the resultant pad reaction is due to variation in magnitude and direction of cutting force resultant as well as variation of friction coefficient at the guide pads. In this chapter the cutting force variations are found out by probabilistic approaches i.e., Linear Statistical Approach and Monte Carlo simulation and the results have been compared in both the methods.

### **3.2 DEVIATION OF THE CUTTING FORCES MAGNITUDE AND DIRECTION**

In this section two methods are discussed for quantifying cutting force uncertainties. The first method uses a Taylor's series expansion to formulate a linear relationship between the random function and the random cutting force parameters. It mainly involves the solution of a system of linear equations and is called the Linear Statistical Approach [79]. The second method is the Monte Carlo simulation which involves the use of a computer, or a programmable hand calculator, and simulates an experiment.



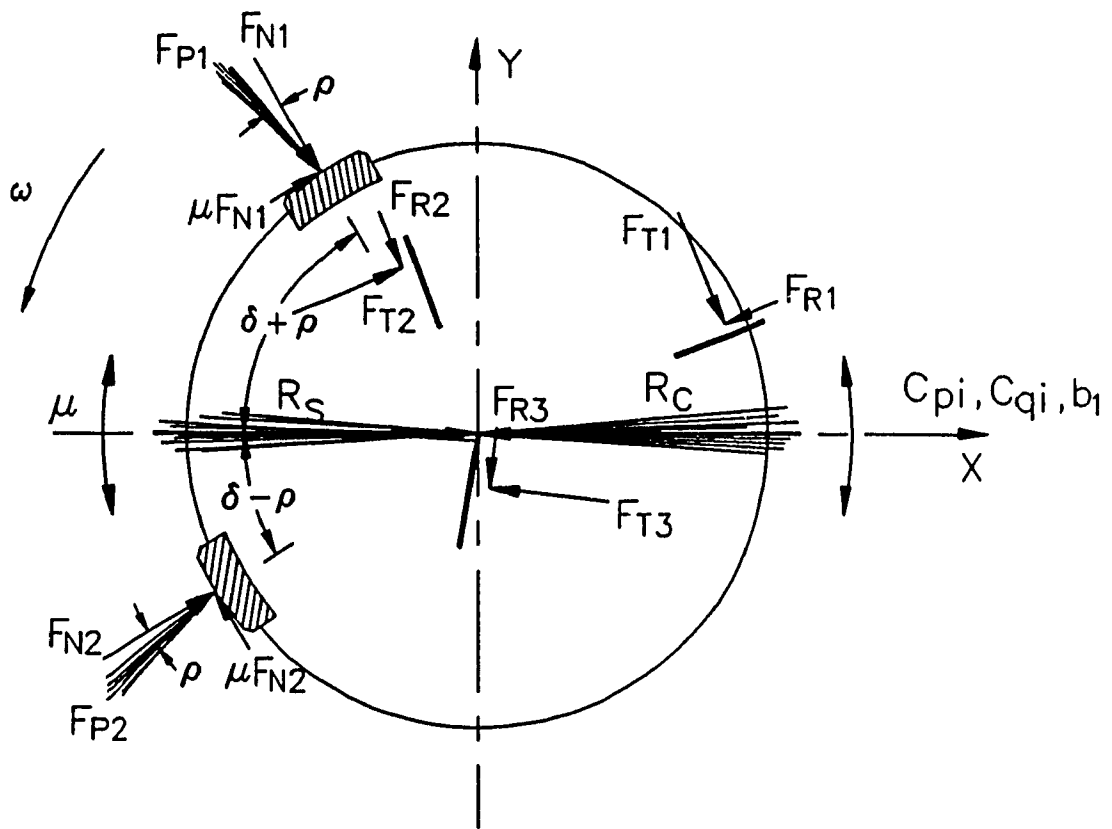


Fig. 3.2 Variations of Resultant Cutting Force and Pad Reactions

### 3.2.1 LINEAR STATISTICAL APPROACH

The statistics of cutting forces which are formulated in this section are based upon a linear statistical model. The mean values and variances of an arbitrary function of  $n$  random variables can be estimated by Taylor's series expansions [79, 80]. This procedure which involves partial derivatives, is easy and doesn't take much computational time. Consider a single function  $y = f(X_1, X_2, X_3, \dots, X_n)$ , where  $X_1, X_2, X_3, \dots, X_n$  are independent random variables that have expected values  $\mu$  which is dependent upon  $n$  random variables  $\mu_{xi}$ , and variances  $V(x_i)$ ,  $[i=1,2,3,\dots,n]$ . To estimate the mean value and standard deviation of function  $y$ , by expanding  $y$  in a Taylor's series about  $\mu_{x1}, \mu_{x2}, \mu_{x3}, \dots, \mu_{xn}$  and it can be written:

$$E(y) = f[E(x_1), E(x_2), E(x_3), \dots, E(x_n)] + \frac{1}{2} \sum_{i=1}^n \frac{\partial^2 y}{\partial x_i^2} [E(x_i) - E(x_i)]^2 \quad (3.1)$$

$$E(y) = f[E(x_1), E(x_2), E(x_3), \dots, E(x_n)] + \frac{1}{2} \sum_{i=1}^n \frac{\partial^2 y}{\partial x_i^2} V(x_i) \quad (3.2)$$

If the value of the second term on the right side in the equation (3.2) is negligible compared to the value of the first term, then

$$E(y) = f[E(x_1), E(x_2), E(x_3), \dots, E(x_n)] \quad (3.3)$$

In order to find the variance by Taylor's series expansion, the variance of the function  $y$  can be written as [79],

$$V(y) = E(y^2) - [E(y)]^2 \quad (3.4)$$

Squaring equation (3.2) yields

$$\begin{aligned} [E(y)]^2 &= [f[E(x_1), E(x_2), \dots, E(x_n)]]^2 \\ &+ [f[E(x_1), E(x_2), \dots, E(x_n)]] \left[ \sum_{i=1}^n \frac{\partial^2 y}{\partial x_i^2} V(x_i) \right] + \left[ \frac{1}{2} \sum_{i=1}^n \frac{\partial^2 y}{\partial x_i^2} V(x_i)^2 \right] \end{aligned} \quad (3.5)$$

To obtain  $E(y^2)$ , square equation (3.2) and take the expected values term by term,

$$\begin{aligned} E(y)^2 &= [f[E(x_1), E(x_2), \dots, E(x_n)]]^2 + \sum_{i=1}^n \left( \frac{\partial y}{\partial x_i} \right)^2 V_i \\ &+ \left[ f[E(x_1), E(x_2), \dots, E(x_n)] \right] \sum_{i=1}^n \frac{\partial^2 y}{\partial x_i^2} V_i \\ &+ \left[ \frac{1}{2} \sum_{i=1}^n \frac{\partial^2 y}{\partial x_i^2} V(x_i)^2 \right] \sum_{i=1}^n \left( \frac{\partial^2 y}{\partial x_i^2} \right) \left( \frac{\partial^2 y}{\partial x_i^2} \right) E[x_i - E(x_i)]^2 \end{aligned} \quad (3.6)$$

The square root of the difference between the equations (3.5) and (3.6) gives the standard deviation of the function  $y$ . If the second and higher order terms are ignored in the equation (3.6) without significant error, then standard deviation of  $y$  can be written as,

$$\sigma_y = \left[ \sum_{i=1}^n \left( \frac{\partial y}{\partial x_i} \right)^2 \sigma_{x_i}^2 \right]^{1/2} \quad (3.7)$$

Equation (3.3) and (3.7) give the estimators of the mean and standard deviation of functions of independent random variables  $X_i$ . A check for accuracy of a linear statistical analysis for a problem where effect of higher-order terms in Taylor's series expansion can be assessed is obtained by a Monte Carlo simulation discussed in the next section.

The random variables such as specific cutting forces  $C_{pi}$ ,  $C_{qi}$  and width of cut of the cutter  $b_i$  are involved in the cutting force equations therefore the mean values of the cutting forces in X and Y directions  $\bar{F}_x$  and  $\bar{F}_y$  respectively and resultant cutting

force magnitude  $\bar{R}_c$  and direction and  $\bar{\lambda}$  can be written as

$$\bar{F}_x = \sum_{i=1}^3 (\bar{C}_{qi} b_i^{x_2} S_i^{y_2} \sin \kappa_i \cos \phi_i - \bar{C}_{pi} b_i^{x_1} S_i^{y_1} \sin \phi_i) \quad (3.8)$$

$$\bar{F}_y = \sum_{i=1}^3 (\bar{C}_{qi} b_i^{x_2} S_i^{y_2} \sin \kappa_i \sin \phi_i + \bar{C}_{pi} b_i^{x_1} S_i^{y_1} \cos \phi_i) \quad (3.9)$$

$$\bar{R}_c = \sqrt{\bar{F}_x^2 + \bar{F}_y^2} \quad \text{and} \quad \bar{\lambda} = \tan^{-1} \left[ \frac{\bar{F}_y}{\bar{F}_x} \right] \quad (3.10)$$

If the second and higher order terms are ignored [79], the variations of the resultant cutting force magnitude can be expressed as

$$\sigma_{R_c} = \left[ \sum_{i=1}^3 \left[ \frac{\partial \bar{R}_c}{\partial C_{pi}} \right]^2 \sigma_{C_{pi}}^2 + \sum_{i=1}^3 \left[ \frac{\partial \bar{R}_c}{\partial C_{qi}} \right]^2 \sigma_{C_{qi}}^2 + \left[ \frac{\partial \bar{R}_c}{\partial b_1} \right]^2 \sigma_{b_1}^2 \right]^{1/2} \quad (3.11)$$

where

$$\frac{\partial \bar{R}_c}{\partial C_{pi}} = \frac{1}{R_c} (\bar{F}_x(-b_i^{x_1} s_i^{y_1} \sin \phi_i) + \bar{F}_y(b_i^{x_1} s_i^{y_1} \cos \phi_i)) \quad (3.12)$$

$$\begin{aligned} \frac{\partial \bar{R}_c}{\partial C_{qi}} = \frac{1}{R_c} (\bar{F}_x (b_i^{x_2} s_i^{y_2} \sin \kappa_i \cos \phi_i) \\ + \bar{F}_y (b_i^{x_2} s_i^{y_2} \sin \kappa_i \sin \phi_i)) \end{aligned} \quad (3.13)$$

$$\begin{aligned} \frac{\partial \bar{R}_c}{\partial b_1} = \frac{1}{R_c} (\bar{F}_x(\bar{C}_{qi} s_1^{y_2} \sin \kappa_1 \cos \phi_1 - \bar{C}_{p1} s_1^{y_2} \sin \phi_1) \\ + \bar{F}_y(\bar{C}_{qi} s_1^{y_2} \sin \kappa_1 \sin \phi_1 + \bar{C}_{p1} s_1^{y_1} \cos \phi_1)); x_2 b_1^{x_2-1} = 1 \text{ for } x_2=1 \end{aligned} \quad (3.14)$$

Similarly by neglecting the higher order terms, the deviation of the resultant cutting force direction can be expressed as

$$\sigma_\lambda = \left[ \sum_{i=1}^3 \left( \frac{\partial \bar{\lambda}}{\partial C_{pi}} \right)^2 \sigma_{C_{pi}}^2 + \sum_{i=1}^3 \left( \frac{\partial \bar{\lambda}}{\partial C_{qi}} \right)^2 \sigma_{C_{qi}}^2 + \left( \frac{\partial \bar{\lambda}}{\partial b_1} \right)^2 \sigma_{b_1}^2 \right]^{1/2} \quad (3.15)$$

Where

$$\frac{\partial \bar{\lambda}}{\partial C_{pi}} = \frac{1}{(\bar{F}_x^2 + \bar{F}_y^2)} (\bar{F}_x(-b_i^{x_1} s_i^{y_1} \sin \phi_i) - \bar{F}_y(b_i^{x_1} s_i^{y_1} \cos \phi_i)) \quad (3.16)$$

$$\frac{\partial \bar{\lambda}}{\partial C_{qi}} = \frac{1}{(\bar{F}_x^2 + \bar{F}_y^2)} (\bar{F}_x(b_i^{x_2} s_i^{y_2} \sin \kappa_i \cos \phi_i) - \bar{F}_y(b_i^{x_2} s_i^{y_2} \sin \kappa_i \sin \phi_i)) \quad (3.17)$$

and

$$\frac{\partial \bar{\lambda}}{\partial b_1} = \frac{1}{(\bar{F}_x^2 + \bar{F}_y^2)} (\bar{F}_x (\bar{C}_{qi} s_1^{y_i} \sin \kappa_i \sin \phi_i + \bar{C}_{pi} s_1^{y_i} \sin \phi_i) - \bar{F}_y (\bar{C}_{qi} s_1^{y_i} \sin \kappa_i \cos \phi_i - \bar{C}_{pi} s_1^{y_i} \cos \phi_i)); \quad x_2 b_1^{x_2-1} = 1 \text{ for } x_2 = 1 \quad (3.18)$$

where  $i = 1, 2, 3$

In the same way the deviations of the cutting forces in X and Y directions can be written as

$$\sigma_{F_x} = \left[ \sum_{i=1}^3 \left( \frac{\partial \bar{F}_x}{\partial C_{pi}} \right)^2 \sigma_{C_{pi}}^2 + \sum_{i=1}^3 \left( \frac{\partial \bar{F}_x}{\partial C_{qi}} \right)^2 \sigma_{C_{qi}}^2 + \left( \frac{\partial \bar{F}_x}{\partial b_1} \right)^2 \sigma_{b_1}^2 \right]^{1/2} \quad (3.19)$$

and

$$\sigma_{F_y} = \left[ \sum_{i=1}^3 \left( \frac{\partial \bar{F}_y}{\partial C_{pi}} \right)^2 \sigma_{C_{pi}}^2 + \sum_{i=1}^3 \left( \frac{\partial \bar{F}_y}{\partial C_{qi}} \right)^2 \sigma_{C_{qi}}^2 + \left( \frac{\partial \bar{F}_y}{\partial b_1} \right)^2 \sigma_{b_1}^2 \right]^{1/2} \quad (3.20)$$

where

$$\frac{\partial \bar{F}_x}{\partial C_{pi}} = -b_i s_i^{y_i} \sin \phi_i \quad (3.21)$$

$$\frac{\partial \bar{F}_x}{\partial C_{qi}} = b_i s_i^{y_i} \sin \kappa_i \cos \phi_i \quad (3.22)$$

$$\frac{\partial \bar{F}_y}{\partial b_1} = c_q s_1^{y_1} \sin \kappa_1 \cos \phi_1 - c_p s_1^{y_1} \sin \phi_1; \quad x_2 b_1^{x_2-1} = 1 \text{ for } x_2 = 1 \quad (3.23)$$

$$\frac{\partial \bar{F}_Y}{\partial C_{pi}} = -b_i s_i^{y1} \cos \phi_i \quad (3.24)$$

$$\frac{\partial \bar{F}_Y}{\partial C_{qi}} = b_i s_i^{y2} \sin \kappa_i \sin \phi_i \quad (3.25)$$

$$\frac{\partial \bar{F}_Y}{\partial b_1} = c_q s_1^{y2} \sin \kappa_1 \sin \phi_1 + c_p s_1^{y1} \cos \phi_1; \quad x_2 b_1^{x_2-1} = 1 \text{ for } x_2 = 1 \quad (3.26)$$

where  $i=1,2,3$

It is to be noted that in all the above expressions when  $i = 1$ , the width of cut of the outer cutter can be written as  $\bar{b}_1$ . This is the most popular technique, in which the variations of any function which involves independent random parameters can be found without going for simulation. The upper and lower limits of the cutting forces in X and Y directions and resultant cutting force magnitude and direction can be found by using the relations,  $\bar{F}_x \pm 3\sigma_{F_x}$ ,  $\bar{F}_y \pm 3\sigma_{F_y}$ ,  $\bar{R}_C \pm 3\sigma_{R_C}$  and  $\bar{\lambda} \pm 3\sigma_{\lambda}$  respectively.

### 3.2.2 MONTE CARLO SIMULATION

Monte Carlo analysis is a powerful engineering tool by which one can perform a statistical analysis of the confidence level (or uncertainty) in engineering problems. It

is particularly useful for complex problems where numerous random variables are related through nonlinear equations. This method is very helpful to visualize as an experiment which is performed by a computer rather than in a laboratory. The main drawback of this method is that it takes a considerable amount of computational time for good accuracy.

The basic step in Monte Carlo simulation is the generation of a set of random numbers which can be generated either numerically or electronically. However, most random number generation is accomplished by digital computers. The magnitude of cutting forces in X and Y directions and magnitude and direction of resultant cutting force are found by repeating large number of replications in random manner by a standard software available from the computer subroutines library.

Further, the variation range of the magnitude of cutting forces in X and Y directions and magnitude and direction of resultant cutting force are obtained. The mean values of the cutting forces calculated this way are given in the Table 3.1 and the deviations obtained by the Linear Statistical Approach and Monte Carlo method are given in Table 3.2. The variations obtained by Monte Carlo method are calculated for 1000 to 30000 replications and can be seen in Table 3.2. The probability density functions of the cutting forces for 30000 replications are shown in Fig. 3.3 to 3.6. These variations of the cutting forces are verified with Linear Statistical Approach and they are in good agreement with Monte Carlo method. Since this method needs random number generator, it takes lot of



computational time for larger number of replications. The Monte Carlo method takes more CPU time than Linear Statistical Approach and that is its major disadvantage.

Table 3.1 Mean values of the cutting forces

Mean values of the cutting forces	Cutting force magnitude in X-direction [kN] $\bar{F}_x$	Cutting force magnitude in Y-direction [kN] $\bar{F}_y$	Resultant cutting force magnitude [kN] $\bar{R}_c$	Resultant support reaction force magnitude [kN] $\bar{R}_s$	Resultant cutting force direction [deg] $\bar{\lambda}$
	3.4414025	9.6559E-06	3.441402	3.4414583	1.607E-04

### 3.3 VARIATION OF PAD REACTION

The forces acting on the pads are shown in Fig. 3.1. The bore wall is rubbed and burnished by these pads. The problem involved in such a complex force system, was first studied by Gorski [81] to resolve the problem he suggested use of friction coefficient at the pads to model the forces. The same approach has been subsequently adopted by Greuner [25], Stockert [62], Weber [78], Pflighar [82], Streicher [83], Osman et al [33, 61], Latinovic [3], Chandrashekar [50], Torabi [56], and Gessesse [1]. The same concept has been used in this analysis.

According to Gorski [81] the radial and tangential reactions are function of tangential friction coefficient  $\mu$  at the guide pads and workpiece and can be written as

Table 3.2 Deviations of the cutting forces

	Linear Statistical Approach	Monte Carlo Method						
		1000 Replications	5000 Replications	10000 Replications	15000 Replications	20000 Replications	25000 Replications	30000 Replications
Deviation in X-direction $\sigma_{F_x}$ (kN)	0.169006095	0.170811	0.169938	0.1678010	0.168818	0.167542	0.168116	
Deviation in Y-direction $\sigma_{F_y}$ (kN)	0.132510673	0.127137	0.132263	0.130650	0.1317490	0.130523	0.129958	
Deviation of Resultant cutting force magnitude $\sigma_{R_c}$ (kN)	0.169005978	0.166050	0.170701	0.169850	0.1676150	0.167433	0.168005	
Deviation of Resultant Cutting force direction $\sigma_{\lambda}$ (deg)	2.206066433	2.133281	2.209044	2.180001	2.203737	2.178159	2.169659	

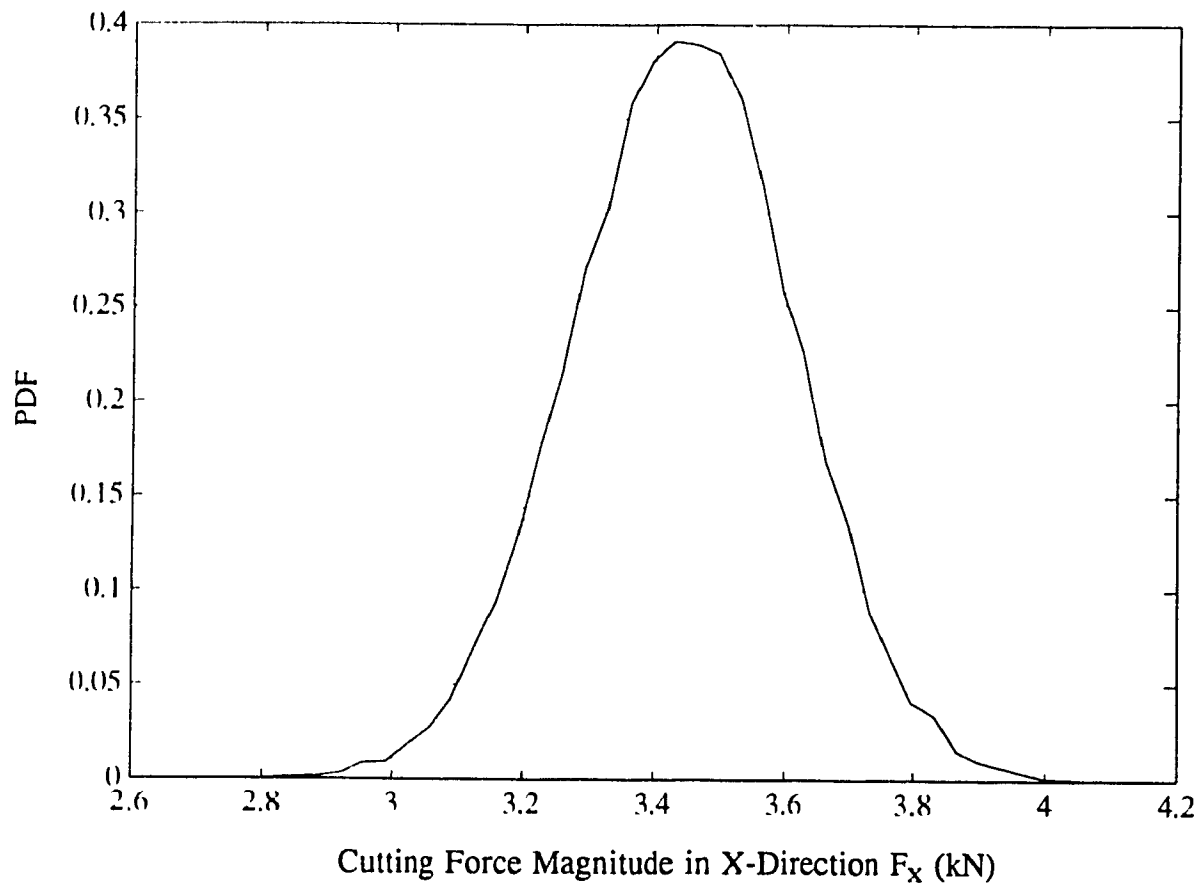


Fig. 3.3 PDF of Cutting Force Magnitude in X-Direction for 30000 Replications

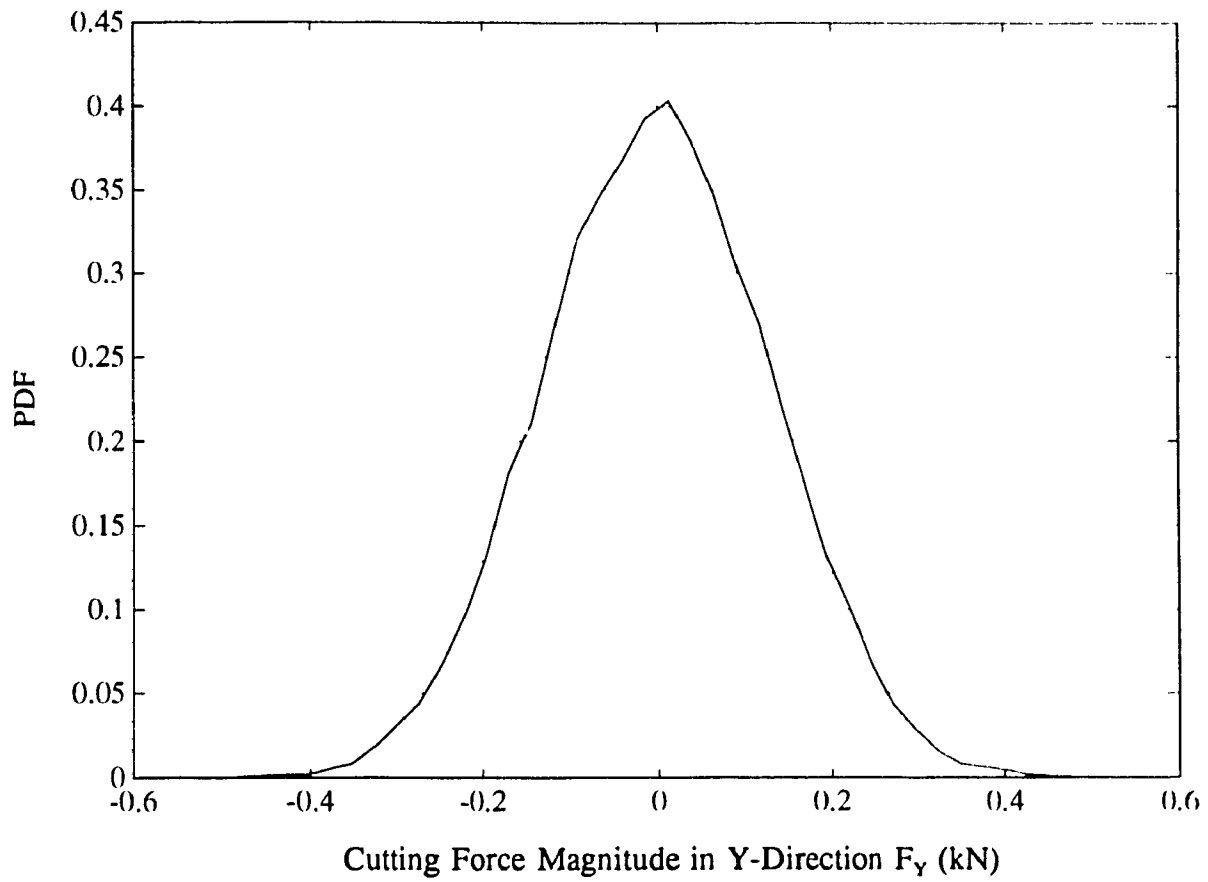


Fig. 3.4 PDF of Cutting Force Magnitude in Y-Direction for 30000 Replications

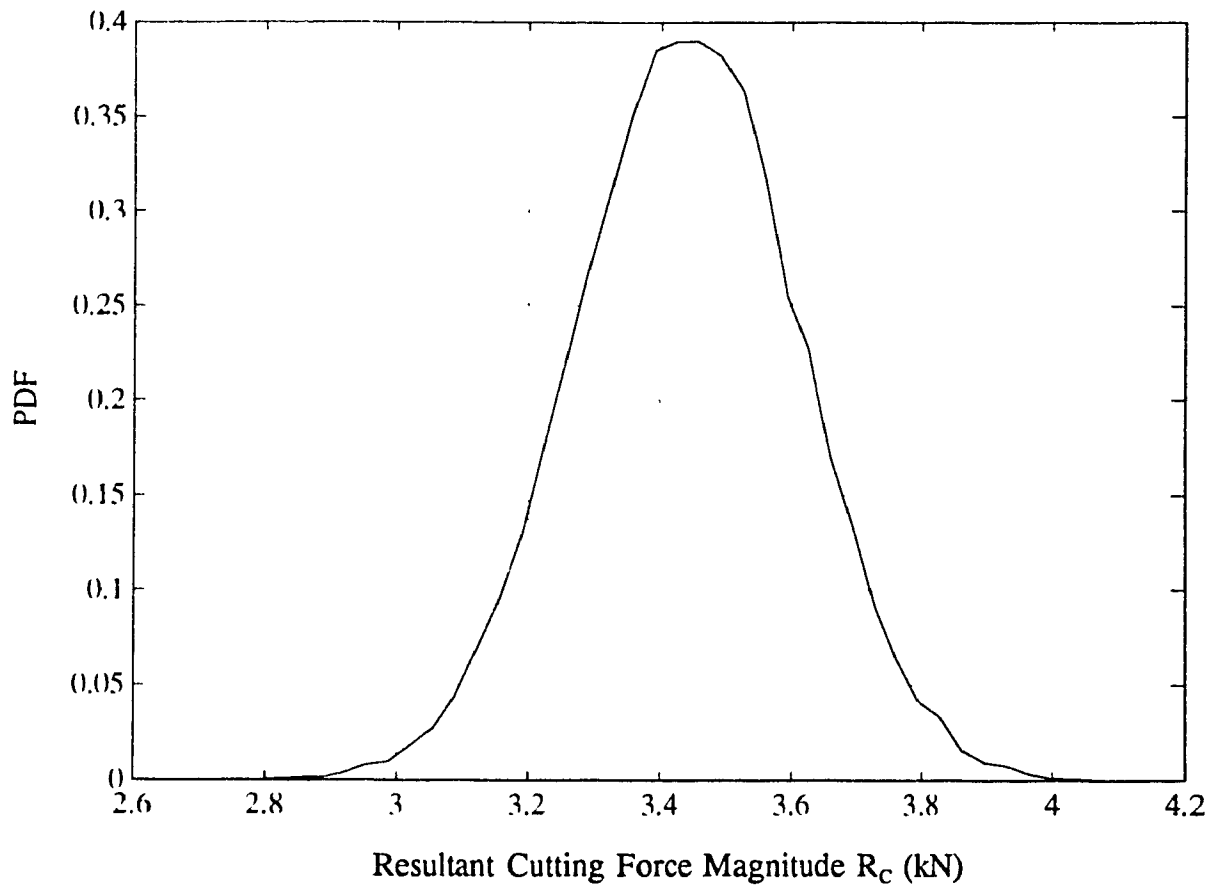


Fig. 3.5 PDF of Resultant Cutting Force Magnitude for 30000 Replications

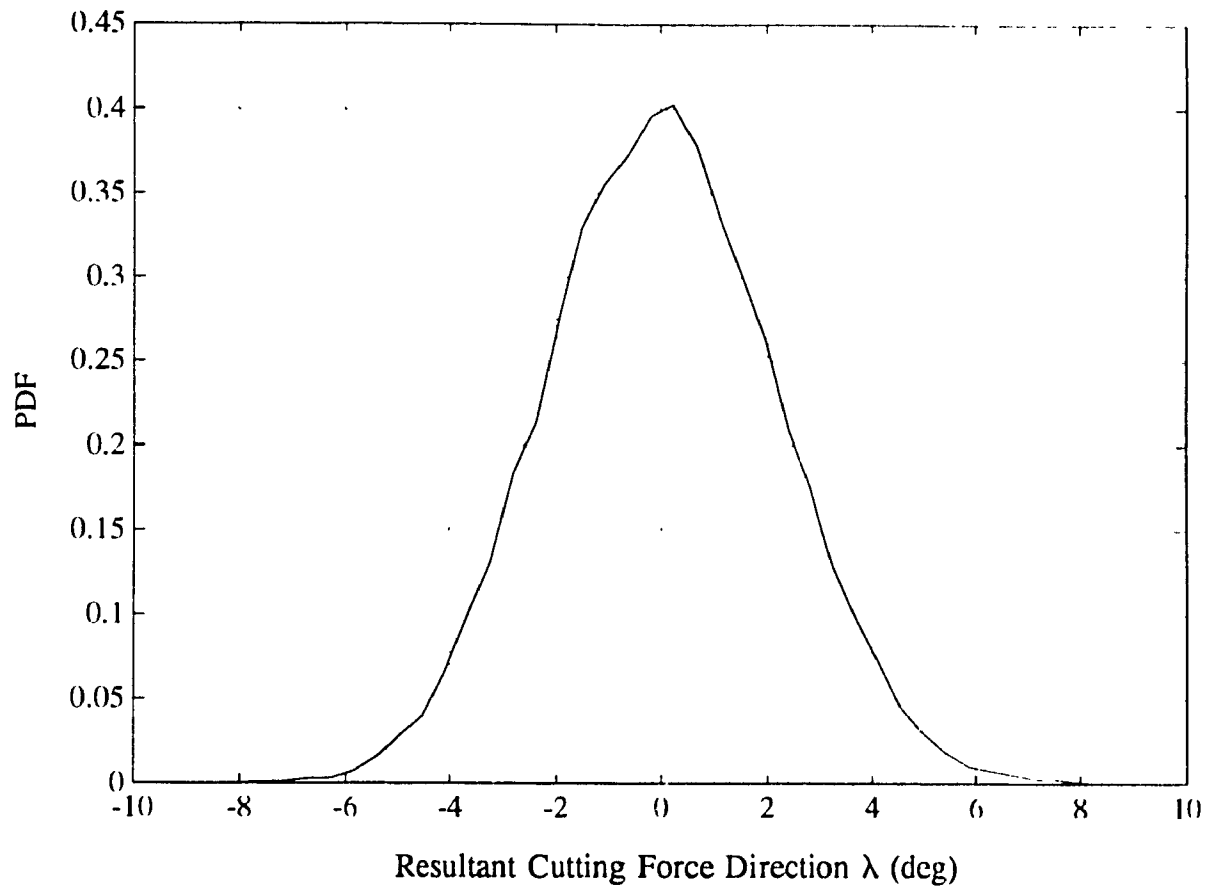


Fig. 3.6 PDF of Resultant Cutting Force Direction for 30000 Replications

$$\mu_i = \frac{F_{Ti}}{F_{Ni}} \quad \text{where } i = 1, \dots, n \quad (3.27)$$

where  $F_{Ti}$ , and  $F_{Ni}$  are pads tangential and normal forces respectively and  $n$  is pad number. From Fig. 2.1 (d) the pad's resultant reaction can be written as

$$F_{Pi} = F_{Ni} (1 + \mu_M^2)^{1/2} \quad (3.28)$$

where  $\mu_M$  is the mean value of the pad coefficient of friction. From Fig. 2.1 (d) the pad normal force can be written as

$$F_{Ni} = \frac{R_{Ci}}{2\sqrt{(1 + \mu_i^2)} \cos \delta} \quad (3.29)$$

where  $R_{Ci}$  is the resultant cutting force and  $\mu_i$  is the friction coefficient,  $\delta$  is the pads included angle and  $i$  designates the replication. By substituting equation (3.29) in equation (3.28) we get

$$F_{Pi} = \frac{R_{Ci}}{2\sqrt{1 + \mu_i^2} \cos \delta} \sqrt{1 + \mu_M^2} \quad (3.30)$$

In order to find the variations of the pad reaction  $F_P$ , it is essential to know the distribution of the parameters incorporated in equation (3.30). It has been discussed that the cutting forces in the deep-hole machining process follow normal distribution [22-25,30,50,67,68,76]. Based on this fact the magnitude and variation of the cutting forces in X and Y directions and magnitude and direction of the resultant cutting force were calculated. The pad reactions vary during machining process because of change of the pads normal and tangential forces at the guide pads. From equation (3.27) it can be seen that the pads normal and tangential forces are function of coefficient of friction. It is

important to know the variation range and distribution of the friction coefficient at the guide pads. Few researchers reported the variation range of the tangential friction coefficient but no information was given about the type of distribution it follows.

Griffiths [66] found that the tangential friction coefficient  $\mu$  depends on feed rate and it decreases as feed increases. The conventional Coulomb friction coefficient remain constant irrespective of the normal force, but its value is heavily dependent on contact surface condition. Greuner [25] found that the coefficient of friction on BTA solid tool ranges from 0.2 to 0.29 for a carbide pad when drilling a steel (C60) workpiece. Weber [78] found that the coefficient of friction varies from 0.2 to 0.39 and Pfléghar [82] reported that for 0.22 to 0.28 for gundrilling. Griffiths [66] has suggested values in the range 0.13 to 0.27 which compare very favourably with other workers who drilled similar steels. However no information is available what type of distribution the tangential friction coefficient  $\mu$  at the guide pads follows during machining of a hole.

The variation range of pad reaction can be calculated by using the equation (3.30). Since the cutting forces in the deep-hole machining process follow normal distribution, a normal distribution can be assumed for coefficient of friction, to find out the variations of pad reactions. However it makes more sense to assume the worst case which will render conservative solution which is the uniform distribution. Both cases were simulated and the probability density function was plotted for pad reactions shown in Fig. 3.7. Numerical values for the standard deviations were found for the uniform



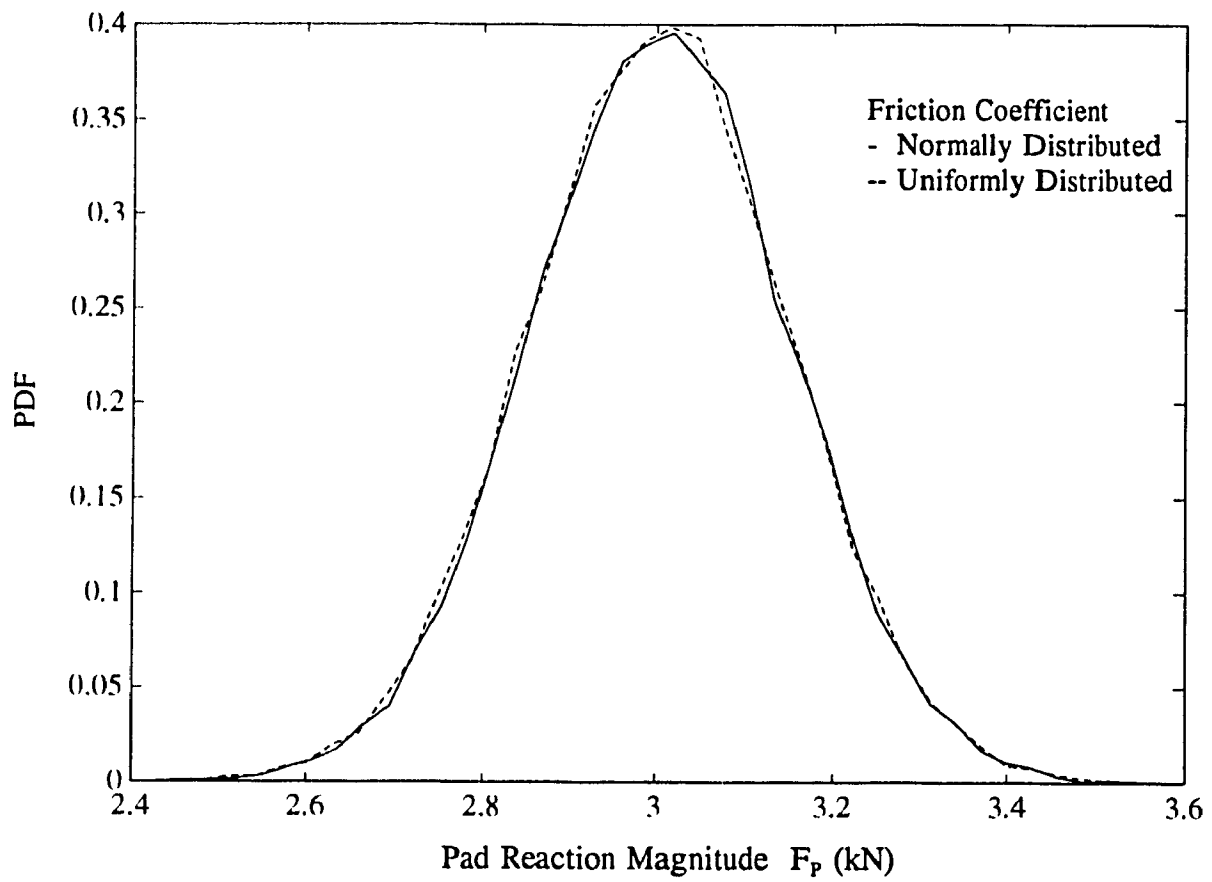


Fig. 3.7 PDF of Pad Reaction Magnitude for 30000 Replications

distribution and normal distribution 0.148158 kN and 0.146641 kN respectively. This reveals that there is an insignificant difference between the two and that normal distribution can be used safely. The upper and lower limits of the pads reaction force can be calculated by using the relation  $\bar{F}_p \pm 3\sigma_{F_p}$ .

### 3.4 CONCLUSIONS

The variations in magnitude of cutting forces in X and Y directions as well as variations in magnitude and direction of the resultant cutting force are found by two probabilistic approaches. First the variations of the cutting forces are found by Linear Statistical Approach and these are verified by Monte Carlo simulation to show that they are in good agreement. From Table 3.2 it can be seen that the results are in very good agreement when the replication size in Monte Carlo simulation is 10000. The PDF of resultant cutting force magnitude for different number of replications are shown in Appendix-B and it can be observed from the figures that the higher the number of replications the smoother the curve resulted. However, the numerical values of standard deviation are practically unaffected. The Monte Carlo method is time consuming and needs higher number of replications for better accuracy, and smoother probability density functions. For convenience, the resultant cutting force has been chosen to be in horizontal direction. The variation of the resultant cutting force magnitude is approximately equal to the variation of the cutting force in X-direction. Though the mean value of the cutting force

in Y-direction is zero, it has non zero variations. However, the resultant cutting force direction varies within the limits of pads included angle which is important for the tool guidance, and static stability. Despite the lack of information on friction coefficient's distribution at the guide pads, the variations of pad reactions are predicted by Monte Carlo simulation by assuming for convenience normal distribution and the worst case an uniform distribution. It can be seen from Fig. 3.7 that in the PDF curves for friction coefficient normally distributed and uniformly distributed do not differ to any significant extend. For simplicity the distribution for friction coefficient can be assumed normal for future analysis, though there is no experimental evidence to confirm this assumption. The magnitude fluctuation of the cutting force resultant and pad reactions is about  $\pm 14.66\%$ . Though the magnitude fluctuations of tangential and radial cutting forces at the cutters are 10% [77], the magnitude variation of resultant cutting force is slightly higher, what is expected. This still leaves about 85% of the mean cutting force resultant for tool support and guidance. Since the magnitude fluctuation of cutting force resultant and pad reactions are equal, the resultant cutting force is always balanced by the resultant pad support reaction. Moreover, this also proves the condition that the magnitude variations of resultant pad reaction is dependent on the variations of the cutting force resultant, in both the magnitude and the direction.

## **CHAPTER 4**

### **STABILITY ANALYSIS OF CUTTING TOOL-BORING BAR IN DEEP-HOLE MACHINING**

#### **4.1 INTRODUCTION**

Since it does not seem feasible to incorporate the conditions of dynamic instability into the design procedure to achieve optimal tool lay outs, the system instability must be considered separately. Basically there are three applications of BTA deep-hole machining system depending upon the workpiece shape and hole size. They are stationary tool-rotating workpiece, rotating tool-stationary workpiece and rotating tool-rotating workpiece. Stationary tool-rotating workpiece system is the most common method for drilling long cylindrical workpieces where the difference between the diameter of the workpiece and the hole being produced is not large. Extremely straight holes can be expected in this application. Rotating tool-stationary workpiece system is used for drilling cylindrical as well as unsymmetrical workpieces of any shape not convenient for rotation. Rotating tool-rotating workpiece system is used whenever straightness requirements are of a prime concern and the workpiece can be rotated. This application gives best accuracy of the holes as compared to the previous two.

In stationary cutting tool and rotating workpiece system the cutting tool-boring bar assembly is subjected to transverse vibrations because of dynamic characteristics of

cutting forces. Gessesse et al [52] and Sakuma et al [84] have investigated the frequency of lateral vibration of the cutting tool-boring bar system. Both assumed that the boundary conditions at the cutting tool - workpiece interface are not affected by force unbalance and static stability of the cutting tool. Pfleghar [55] proposed static stability analysis in deep-hole machining and he concluded that 3 modes of static stability can occur during machining process. In this analysis boundary conditions at the cutting tool-workpiece contact are studied, since the cutting tool edge subjects to a variety of boundary conditions depending on the modes of static stability of the cutting tool during hole-making process. Besides the cutting forces acting on the cutting edges, there are pads' reactions at the guide pads as shown in Fig. 4.1 and as already stated these reactions play an important role in hole quality, cutting tool's guidance and stability. An unstable cutting tool produces a bad surface finish and a poor operating condition which will lead to the quick breakage of the cutting tool. In order to ensure that the designed cutting tool is stable, it has to satisfy certain stability criteria, both static and dynamic stability. Static stability involves the study of the cutting tool guidance, the forces at the cutting edges as well as at the guide pads, whereas dynamic stability involves the study of the instability caused by the system vibrations. Gessesse et al [52] has conducted an experimental study of the dynamic stability of the cutting tool-boring bar system and its effect on hole quality. This study considers different boundary conditions which can occur in actual practice. The analysis concerns with the identification of such boundary conditions and vibrating modes yielded by these conditions.

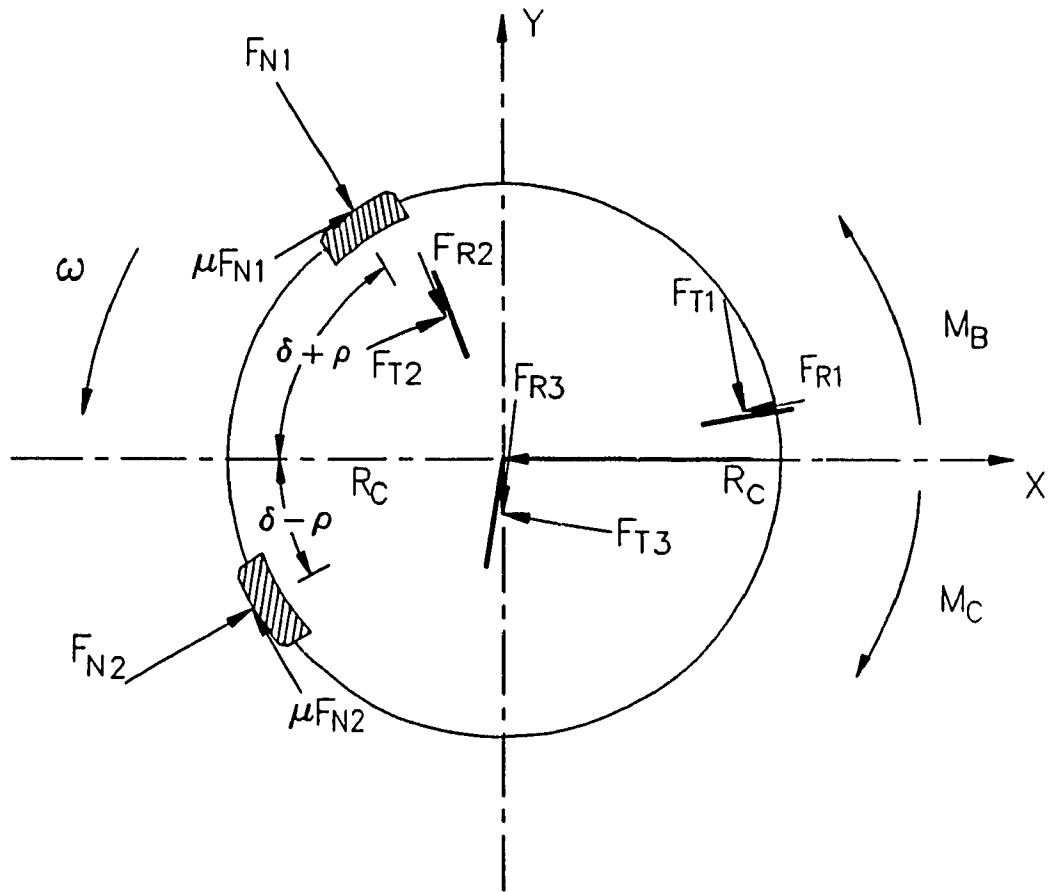


Fig. 4.1 Tool Force System

## 4.2 STATIC STABILITY ANALYSIS

Static stability analysis in deep-hole machining was first carried out by Pflagher [55]. The forces generated during machining process at the cutting edges as well as at the guide pads fluctuate randomly because of variations in the cutting parameters and friction coefficient at the guide pads. In order to maintain tool stability and acceptable hole quality, the resultant cutting force should be balanced by the total support reactions through out the machining process. For tool stability the direction of resultant of pads' reactions should always bisect the included angle of the pads. The support reaction acting on each of the pads depends on both the magnitude and the direction of the resultant cutting force, and the pads included angle. The limits allowed for included angle of the supporting pads are established by experience at  $90^\circ$  and  $110^\circ$ . But the maximum pads included angle of  $98^\circ$  is usually recommended. One of the guide pad should be placed nearly opposite to the outer cutter in order to control the hole size. Latinovic and Osman [60] and Latinovic et al [61] developed staggered and unsymmetrical multi edge cutting tools with a predetermined resultant cutting force magnitude and direction, where the principle that the resultant support reaction bisects the pads included angle is used in the tool design. The problem arises from the fact that the resultant of the two pad reactions does not completely satisfy the equilibrium condition for the static moment of the two pads reactions and the cutting force resultant. This non-zero moment may cause an instability of the tool.

Pfleghar [55] used this moment as a criteria for the stability of the tools, subjected to cutting forces as well as pad reactions. Based on his formulation, the degree of stability for both pads may be written as

$$S_i = \frac{M_{hi}}{M_{ti}} \quad \text{where } i=1,2 \quad (4.1)$$

Where  $S_i$  is the degree of stabilities of the guide pads,  $M_{hi}$  is called holding moment and  $M_{ti}$  is called tilting moment. From Fig. 4.1 the cutting moment  $M_C$  about the centre of the boring head is given by

$$M_C = F_{T1} \left( \frac{b_1}{2} + b_2 + b_3 \right) + F_{T2} \left( \frac{b_2}{2} + b_3 \right) + F_{T3} \left( \frac{b_3}{2} \right) \quad (4.2)$$

The driving moment  $M_B$  which opposes the moments of forces from the cutters and reactions from the guide pads can be written as

$$M_B = M_C + (\mu F_{N1} + \mu F_{N2}) (d/2) \quad (4.3)$$

In order to have good stability the resultant cutting force  $R_C$  should always bisect the included angle of the guide pads. Hence the holding moment  $M_{h1}$  and tilting moment  $M_{t1}$  with respect to guide pad 1 can be written as

$$M_{h1} = M_C + R_C (d/2) \sin(\delta + \rho) \quad (4.4)$$

$$M_{t1} = M_N + F_{N2} (d/2) \sin 2\delta \quad (4.5)$$

Similarly for guide pad 2 the holding moment  $M_{h2}$  and tilting moment  $M_{t2}$  can be found by writing moments about the guide pad 2

$$M_{h2} = (F_{N1} + F_{N2}) (d/2) \mu + R_C (d/2) \sin(\delta - \rho) \quad (4.6)$$

$$M_{t2} = F_{N1} (d/2) [\sin 2\delta + \mu (1 - \cos 2\delta)] \quad (4.7)$$



The overall degree of stability  $S$  of the tool constitutes a smaller of the  $S_1$  and  $S_2$  which is responsible for tool instability. Thus the critical degree of stability of the tool  $S$  is

$$S = S_1 \text{ if } S_1 < S_2; \text{ and } S = S_2 \text{ if } S_2 < S_1$$

The type of equilibrium can be determined by the value of degree of stability as follows

Stable equilibrium:  $S > 1.0$

Indifferent equilibrium:  $S = 1.0$

Unstable equilibrium:  $S < 1.0$

The degree of stability  $S$  greater than one indicates that the resultant pad force swings between the two pads. Indifferent equilibrium, i.e.,  $S$  equal to unity, indicates that one of the pad force is zero and resultant reaction force passes through the other pad. Practically this is not a good balance, because under dynamic conditions the tool could undergo unstable behaviour. The factors that could lead to instability of tool are random variation of parameters that are affecting the cutting forces and pads reactions. Finally, if the degree of stability is less than one, the tool is not supported. For a reasonable hole quality and statically stable cutting tool, the degree of stability should always be greater than one.

A high degree of stability depends on condition of the cutting edge, the location and partition of the cutting edges and location of the guide pads. A high degree of stability indicates stable support of cutting head against the bore wall. Pflgar [55] has conducted experiments with various tools of different positions of guide pads and showed that tools with high degree of stability perform better. Such tools produce bores of

higher quality. Furthermore he found that maximum degree of stability can be obtained when the difference in pads position angle is about  $90^0$ . Torabi [56] developed a staggered multi edge cutting tool which has a degree of stability of 1.26 and Gessesse [1] showed that a commercially available solid boring tool with single cutting edge has a degree of stability of 1.68.

#### **4.3 MATHEMATICAL MODELING OF THE CUTTING TOOL-BORING BAR SYSTEM'S DYNAMICS**

During machining process, depending upon the degree of stability  $S$ , the boring bar with the cutting tool attached to it can be considered subjected to different end conditions. A mathematical model of the cutting tool-boring bar system is proposed based on the following factors:

- The boring bar is considered as a continuous beam clamped at the bar driver with the stiffness at this end being infinite.
- An intermediate support is given to the boring bar by the pressure head and proper type of stuffing box is provided at this contact. Hence a simple support conditions are assumed at this contact.
- Since the tool floats at the guide pads, different end conditions such as a simple end, clamped end or free end conditions can be assumed, provided the work-piece is sufficiently rigid to ignore its deflection at the cutting edge.
- The damping effect at the cutting edges and the guide pads is ignored at this

stage, since it would require much more effort and extended research to account for it.

The cutting tool-boring bar system now can be considered as multi-span beam shown in Fig. 4.2. Transverse vibrations of multi-span beams have been studied by numerous authors [85-88]. Accordingly the transverse vibrations of the boring bar in the X-Y plane which is assumed to be a plane of symmetry for any cross-section can be formulated. When the boring bar undergoes free vibrations, the governing differential equations are given by

$$EI \frac{\partial^4 u_i}{\partial X^4}(X,t) + \frac{\gamma A}{g} \frac{\partial^2 u_i}{\partial t^2}(X,t) = 0, \quad i=1,2 \quad (4.8)$$

where  $EI$  is the flexural rigidity,  $\gamma$  is the specific weight,  $A$  is the area of cross-section,  $u_1(X,t)$  and  $u_2(X,t)$  are the deflections of the centre lines of the left and right portions of the boring bar,  $X$  denotes the length coordinate, and  $t$  is the time. A solution  $u_i(X,t)$  is sought by commonly used variable separation method in a form of

$$u_i(X,t) = \xi_i(X) q(t) \quad i=1,2 \quad (4.9)$$

Substitution of equation (4.9) in equation (4.8) results the following differential equations:

$$\xi_i''''(X) - \beta^4 \xi_i(X) = 0, \quad i=1,2 \quad (4.10)$$

$$\text{and } \ddot{q}(t) + \omega^2 q(t) = 0 \quad (4.11)$$

$$\text{where } \beta^4 = \omega^2 L^4 \gamma A / (EIg) \quad (4.12)$$

The general solutions of the ordinary differential equations (4.10) and (4.11) are given by

$$\xi_1(X) = A_1 \cosh\beta X + B_1 \sinh\beta X + C_1 \cos\beta X + D_1 \sin\beta X \quad (4.13)$$

$$\xi_2(X) = A_2 \cosh\beta X + B_2 \sinh\beta X + C_2 \cos\beta X + D_2 \sin\beta X \quad (4.14)$$

$$q(t) = P \cos \omega t + Q \sin \omega t \quad (4.15)$$

The constants  $A_1, B_1, C_1, D_1, A_2, B_2, C_2,$  and  $D_2,$  given in equations (4.13) and (4.14) need to be calculated by prescribing different boundary conditions at bar holder, pressure head support and cutting edge tool contact and the constants  $P$  and  $Q$  given in equation (4.15) can be evaluated from the initial conditions.

#### 4.4 FREQUENCY ANALYSIS OF THE CUTTING TOOL-BORING BAR

Depending upon the degree of stability by Pflgar at the guide pads, the frequency analysis of the cutting tool-boring bar assembly can be classified into three different cases. In the first case, both guide pads are supported and the end conditions at the cutting edge can be considered clamped end as shown in Fig. 4.2. This type of stability occurs when the resultant reaction force swings between the pads included angle and the outer cutter is located opposite to one of the guide pads. The boundary conditions assumed at the cutting tool-workpiece interaction during stable equilibrium are clamped end conditions and they are given in Table 4.1.

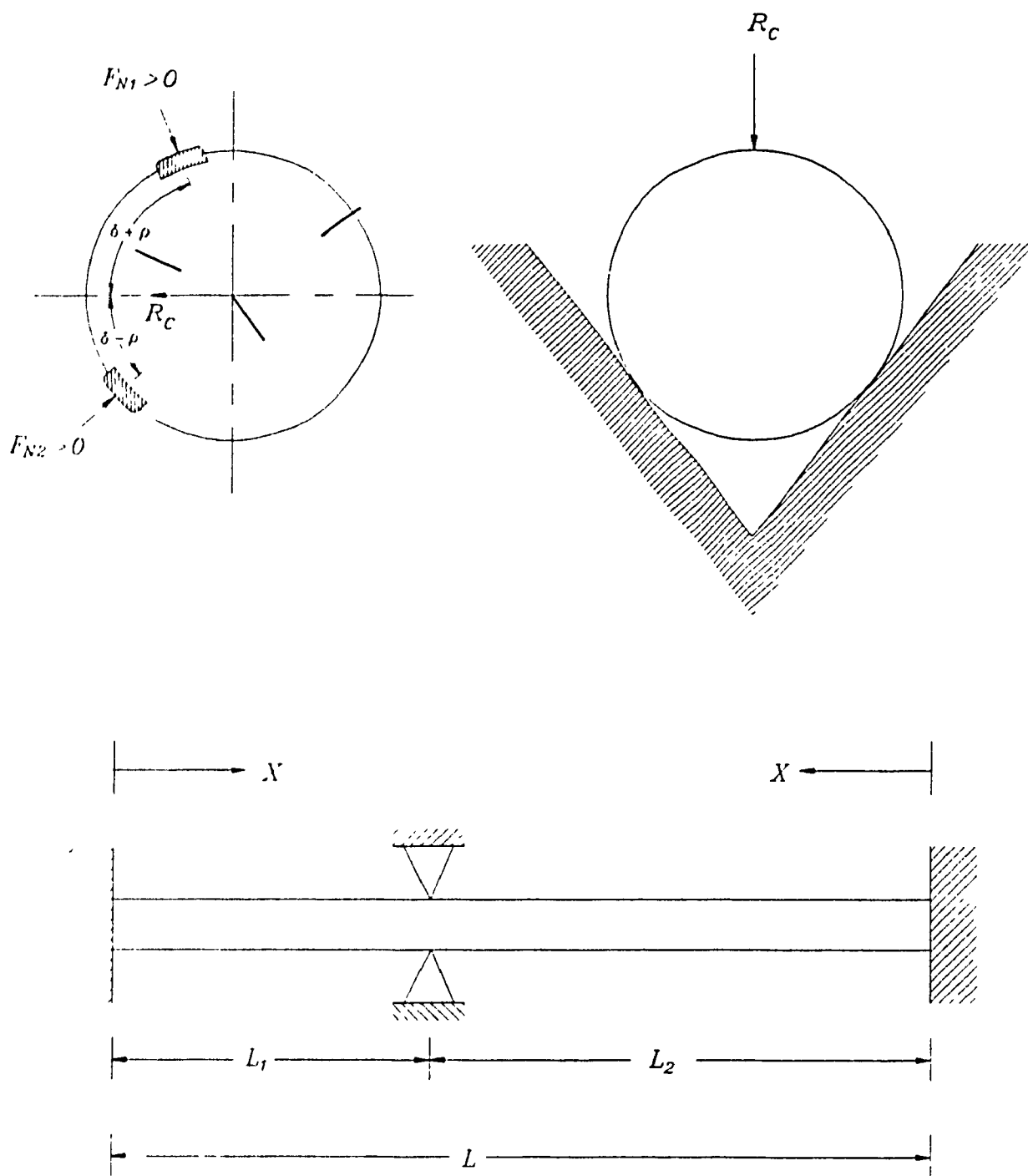


Fig. 4.2 Model of Cutting Tool-Boring Bar Assembly at Stable Equilibrium

Table 4.1 Clamped-Clamped with intermediate simple support

Boundary conditions at the cutting edge and boring bar holder	Boundary conditions at the intermediate pressure head support
$\xi_1(0) _{x=0} = \xi_2(0) _{x=0} = 0$	$\xi_1(L_1) _{x=L_1} = \xi_2(L_2) _{x=L_2} = 0$
$\xi_1'(0) _{x=0} = \xi_2'(0) _{x=0} = 0$	$\xi_1'(L_1) _{x=L_1} = -\xi_2'(L_2) _{x=L_2}$
	$\xi_1''(L_1) _{x=L_1} = \xi_2''(L_2) _{x=L_2}$

By substituting the above boundary conditions in equations (4.13) and (4.14), the frequency equation for a stable equilibrium can be written as follows:

$$\begin{aligned}
 & (\cosh \beta L_1 \cos \beta L_1 - 1)(\cosh \beta L_2 \sin \beta L_2 - \sinh \beta L_2 \cos \beta L_2) \\
 & = (\cos \beta L_1 \sinh \beta L_1 - \sin \beta L_1 \cosh \beta L_1)(\cosh \beta L_2 \cos \beta L_2 - 1)
 \end{aligned} \tag{4.16}$$

The corresponding modal shape expressions can be written as

$$\xi_1(X) = C \left\{ \left( \sin \left( q_r \frac{X}{L_1} \right) - \sinh \left( q_r \frac{X}{L_1} \right) + \alpha_1 \left( \cos \left( q_r \frac{X}{L_1} \right) - \cosh \left( q_r \frac{X}{L_1} \right) \right) \right) \right\} \tag{4.17}$$

$$\xi_2(X) = C^* \left\{ \alpha_2 \left( \sin \left( q_r^* \frac{X}{L_2} \right) - \sinh \left( q_r^* \frac{X}{L_2} \right) \right) + \alpha_3 \left( \cos \left( q_r^* \frac{X}{L_2} \right) - \cosh \left( q_r^* \frac{X}{L_2} \right) \right) \right\} \tag{4.18}$$

where  $C$  and  $C^*$  are arbitrary amplitude constants,  $q_r = \beta L_1$ , and  $q_r^* = \beta L_2$

$$\alpha_1 = \frac{(\sin \beta L_1 - \sinh \beta L_1)}{(\cos \beta L_1 - \cosh \beta L_1)} ; \quad \alpha_2 = \frac{(1 - \cos \beta L_1 \cosh \beta L_1)(\cosh \beta L_2 - \cos \beta L_2)}{(\cos \beta L_1 - \cosh \beta L_1)(1 - \cos \beta L_2 \cosh \beta L_2)}$$

$$\text{and } \alpha_3 = \frac{(\sinh \beta L_2 - \sin \beta L_2)}{(\cos \beta L_2 - \cosh \beta L_2)}$$

In the second case, the cutting tool is in indifferent equilibrium and the conditions at the cutting edge can be approximated by simple support as shown in Fig. 4.3. This is the case when either trailing or leading pad is not supported at all. According to some investigations one of the guide pads would not be supported in 60% of the BTA tools during the machining process and 100% of the BTA tools would be subjected to this unstable condition during the initial cut [89]. Generally most of these tools and gundrills are subjected to unstable condition during the initial cut because the cutting force resultant is not pointing between the guide pads. The boundary conditions for this case are given in Table 4.2.

Table 4.2 Clamped-Simple with intermediate simple support

Boundary conditions at the cutting edge and boring bar holder	Boundary conditions at the intermediate pressure head support
$\xi_1(0) _{x=0} = \xi_1''(0) _{x=0} = 0$	$\xi_1(L_1) _{x=L_1} = \xi_2(L_2) _{x=L_2} = 0$
$\xi_2(0) _{x=0} = \xi_2'(0) _{x=0} = 0$	$\xi_1'(L_1) _{x=L_1} = -\xi_2'(L_2) _{x=L_2}$
	$\xi_1''(L_1) _{x=L_1} = \xi_2''(L_2) _{x=L_2}$

Similarly for indifferent equilibrium the frequency equation can be written as

$$\begin{aligned} & (\cos \beta L_2 \sinh \beta L_2 - \sin \beta L_2 \cosh \beta L_2)(\cosh \beta L_1 \sin \beta L_1 - \sinh \beta L_1 \cos \beta L_1) \\ & = (1 - \cosh \beta L_2 \cos \beta L_2) (2 \sin \beta L_1 \sinh \beta L_1) \end{aligned} \quad (4.19)$$

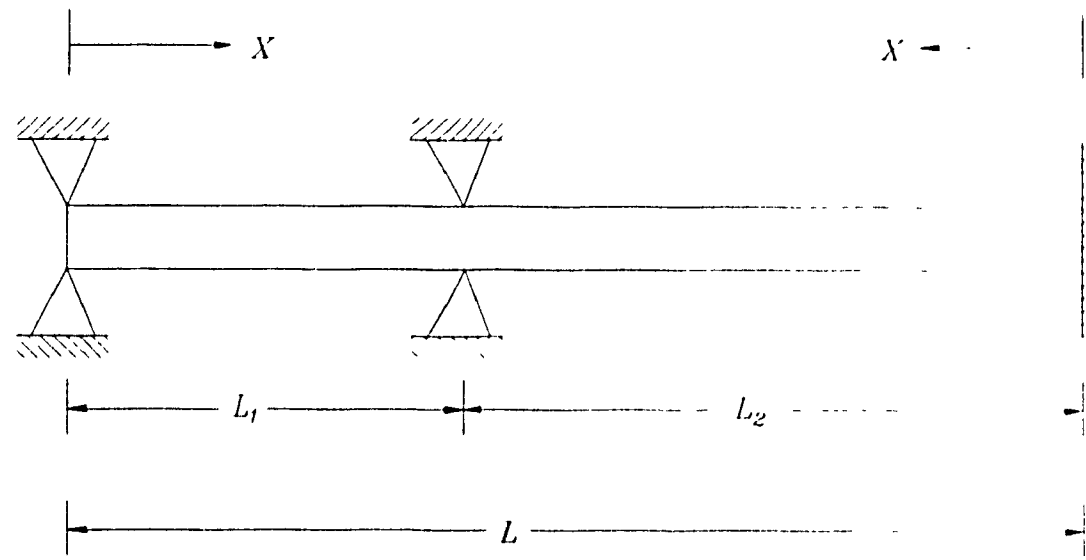
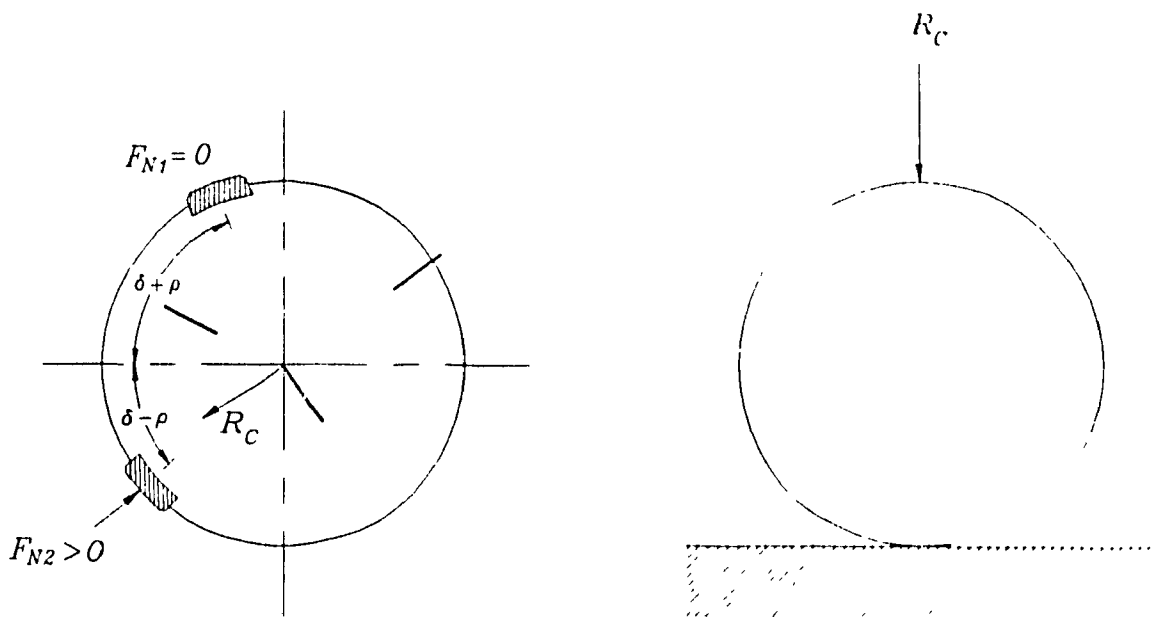


Fig. 4.3 Model of Cutting Tool-Boring Bar Assembly at Indifferent Equilibrium



The modal shape expressions can be written for indifferent equilibrium as

$$\xi_1(X) = C \left\{ \sinh\left(q_r \frac{X}{L_1}\right) - \alpha_1 \left( \sin\left(q_r \frac{X}{L_1}\right) \right) \right\} \quad (4.20)$$

$$\xi_2(X) = C \cdot \left\{ \alpha_2 \left( \sinh\left(q_r^* \frac{X}{L_2}\right) - \sin\left(q_r^* \frac{X}{L_2}\right) \right) + \alpha_3 \left( \cosh\left(q_r^* \frac{X}{L_2}\right) - \cos\left(q_r^* \frac{X}{L_2}\right) \right) \right\} \quad (4.21)$$

where  $\alpha_1 = \frac{\sin\beta L_1}{\sinh\beta L_1}$  ;  $\alpha_2 = \frac{(\sin\beta L_1 \cosh\beta L_1 - \sinh\beta L_1 \cos\beta L_1)(\cosh\beta L_2 - \cos\beta L_2)}{2\sinh\beta L_1(\cosh\beta L_2 \cos\beta L_2 - 1)}$

and  $\alpha_3 = \frac{(\sin\beta L_2 - \sinh\beta L_2)}{(\cosh\beta L_2 - \cos\beta L_2)}$

In the third case, the cutting tool is in unstable equilibrium and the end conditions at the cutting edge can be considered as a free end as shown in Fig. 4.4. This unstable condition would occur due to a false cutting tool geometry leading to a case when the tool is not supported by the pads, and only 'encastre' effect will prevent the tool from deviating away from the straight direction. Similar set of conditions occur when the boring bar is attached to conventional cutting tools such as spade drills, twist drills, boring tools, and reamers. The boundary conditions at unstable equilibrium are given in Table 4.3.

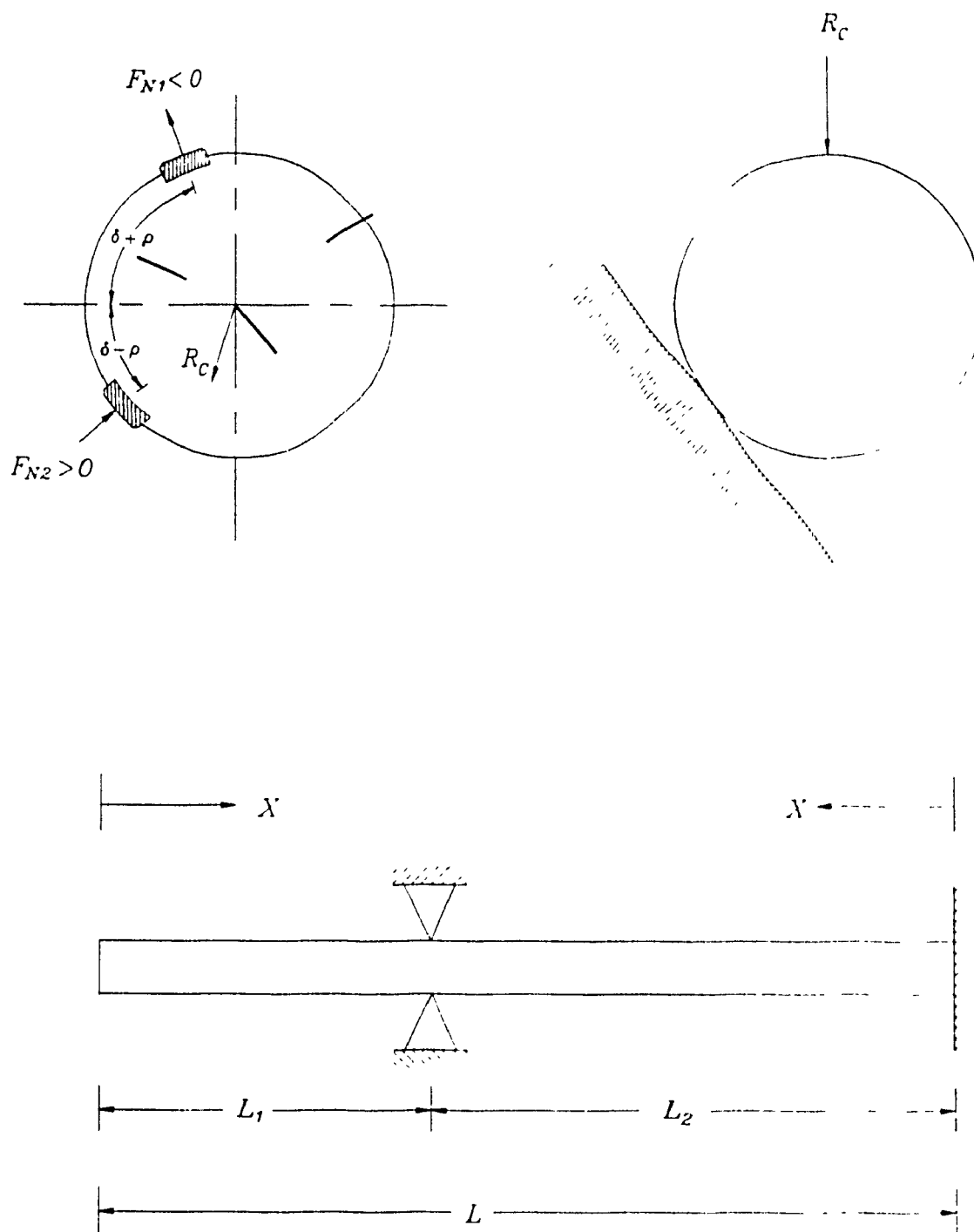


Fig. 4.4 Model of Cutting Tool-Boring Bar Assembly at Unstable Equilibrium

Table 4.3 Clamped-Free with intermediate simple support

Boundary conditions at the cutting edge and boring bar holder	Boundary conditions at the intermediate pressure head support
$\xi_1''(0) _{x=0} = \xi_1'''(0) _{x=0} = 0$	$\xi_1(L_1) _{x=L_1} = \xi_2(L_2) _{x=L_2} = 0$
$\xi_1(0) _{x=0} = \xi_1''(0) _{x=0} = 0$	$\xi_1'(L_1) _{x=L_1} = -\xi_2'(L_2) _{x=L_2}$
	$\xi_1''(L_1) _{x=L_1} = \xi_2''(L_2) _{x=L_2}$

Finally the frequency equation for unstable equilibrium can be written as

$$(1 + \cosh \beta L_1 \cos \beta L_1) (\cos \beta L_2 \sinh \beta L_2 - \sin \beta L_2 \cosh \beta L_2) \\ = (\cosh \beta L_1 \sin \beta L_1 - \sinh \beta L_1 \cos \beta L_1) (\cosh \beta L_2 \cos \beta L_2 - 1) \quad (4.22)$$

The modal shape expressions for unstable equilibrium can be written as

$$\xi_1(X) = C \left\{ \sinh \left( q_r \frac{X}{L_1} \right) + \sin \left( q_r \frac{X}{L_1} \right) - \alpha_1 \left( \cosh \left( q_r \frac{X}{L_1} \right) + \cos \left( q_r \frac{X}{L_1} \right) \right) \right\} \quad (4.23)$$

$$\xi_2(X) = C \cdot \left\{ \alpha_2 \left( \sinh \left( q_r \frac{X}{L_2} \right) - \sin \left( q_r \frac{X}{L_2} \right) \right) + \alpha_3 \left( \cosh \left( q_r \frac{X}{L_2} \right) - \cos \left( q_r \frac{X}{L_2} \right) \right) \right\} \quad (4.24)$$

where  $\alpha_1 = \frac{(\sinh \beta L_1 + \sin \beta L_1)}{(\cosh \beta L_1 + \cos \beta L_1)}$

$$\alpha_2 = \frac{(\cos \beta L_1 \sinh \beta L_1 - \sin \beta L_1 \cosh \beta L_1) (\cosh \beta L_2 - \cos \beta L_2)}{(\sin \beta L_2 \cosh \beta L_2 - \sinh \beta L_2 \cos \beta L_2) (\cos \beta L_1 + \cosh \beta L_1)}$$

$$\text{and } \alpha_3 = \frac{(\sin \beta L_2 - \sinh \beta L_2)}{(\cosh \beta L_2 - \cos \beta L_2)}$$

The natural frequencies of the boring bar in all three cases can be calculated by use of equation (4.6),

$$\omega_n = \left( \frac{q_r + q_r^*}{L_1 + L_2} \right)^2 \left[ \frac{EIg}{\gamma A} \right]^{\frac{1}{2}} \quad (4.25)$$

$$\text{where } I = \frac{\pi}{64}(d_0^4 - d_i^4) \text{ and } A = \frac{\pi}{4}(d_0^2 - d_i^2) \quad (4.26)$$

Following numerical values are used for illustration.

$$E = 2 \times 10^{11} \text{ N/m}^2, \gamma = 76036 \text{ N/m}^3, d_i = 0.0135 \text{ m}, d_0 = 0.022 \text{ m and } L_1 + L_2 = 2.5 \text{ m}$$

#### 4.7 CONCLUSIONS

Different boundary conditions at the cutting tool-workpiece contact during machining process have been identified in this analysis based on the Pfléghar's static stability criterion. By doing so it was possible to obtain boring bar-tool dynamic response, for the three end conditions. Results of these selected numerical examples show that the natural frequencies of the first transverse mode of the cutting tool-boring bar varies between 18.31 Hz to 26.57 Hz. The mode shapes of the cutting tool-boring bar for the stable, indifferent and unstable equilibrium were obtained for the tool penetration of 500

mm and are plotted in Figures 4.5, 4.6, and 4.7. Furthermore the tool penetrations from 0.1 mm to 500 mm are given to the workpiece in all the three cases and the corresponding first five natural frequencies are given in the Tables 4.4, 4.5, and 4.6. Plots of natural frequencies versus tool penetrations for all the three conditions can be seen in Figures 4.8, 4.9 and 4.10. Gessesse and Latinovic [52] concluded that an instability called spiralling could occur because of tool bluntness, circle land on the circumference, position of pads, coincidence of the natural lateral frequency with appropriate number of lobes occurring. Cronenjager et al [59] concluded that spiralling can occur during initial cut, excessive buckling of the boring bar, and due to non-homogeneous material of the workpiece. The natural frequencies of the boring bar for all the end conditions are verified with those of Gessesse's [1] experimental results and the best agreement was found between his experimental results and those yielded by simple support end conditions of the bar at the cutting tool. Certainly these frequencies are pure theoretical response and if they are used in machine shop practice, a due precaution should be exercised. However, they can serve as a good guide in selecting the machine tool speed for each hole size. Avoiding the critical speeds would lead to a most likely stable, vibration free operation.

Table 4.4 Natural frequencies for different tool penetrations in Stable equilibrium

Tool Penetrations (mm)	Natural frequencies (Hz)				
	$\omega_{n1}$	$\omega_{n2}$	$\omega_{n3}$	$\omega_{n4}$	$\omega_{n5}$
25	27.10	75.70	149.33	245.26	337.41
50	27.68	77.37	152.49	248.25	324.11
100	28.89	80.87	158.76	246.31	300.15
150	30.20	84.60	164.29	229.90	298.74
200	31.62	88.51	166.81	212.93	308.53
250	34.14	92.51	162.05	206.43	321.86
300	34.80	96.41	151.50	210.09	336.08
350	36.56	99.62	140.98	218.39	347.09
400	38.46	100.90	134.94	228.64	342.32
450	40.50	98.79	132.27	239.40	321.76
500	42.66	94.97	135.33	247.91	302.76

Table 4.5 Natural frequencies for different tool penetrations in Indifferent equilibrium

Tool Penetrations (mm)	Natural frequencies (Hz)				
	$\omega_{n1}$	$\omega_{n2}$	$\omega_{n3}$	$\omega_{n4}$	$\omega_{n5}$
25	26.49	74.27	145.36	219.66	274.60
50	27.03	75.81	147.33	210.74	272.49
100	28.17	78.96	148.61	194.33	278.93
150	29.41	82.10	144.01	185.98	289.87
200	30.73	84.94	132.47	188.34	302.44
250	32.14	86.81	122.71	195.05	314.83
300	34.64	86.44	116.88	204.64	321.80
350	35.21	84.10	116.05	214.07	311.29
400	36.84	78.08	118.89	222.07	290.55
450	38.47	72.92	124.75	227.05	275.01
500	39.97	68.40	129.76	221.68	274.74

Table 4.6 Natural frequencies for different tool penetrations in unstable equilibrium

Tool Penetration (mm)	Natural frequencies (Hz)				
	$\omega_{n1}$	$\omega_{n2}$	$\omega_{n3}$	$\omega_{n4}$	$\omega_{n5}$
25	18.38	42.06	79.67	150.75	245.89
50	18.39	49.59	80.55	154.66	248.58
100	18.19	38.29	82.99	159.56	245.38
150	17.67	36.93	86.07	164.76	227.89
200	16.90	36.43	89.57	166.72	211.12
250	15.97	36.62	94.30	161.08	205.49
300	14.96	37.34	96.97	150.06	209.72
350	14.97	38.47	99.94	139.56	218.23
400	14.02	39.92	100.84	132.83	228.56
450	12.13	41.63	98.26	131.63	239.35
500	11.32	44.55	94.14	135.02	245.90

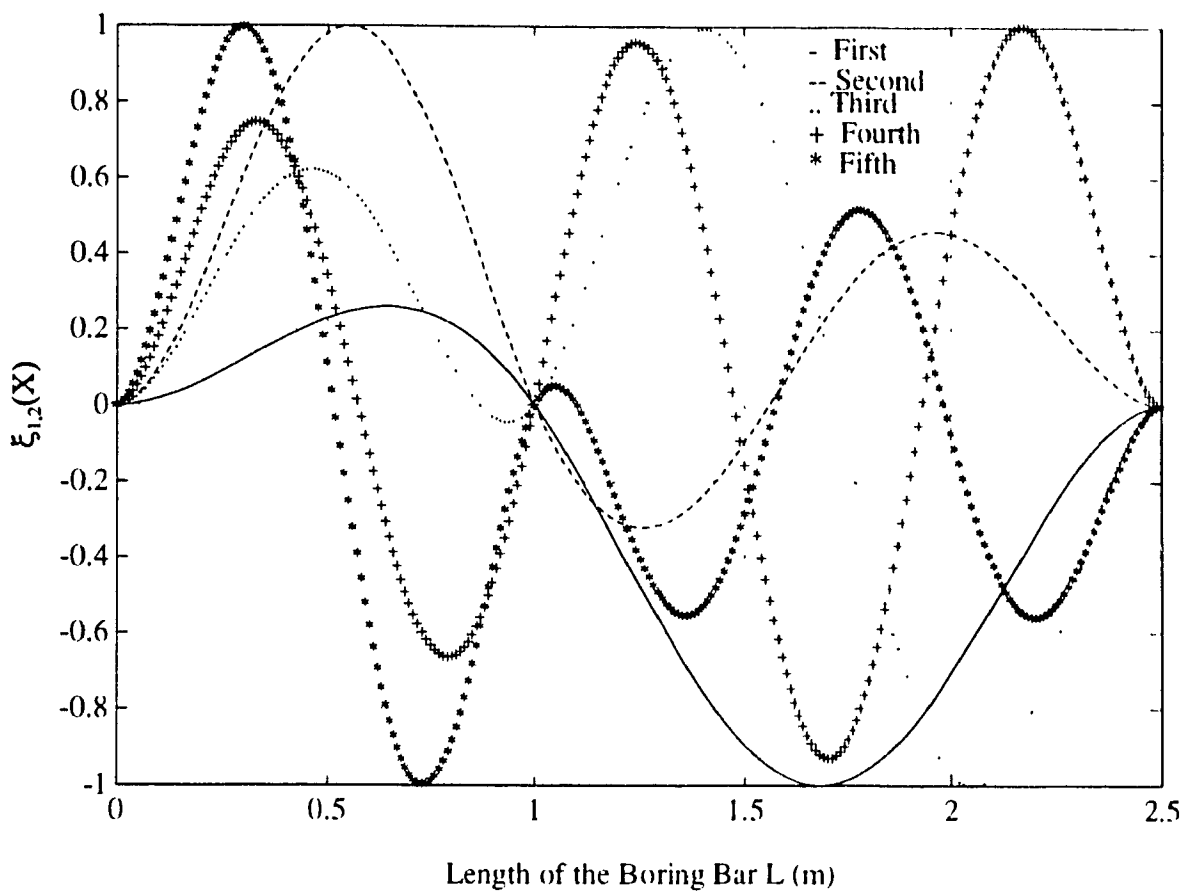


Fig. 4.5 Mode Shapes of the Cutting Tool - Boring Bar Assembly at Stable Equilibrium



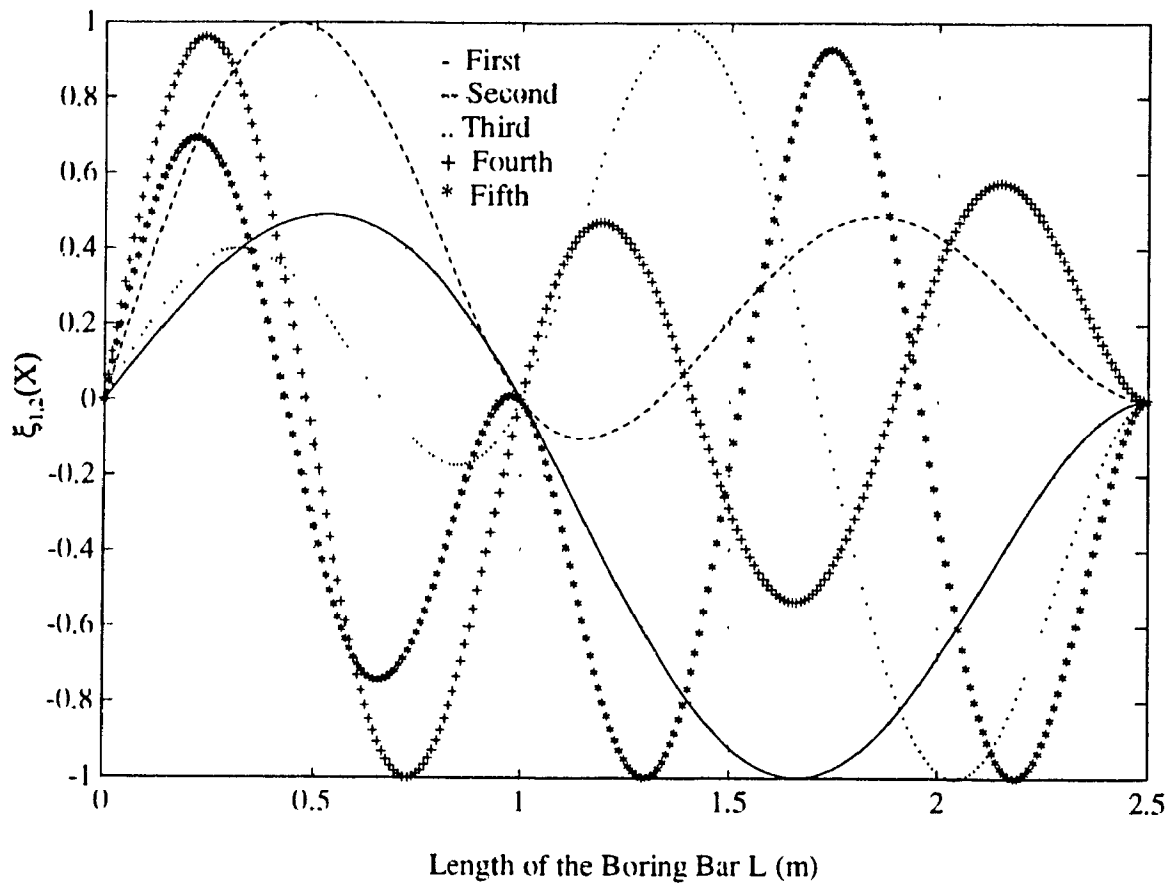


Fig. 4.6 Mode Shapes of the Cutting Tool - Boring Bar Assembly at Indifferent Equilibrium

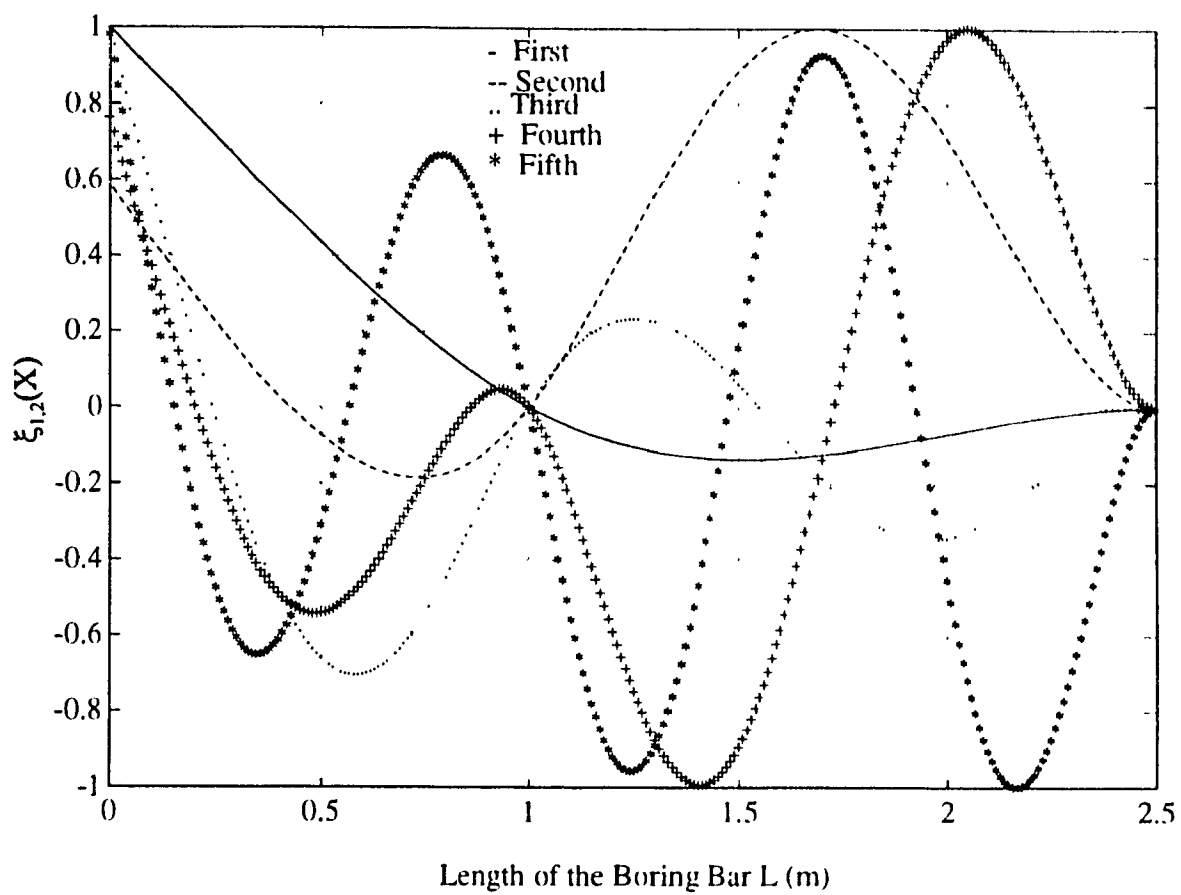


Fig. 4.7 Mode Shapes of the Cutting Tool - Boring Bar Assembly at Unstable Equilibrium

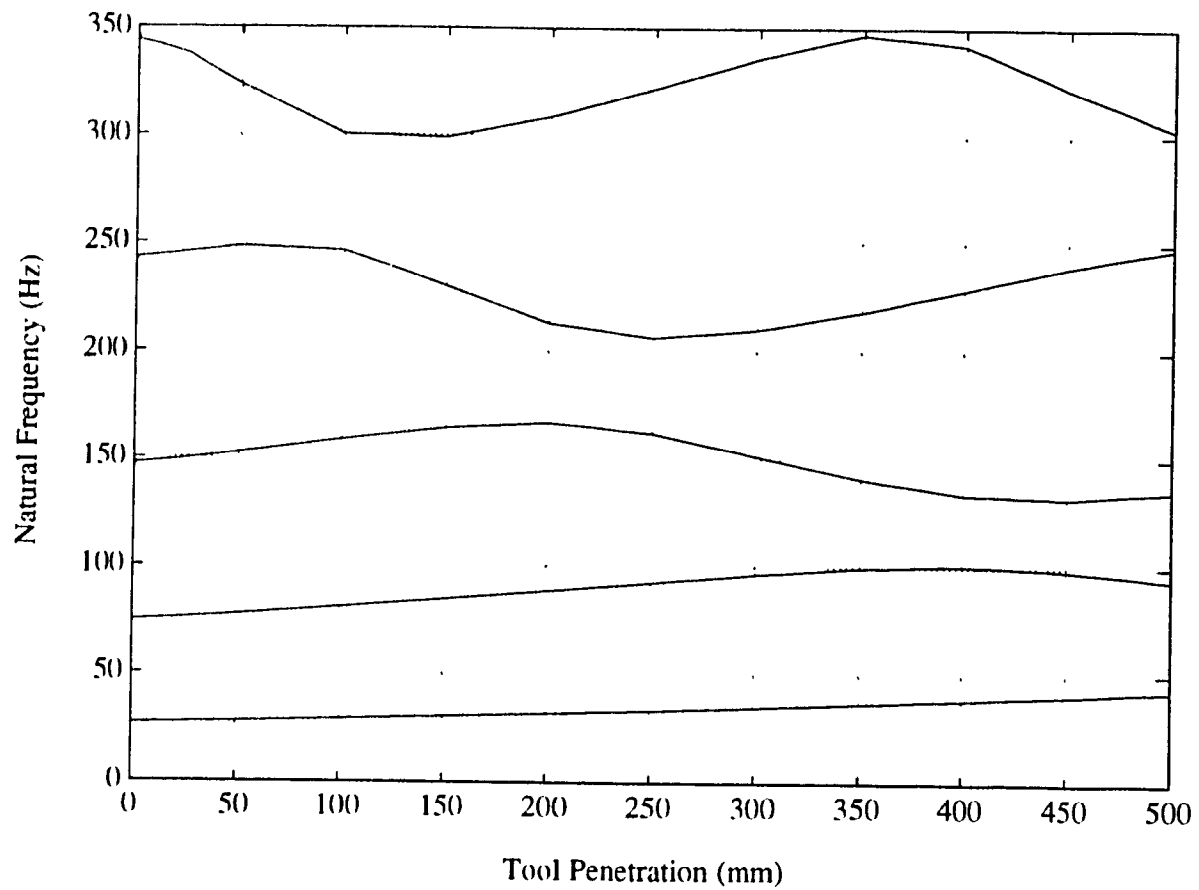


Fig. 4.8 Lateral Natural Frequencies of the Cutting Tool-Boring Bar Assembly at Different Tool Penetrations in Stable Equilibrium

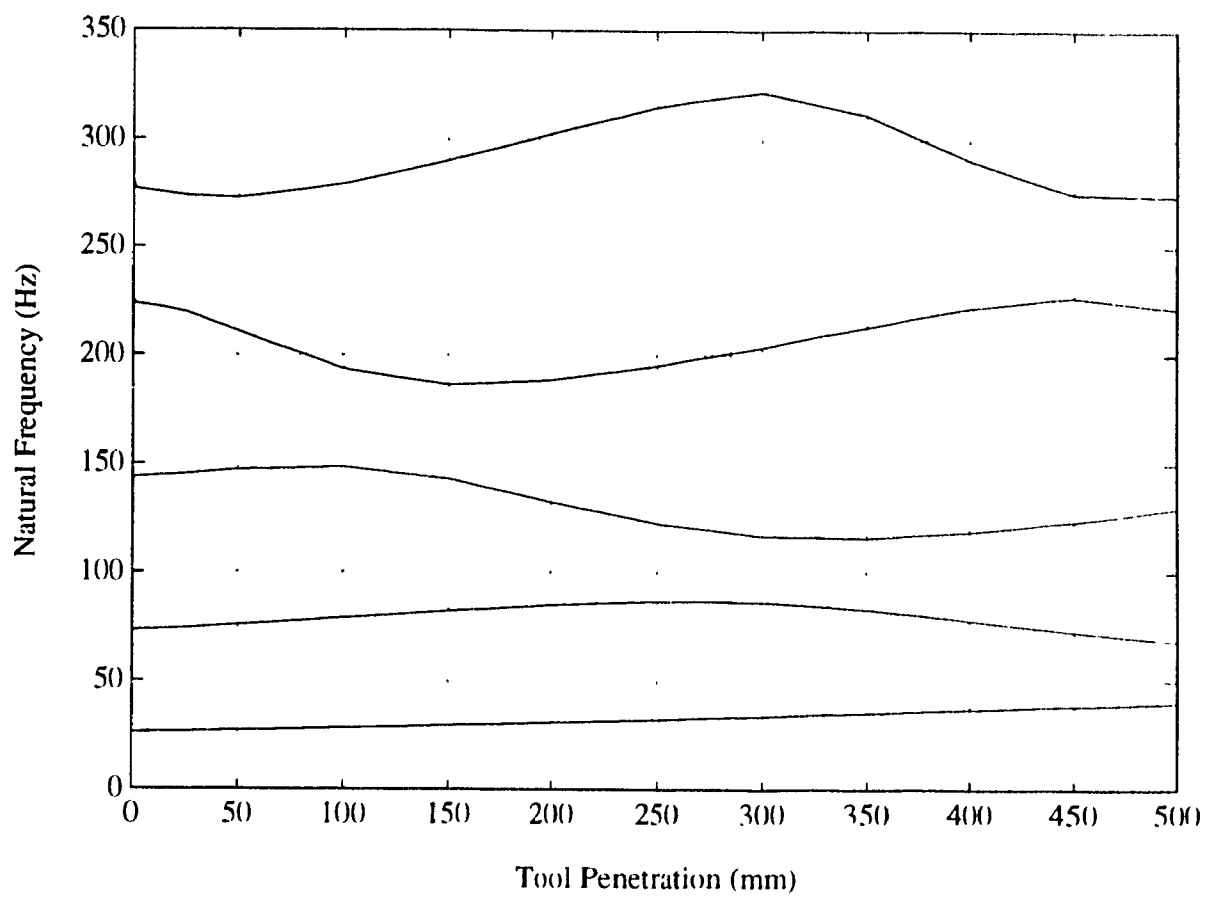


Fig. 4.9 Lateral Natural Frequencies of the Cutting Tool-Boring Bar Assembly at Different Tool Penetrations in Indifferent Equilibrium

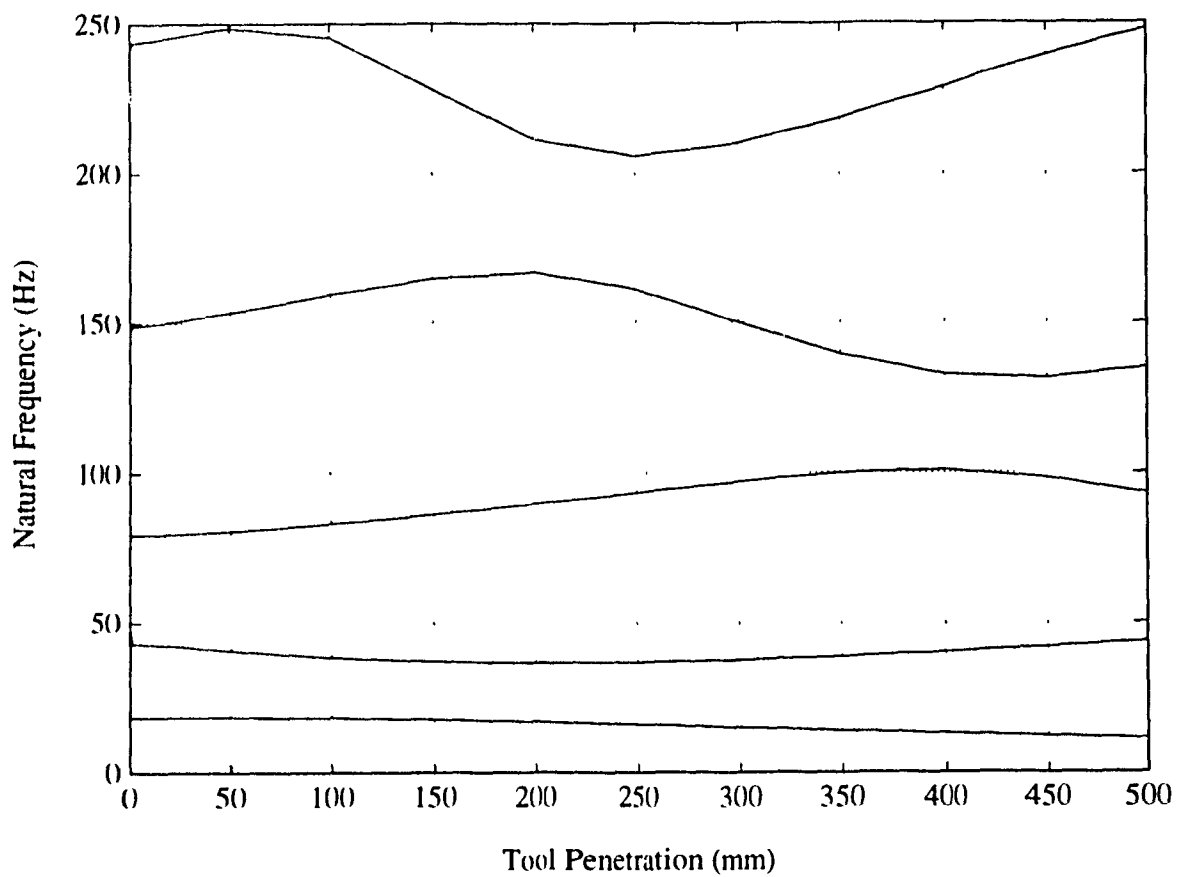


Fig. 4.10 Lateral Natural Frequencies of the Cutting Tool-Boring Bar Assembly at Different Tool Penetrations in Unstable Equilibrium

## **CHAPTER 5**

### **SUMMARY, CONCLUSIONS AND RECOMMENDATIONS**

#### **5.1 SUMMARY**

In this analysis, an analytical formulation of tool cutting force system for a BTA multi-edge cutting tool with staggered cutters and a procedure of optimizing a tool design in such a way that the tool maintains equal pad reactions is carried out. The salient feature of the design is that staggered cutters with different width of cut are unsymmetrically located on the boring head, so that a non zero resultant cutting force is transmitted to the bore-wall at all times with equal pad reactions. The random parameters affecting cutting forces in the machining process are identified and the cutting forces are formulated in terms of these parameters. The novel feature is that the optimization procedure is accomplished by formulating a multi-variable, nonlinear, stochastic objective function and several constraints.

##### **5.1.1 MATHEMATICAL MODEL AND OPTIMUM TOOL DESIGN**

To formulate the cutting force system for the BTA tool with staggered cutters, the mathematical model of cutting force system was adopted based on a combined cutting mechanics and empirical approach proposed earlier. In this approach, the three cutting force components namely tangential, radial and feed forces are formulated using metal

cutting mechanics. But the equations of the cutting force components are written as an empirical function of width of cut and uncut chip thickness. The resultant cutting force is formulated in terms of these cutting force components and the angular location of each cutter.

An objective function is formulated based on the mathematical model developed for the cutting forces. The objective is to minimize the difference of the cutting force resultant and desired resultant pads reaction for a good tool guidance. In order to account for the variations of the cutting forces, a probabilistic model is used for the objective function. Several constraints are incorporated to secure a feasible tool design. The resulting multi-variable, constrained, non-linear stochastic optimization problem has been solved by using Interior Penalty Method.

### **5.1.2 CUTTING FORCES AND PAD REACTIONS VARIATIONS**

The cutting forces in machining process are dynamic in nature with random characteristics. The magnitude of the cutting forces during machining process vary because of the randomness of the parameters involved. Given the variations in magnitude of the cutting force components the variations in magnitude and direction of the cutting force resultant are found using two probabilistic methods such as Linear Statistical Approach and Monte Carlo Simulation. The magnitude variations of pad reactions are predicted by attempting a normal distribution and an uniform distribution

to the coefficient of friction at the guide pads, because of lack of information on friction coefficient's distribution. The difference caused by use of the two distributions turned out insignificant and consequently for convenience, the normal distribution is recommended in future for the probabilistic model.

### **5.1.3 FREE TRANSVERSE VIBRATIONS OF CUTTING TOOL-BORING BAR**

The static stability of the BTA tool with staggered cutters is studied by Pfléghar's method. Different boundary conditions are identified at the cutting tool-workpiece contact depending upon the stability conditions at the tool guide pads. These are approximated with clamped end, simple support and free end. Boring bar holder is represented as a clamped end and simple support is used at the pressure head. These approximations are the representations of most probable boundary conditions during cutting process. The first five transverse mode shapes of the cutting tool - boring bar system for a tool penetration of 500 mm as well as the natural frequencies at varied tool penetrations from 0.1 mm to 500 mm are determined.

## **5.2 CONCLUSIONS**

During the analytical investigation on the stochastic optimization of a BTA tool with staggered cutters, cutting forces and pad reactions variations as well as the free transverse vibrations of the cutting tool - boring bar, the following conclusions



can be made:

- (i) An analytical formulation of the tool cutting force system and a procedure of optimum design with equal pad reactions for BTA tools with staggered cutters have been proven an adequate means for tool optimization using the stochastic approach.
- (ii) The predetermined pad reactions are chosen in the optimization in such a way that the varying cutting force resultant is transmitted to the bore-wall evenly to both pads. The optimum resultant cutting force exerts adequate even pressure onto the bore-wall which in turn guides the tool and prevents its separation from the bore-wall.
- (iii) The objective function is minimized in such a way that the cutting force resultant and pads resultant reactions are balanced. A probabilistic approach is selected in order to handle the objective function, which accommodates the variations of the random parameters in the machining process. The random parameters identified in the machining process are cutting forces expressed in terms of the unit cutting forces and width of cut, both being random in nature. The model handled the variations of the unit cutting forces and width of cut of the outer cutter, for the given variances.
- (iv) The variations in magnitude of cutting forces and variations in magnitude and direction of the cutting force resultant are calculated by two probabilistic approaches, the Linear Statistical Approach and Monte Carlo simulation. The results obtained by the two methods are in good agreement. However, Monte

Carlo simulation is time consuming and needs large number of replications for good accuracy. The Linear Statistical Approach is proposed for use in the future.

- (v) Due to lack of information on the friction coefficient's variation the magnitude variations of pad reactions are assessed by assuming two distributions the normal distribution and the uniform the distribution; the first being most convenient, and the second being the worst case. However, an insignificant difference in the deviation of pad reactions resulted from the two. Hence the normal distribution for the friction coefficient at the guide pads is recommended for convenience for the future use.
- (vi) Results show that the cutting force resultant direction varies within the limits of pads included angle which is important for the tool guidance, and static stability. The magnitude fluctuation of pad reactions indicate that these are always maintained at safe values greater than zero, which secures the tool guidance.
- (vi) The static stability of the cutting tool is studied by Pfléghar's static stability analysis. Different boundary conditions at the cutting tool - workpiece contact during machining process have been identified depending upon the degree of stability of the tool by this method. The free transverse vibrations of the cutting tool - boring bar are studied for the identified boundary conditions at the cutting tool workpiece contact. The natural frequencies of the first transverse mode of the cutting tool-boring bar varied between 18.31 Hz to 26.57 Hz, depending on the degree of static stability of the tool.

### 5.3 RECOMMENDATIONS

The following are the recommendations to be considered in the future for further investigation.

- (i) In order to compare the studied performance of the BTA tool with staggered cutters, a prototype should be built and tested along with the commercially available tools in terms of hole run out, surface finish, hole roundness and performance with various specimens at different conditions.
- (ii) The variations in magnitude and direction of the cutting force resultant and pad reactions have to be verified experimentally, which is important for tool guidance and burnishing action. The variations of the feed rate should be incorporated into the cutting force components through the variation of depth cut to make further improvement in the assessment of cutting force resultant variations.
- (iii) The efforts should continue to further investigate dynamic stability of boring bar-cutting tool-work piece system particularly when slender workpieces are drilled. The dynamic instability of the system seems to be a major obstacle to achieve good quality of holes in the machine shops practice.

## REFERENCES

- 1 Gessesse, Y.B., "Stability of Deep-Hole BTA Machining Process", M.A.Sc. Thesis, Concordia University, Montreal, 1990.
- 2 M.O.M. Osman, "The BTA Technique - Fast Hole Machining", Tooling & Production, No. 2, pp. 49-51, 1975.
- 3 Latinovic, V.N., "An Investigation of the Theoretical and Design Aspects of Unsymmetrical Multi-Cutting Action in Deep-Hole Machining", D-Eng. Thesis, Concordia University, Montreal, 1978.
- 4 Steeds, W., "A History of Machine Tools 1700-1910", Oxford at Clarendon Press, pp. 1-24, 1969.
- 5 Thorne, W.H., "Twist Drills", ASME Transactions, Vol. 3, pp. 130-137, 1886.
- 6 Griffiths, B.J., "The Machining Action During Deep-Hole Boring and the Resultant Hole Form and Force System", Proc. of 2nd International Conference on Production Res., Copenhagen, 1973.
- 7 Turner, C.F., "Practical Aspects of Producing Holes", International Conference on Deep Hole Drilling and Boring, Brunel University, May 1975.
- 8 Amarego, E.J.A., and Brown, R.H., "The Machining of Metals", Prentice- Hall Inc., 1969.
- 9 Merchant, M.E., "Basic Mechanics of Cutting Process", J. Applied Mechanics, Vol. 11, pp. 168-175, 1944.
- 10 Merchant, M.E., "Mechanics of the Metal Cutting Process in Orthogonal Cutting and the Type 2 Chip", J. Applied Physics, Vol. 16, No. 5, pp. 267-275, 1945.

- 11 Shaw, M.C., Cook, N.H., and Smith, P.A., "The Mechanics of Three-Dimensional Cutting Operations", ASME Transactions, Vol. 74, pp. 1055-1067, 1952.
- 12 Oxford, C.J.Jr., "On the Drilling of Metals, 1-Basic Mechanics of Process", ASME Transactions, Vol. 77, pp. 103-114, 1955.
- 13 Shaw, M.C., and Oxford, C.J.Jr., "On the Drilling of Metals, 2-The Torque and Thrust on Drilling", ASME Transactions, Vol. 79, pp. 139-148, 1957.
- 14 Alberht, P., "Dynamics of the Metal-Cutting Process", ASME Transactions, Journal of Engineering for Industry, pp. 429-441, 1965.
- 15 Williams, R.A., "Dynamic Geometry of a Twist Drill", International Journal of Production and Research, Vol. 7, No. 4, pp. 253-267, 1969.
- 16 Bickel, E., "Die Wechselnden Kräfte bei der Spanbildung", Annals CIRP, Vol. 12, No. 4, pp.206, 1966.
- 17 Kwiatkowski, A.W., and Bennet, F.E., "Application of Random Force Excitation to the Determination of Receptances of Machine Tool Structures", Advances MTDR Conference, 1965.
- 18 Kwaitkowski, A.W., and Al Samarai, H.M., "Progress in the Application of Random Signal Analysis Methods to the Identification of Machine Tool Structures", Advances MTDR, pp. 591, 1968.
- 19 Peklenik, J., and Kwiatkowski, A.W., "New Concepts in Investigating the Manufacturing by Means of Random Process Analysis", Proc. IMTDR Conference, pp. 683, 1965.

- 20 Optiz, H., and Weck, M., "Determination of Transfer Function by Means of Spectral Density Measurements and its Applications to the Dynamic Investigation of Machine Tools under Working Conditions", Advances in MTDR., pp. 349, 1969.
- 21 Osman, M.O.M, and Sankar, T.S., "Short-Time Acceptance Test for Machine Tools Based Upon Random Nature of Cutting Forces", ASME Transactions, Journal of Engineering for Industry, Vol. 94, No. 4, pp. 1020-1024, 1972.
- 22 Maragos, S.K., "Measurement and Modeling of the Cutting Force Fluctuations During Machining", M.Eng.Thesis, Sir George Williams University, Montreal, 1973.
- 23 Rakhit, A.K., Sankar, T.S., and Osman, M.O.M., "The Effect of Stochastic Response of Machine-Tool-Workpiece on Formation of Surface Texture in Turning", ASME Vibration Conference, Cincinnati, 1973.
- 24 Chahil, G.S., "Measurement and Modeling of Torque and Thrust in Twist Drilling Operation", M.Eng. Thesis, Concordia University, Montreal, 1976.
- 25 Greuner, B., "Beitrag zur Frage des Krafte ans Schneide und Fuhrungsleisten an einsehheidigen hartmetallbestuckfen Tiefbohrwerkzeugen", Dr. Ing. Thesis, Technischen Universitat, Hannover, 1970.
- 26 Gildemeister-Heidenrich and Harbeck, "Was Baited Modernes Tiefbohren der Fertigungstechnik Heute?", Vortragsveranstaltung, Remscheid, May, 1973.
- 27 Pearson, H.J., "High-Speed Boring" - Parts 1, 2, 3 and 4. Production Technology, March, April, July 1962 and May 1963.

- 28 Swinehart, H.J., "Gundrilling, Trepanning and Deep-Hole Machining", ASTME, Dearborn, Mich., 1967.
- 29 Hutson, G.A., "Modernization of Gun Tube Boring Facilities", Bent R & E Laboratories, Technical Report WVT-7016, New York, 1970.
- 30 Griffiths, B.J., "The Machining Action During Deep-Hole Boring and the Resultant Hole Form and Force System", Proc. 2nd International Conference on Production Res., Copenhagen, 1973.
- 31 Osman, M.O.M., and Greuner, B., "Entwicklunstendenzen Eines BTA - Werkzeuges zum Bohren ins Volle", TZ fur praktische Metallbearbeitung, Vol. 68, No. 5, pp. 166-168, 1974.
- 32 Pflighar, F., "The Aspect of Stability in Designing Deep-Hole Drilling and Boring Tools", 2 nd International Conference on Deep-Hole Drilling and Boring, Brunel University, 1979.
- 33 Osman, M.O.M., and Latinovic, V., "On the Development of Multi-Edge Cutting for BTA Deep-Hole Machining", ASME Trans., J. Eng. for Industry, Vol.98, No. 2, pp. 474-480, 1976.
- 34 Osman, M.O.M., and Mansour, W.M., "Lubrication of Journal Bearings", Design Engineering, Vol. 15, No. 10, pp. 56-60, Oct. 1969.
- 35 Griffiths, B.J., "An Introduction to Deep Hole Drilling and Boring", International Conference on Deep Hole Drilling and Boring, Brunel University, May 1975.
- 36 Greuner, B., "Deep Hole Boring and Finishing Techniques and their Application to the Manufacture of Hydraulic Cylinders", International Conference on Deep

- Hole Drilling and Boring, Brunel University, May 1975.
- 37 Faber, K., "Deep Hole Drilling Using the Ejector System", International Conference on Deep Hole Drilling and Boring Brunel University, May 1975.
- 38 Corney, J., and Griffiths, B., "A study of the Cutting and Burnishing Operation During Deep-Hole Drilling and its Relationship to Drill Wear", Int. Journal of Prod. and Research, Vol. 14, No.1, pp. 1-9, 197
- 39 Buck, G., "Chip Forms in Drilling With Gun Drills", International Conference on Deep Hole Drilling and Boring, Brunel University, May 1975.
- 40 Streicher, P., "Drilling With Long Gun Drills", International Conference on Deep Hole Drilling and Boring, Brunel University, May 1975.
- 41 Lundgren, E., "The Role of the Cutting Geometry in Deep-Hole Drilling", International Conference on Deep Hole Drilling and Boring, Brunel University, May 1975.
- 42 Fink, P. "Economic Efficiency of Deep Hole Boring: Optimum Cutting Conditions", International Conference on Deep Hole Drilling and Boring, Brunel University, May 1975.
- 43 Griffiths, B.J., "The Surface Integrity of Holes Produced by the Deep Drilling Process", International Conference on Deep Hole Drilling and Boring, Brunel University, May 1975.
- 44 Tuffentsammer, K., "Feasibility of Controlled Adaption in Deep Hole Boring", International Conference on Deep Hole Drilling and Boring, Brunel University, May 1975.



- 45 Zwingmann, G., "Cooling Lubricants for Deep Drilling", International Conference on Deep Hole Drilling and Boring, Brunel University, May 1975.
- 46 Davies, J., "Deep Hole Boring Within Rolls Royce (1971) Ltd., Small Engine Division", International Conference on Deep Hole Drilling and Boring, Brunel University, May 1975.
- 47 Dicken, T.E.A., "Applications of Deep Hole Boring at Royal Ordnance Factory, Nottingham", International Conference on Deep Hole Drilling and Boring, Brunel University, May 1975.
- 48 Trinkaus, W.H., "A High-Powered Tool for King-Sized Drilling", Manufacturing Engineering, August 1975, From SME Tech. Paper TE 75-451, Presented at Upper Midwest Conference, St. Paul, Minnesota, May 1975.
- 49 Latinovic, V., and Osman, M.O.M., "Unsymmetrical Multi-Edge Cutting in Deep-Hole Machining-Design Concept and Analysis", Proc. NAMRC-IV, pp. 255-262, May 1976.
- 50 Chandrashekhar, S., "An Analytical and Experimental Stochastic Modelling of the Resultant Force System in BTA Deep-Hole Machining and its Influence on the Dynamics of the Machine Tool Workpiece System", Ph.D. Thesis, Concordia University, Montreal, 1984.
- 51 Torabi, S.J., and V.N. Latinovic, "Improved Version of Optimal BTA Tools with Staggered Disposable Carbide Inserts", CSME Mechanical Engineering Forum 1990, pp. 1-6.
- 52 Gessesse, Y.B., and Latinovic, V.N., "Effects of the Stiffness Characteristics of

- the Stuffing Box on Boring Bar Vibrations", International Journal of Production Research, Vol. 29, No. 3, 1991
- 53 Gessesse, Y.B., Latinovic, V.N., and Osman, M.O.M., "Effect of Boring Bar Natural Modes on Bore Quality in BTA Machining", pp. 604-609, Proc. of CSME Forum Transport 1992+, Montreal, Vol. 2, pp. 604-609, June 1992.
- 54 Rama K.P. Koganti, V.N. Latinovic, and A.K.W. Ahmed, "Frequency Analysis of Cutting tool-Boring Bar in Deep-Hole Machining", 11 th International Modal Analysis Conference, Florida, Vol. 2, pp. 934-940, February 1993.
- 55 Pflregar, F., "The Aspect of Stability in Designing Deep-Hole Drilling and Boring Tools", 2 nd International Conference on Deep-Hole Boring and Drilling, 1979.
- 56 Torabi, S.J., "Improved version of BTA Deep-Hole Drilling tools with staggered disposable carbide inserts", M.Eng. Thesis, Concordia University, Montreal, 1990.
- 57 Renz, M., and Cawdery, D.O., "The Concept of Gun Drilling, Design and Development of Machines and Tools", International Conference on Deep-Hole Boring and Drilling, Brunel University, May 1975.
- 58 Swinehart, H.J., "Gundrilling, Trepanning and Deep-Hole Machining", ASTME, Dearborn, 1976.
- 59 Cronjäger, L., Stockert, R., Weber, U., "Vibration and their Effect on Accuracy in Deep-Hole Boring", 3rd International Conference on Deep Hole Machining and Boring, Brunel University, 1979.

- 60 V.N. Latinovic and M.O.M. Osman, "Optimal design of BTA deep-hole cutting tools with staggered cutters", *Int. Journal of Production Research*, Vol. 27, No. 1, pp. 153-173, 1989.
- 61 V.N. Latinovic, R. Blakely and M.O.M. Osman "Optimal design of Multi-edge cutting tools for BTA Deep-Hole Machining", *Transactions of the ASME*, Vol. 101, pp. 281-290, 1979.
- 62 Stockert, R., "Beitrag zur optimaten Auslegung Von Tiefbohrwerkzeugen", Dr. - Ing. Thesis, Universitat Dortmund, 1978.
- 63 Sakuma, K., Taguchi, and K. Katsuki, A., "The Influence of Tool Geometry on Axial Hole Deviation in Deep Drilling: Comparison of Single Edge and Multi-Edge Tools", *Int. J. of JSME*, Vol. 30, No. 265, pp. 1167-1174, 1987.
- 64 Kronenberg, M., "Machining Science and Application", Pergamon Press, 1966.
- 65 VDF - "Waggerecht Tiebohrmaschinen", VDF - Prospect Nr. 148D (Horizontal Deep-Hole Machines, VDF-Catalogue No. 148D Verbrindliche Ausführung, pp. 24, Sept. 1969.
- 66 Griffiths, B.J., "An Investigation into the Role of the Burnishing Pads in the Deep-Hole Drilling Process", Ph.D. Thesis, Brunel University, 1982.
- 67 Stockert, R., "Zerspankraftverteilung über der Schneide von BTA-Vollbohrköpfen Zerspankraftverlauf über dem Bohrweg", *Tiefbohrer*, Dortmund Univ., pp. 16-19, 1976.
- 68 Weber, U., "Messen der Zerspankraft beim Tiefbohren", *Tiefbohren*, Dortmund Univ., pp. 9-12, 1976.

- 69 Cronjäger, L., "Entwicklungsstand des Tiefbohren Metalischer Werkstoofe", Tiebohren '77, VDI-Berichte, Nr. 301, pp. 5-11, 1977.
- 70 A. Charnes and W. Cooper, "Chance Constrained Programming", Management Science 6, pp. 73-79, 1959.
- 71 Rao, S.S., "Structural Optimization by Chance Constrained Programming Techniques", Computers and Structures, Vol. 12, pp. 777-781, 1980.
- 72 Rao, S.S., "Optimization: Theory and Applications", Wiley, New York, 1978.
- 73 S.F. Józwiak, "Minimum Weight Design of Structures with Random Parameters", Computers and Structures, Vol. 23, No. 4, pp. 481-485, 1986.
- 74 J.W. Davidson, L. P. Felton, and G.C. Hart, "Optimum Design of Structures with Random Parameters", Computers and Structures, Vol. 7, pp. 481-486, 1977.
- 75 Garret N. Vanderplaats, "Numerical Optimization Techniques for Engineering Design with Applications", McGraw-Hill Book Company, New York.
- 76 Chandrashekhar, S., Osman, M.O.M, and Sankar, T.S., "An Experimental Investigation for the Stochastic Modeling of the Resultant Force System in BTA Deep-Hole Machining", Int. J. of Prod. Res, Vol. 23, No. 4, pp. 657-673, 1985.
- 77 Cronjäger, L., "Entwicklungsstand des Tiefbohren Metalischer Werkstoofe", Tiebohren '77, VDI-Berichte, Nr. 301, pp. 5-11, 1977.
- 78 Weber, U "Beitarag zur Messtechnischen Erfassung des Tiefbohrprozesses", Dr. - Ing. Thesis, Universitat Dortmund, 1978.
- 79 Gary C. Hart, "Uncertainty Analysis, Loads, and Safety in Structural Engineering", Prentice-Hall Inc., Englewood Cliffs, New Jersey, 1982.

- 80 Edward B. Haugen, "Probabilistic Mechanical Design", Wiley , New York, 1980.
- 81 Gorski, E., "Narzedia do Wiercenia i Rostaczania glebokich Otworow", Warszawa, Panstwowe Wydawnictwa Techniczne, 1961.
- 82 Pflegar, F., "Verbesserung der Bohrungsqualitat beim Arbeiten mit Einlippen Tiefbohrwerkzeugen", Technischer Verlag Gunter Grossman GmbH, Stuttgart Vaihingen, 1976.
- 83 Streicher, P., "Tiefbohren der Metalle", Fachbuchreihe Vogel-Verlag, Werkzeugmaschine Internationale, 1975.
- 84 Sakuma, K., Taguchi, K., and Katsuki, A., "Study on Deep-Hole Boring by BTA System Solid Boring Tool: Behaviour of Tool and its Effects of Profile of Machined Hole", Bulletin of the Japanese Society of Production Engineers, Vol. 14, pp. 143-148, September 1980.
- 85 M.J. Maurizi, and D.V. Bambill De Rossit, "Free Vibration of a Clamped-Clamped Beam with an Intermediate Elastic Support", Journal of Sound and Vibration, Vol. 119, No. 1, pp. 173-176, 1987.
- 86 D.J. Gorman "Free Lateral Vibration Analysis of Double-Span Uniform Beams", International Journal of Mechanical Sciences, Vol. 16, pp. 345-351, 1974.
- 87 C. Kameswara Rao, "Frequency Analysis of Clamped-Clamped Uniform Beams with Intermediate Elastic Support", Journal of Sound and Vibration, Vol. 133, No. 3, pp. 502-509, 1989.
- 88 R.D. Blevins, "Formulas for Natural Frequency and Mode Shape", New york,

Van Nostrand Reinhold Co., 1979.

- 89 Astahov, V., "Effect of Selfstabilizing in BTA Tools", *Rezanie i Instrument* (in Russian), No. 38, pp. 42-54, 1989.

**APPENDIX - A**

**LISTING OF COMPUTER PROGRAMS, AND PRINTOUTS OF RESULTS**

```

C      OPTIMUM DESIGN OF BTA TOOL WITH STAGGERED CUTTERS BY
C      STOCHASTIC OPTIMIZATION
C      INTERIOR PENALTY METHOD USING HOOK AND JEAIVES ROUTINE
      IMPLICIT DOUBLE PRECISION(A-H,O-Z)
      PARAMETER(N=5, M=11)
      REAL XX(N),Q(N),XXX(N),F(N),X(N),G(M),EPS(N),YY(N)
      REAL FR(3),FT(3)
      OPEN (UNIT=10,FILE='BTA61.DAT',STATUS='NEW')
      OPEN (UNIT=11,FILE='BTA62.DAT',STATUS='NEW')
      RAD=(3.1415927/180.0)
      DEG=(180./3.1415927)
      EPSY=0.1E-4
      DO 1 I=1,N
      EPS(I)=0.10
1      CONTINUE
      R=1.
*****
*      INITIAL GUESS      *
*****
      YY(1)=35.125
      YY(2)=160.125
      YY(3)=290.
      YY(4)=7.1625
      YY(5)=51.
      XX(1)=YY(1)*RAD
      XX(2)=YY(2)*RAD
      XX(3)=YY(3)*RAD
      XX(4)=YY(4)
      XX(5)=YY(5)*RAD

      CALL OBJECT(FUN,OBJ,XX,N,G,M,R,RC,RS,FR,FT,FX,FY,PH,T7,T8,
+      DFX,DFY,DRC,DL,PF1,PF2)
      SS=0.0
      DO 2 I=1,M
      SUM=-1/G(I)
      SS=SS+SUM
2      CONTINUE
      R=ABS(OBJ)/SS
      COUNT=0
      C=0.1

      CALL OBJECT(FUN,OBJ,XX,N,G,M,R,RC,RS,FR,FT,FX,FY,PH,T7,T8,
+      DFX,DFY,DRC,DL,PF1,PF2)
      FI=OBJ
5      K=0
      CALL HOOK(XX,N,FO,G,M,R,XXX,OBJ,EPS,RC,RS,FR,FT,FX,FY,PH,
+      T7,T8,DFX,DFY,DRC,DL,PF1,PF2)
      DELTA=ABS(OBJ-FI)/ABS(OBJ)
      IF (DELTA.LT.EPSY) GOTO 16
      FI=OBJ
      DO 6 I=1,N
6      XX(I)=XXX(I)
      R=R*C
c      WRITE(10,*) 'PENALTY PARAMETER',R

```



```

C   WRITE(10,*)
    COUNT=COUNT+1
    PRINT*,COUNT
    IF (count.GT.15) THEN
C   PRINT*, 'COUNT VALUE EXCEEDED',COUNT
    GOTO 16
    ENDIF
    GOTO 5
16  WRITE(10,*)
    WRITE(10,*)
    WRITE(10,*) '* FINAL CONVERGENCE ANALYSIS'
    WRITE(10,*) 'OBJECTIVE FUNCTION VALUE: F(X) =',OBJ
    WRITE(10,*) 'MEAN VALUE OF THE OBJECTIVE FUNCT: = ',T7
    WRITE(10,*) 'STANDARD DEVIATION: OF THE OBJECTIVE FUNCT. =',T8
    WRITE(10,*)
    YY(1)=XX(1)*DEG
    YY(2)=XX(2)*DEG
    YY(3)=XX(3)*DEG
    YY(4)=XX(4)
    YY(5)=XX(5)*DEG
    WRITE(10,*) 'APPROXIMATION OF SOLUTION: X ='
    DO 17 I=1,N
17  WRITE(10,*) YY(I)
    WRITE(10,*)
    WRITE(10,*)
    WRITE(10,*)
    WRITE(10,*) '*****'
    WRITE(10,*)
    WRITE(10,*) 'RESULTANT CUTTING FORCE MAGNITUDE RC',RC
    WRITE(10,*) 'DEVIATION IN RC  DRC',DRC
    WRITE(10,*)
    WRITE(10,*) 'RESULTANT CUTTING FORCE POSITION ANGLE LDA',PH
    WRITE(10,*) 'DEVIATION IN LDA  DLDA',DL
    WRITE(10,*)
    WRITE(10,*) 'TOTAL RESULTANT SUPPORT REACTION RS',RS
    WRITE(10,*)
    WRITE(10,*) 'CUTTING FORCE MAGNITUDE IN X-DIRECTION FX',FX
    WRITE(10,*) 'DEVIATION IN FX  DFX ',DFX
    WRITE(10,*)
    WRITE(10,*) 'CUTTING FORCE MAGNITUDE IN Y-DIRECTION FY',FY
    WRITE(10,*) 'DEVIATION IN FY  DFY',DFY
    WRITE(10,*)
    WRITE(10,*) 'RADIAL CUTTING FORCES FR(I)', (FR(I),I=1,3)
    WRITE(10,*) 'TANGENTIAL CUTTING FORCES FT(I)', (FT(I),I=1,3)
    WRITE(10,*)
    WRITE(10,*) 'STATIC STABILITY COEFFICIENTS',PF1,PF2
    WRITE(10,*)
    WRITE(10,*) '*****'
    END

```

```

*****
*       HOOK AND JEAIVES ROUTINE       *
*****

```

```

SUBROUTINE HOOK (XX,N,FO,G,M,R,XXX,OBJ,EPS,RC,RS,FR,FT,FX,
+  FY, PH,T7,T8,DFX,DFY,DRC,DL,PF1,PF2)
IMPLICIT DOUBLE PRECISION(A-H,O-Z)
REAL EPS(N),XXX(N),F(5),XX(N),X(5),FO,G(M),YY(5),FR(3),FT(3)
DEG=(180./3.1415927)
ALPHA=1.0
BETA=0.5
MAXK=500
NKAT=50
EPSY=0.1e-4
DO 20 I=1,N
X(I)=XX(I)
F(I)=0.0
20  CONTINUE
KFLAG=0
KAT=0
KK1=0
FO=0
25  KCOUNT=0
FBEST=F(N)

CALL OBJECT(FUN,OBJ,XX,N,G,M,R,RC,RS,FR,FT,FX,FY,PH,T7,T8,
+  DFX,DFY,DRC,DL,PF1,PF2)
KK1=KK1+1
BO=FUN
      IF (KK1.EQ.1) THEN
      FO=FUN
      GO TO 30
      ENDIF
      IF (BO.GT.FO) THEN
      KFLAG=1
      ENDIF
      IF (BO.LT.FO) THEN
      FO=BO
      ENDIF
30  DO 100 I=1,N
      XXX(I)=XX(I)
      BASE=XX(I)
      XX(I)=XX(I)+EPS(I)

CALL OBJECT(FUN,OBJ,XX,N,G,M,R,RC,RS,FR,FT,FX,FY,PH,T7,T8,
+  DFX,DFY,DRC,DL,PF1,PF2)
KK1=KK1+1
F(I)=FUN
c  WRITE(10,*) '*****FIRST EXPLOR*****'
c  WRITE(10,*) 'FUNCTION IS',FUN,obj
c  WRITE(10,*) 'VARIABLES ARE',XX
      IF(F(I).LT.FO) GOTO 90
      XX(I)=XX(I)-2.0*EPS(I)
CALL OBJECT(FUN,OBJ,XX,N,G,M,R,RC,RS,FR,FT,FX,FY,PH,T7,T8,
+  DFX,DFY,DRC,DL,PF1,PF2)
KK1=KK1+1
F(I)=FUN
c  WRITE(10,*) '*****SECOND EXPLOR*****'

```

```

c    WRITE(10,*), 'FUNCTION IS',FUN,obj
c    WRITE(10,*), 'VARIABLES ARE',XX
    IF (F(I).LT FO) GOTO 90
    XX(I)=BASE
c    WRITE(10,*), '*****NO CHANGE IN BOTH THE MOVES*****'
    IF(I.EQ.1) GOTO 70
    F(I)=F(I-1)
    GOTO 80
70   F(I)=BO
80   KCOUNT=KCOUNT+1
    GOTO 100
90   FO=F(I)
    XXX(I) = XX(I)
100  CONTINUE
    IF (KK1.GT.MAXK) THEN
c    WRITE(10,*), 'FUNCTION EXCEEDED MAXK'
    GOTO 250
    ENDIF
    IF (KAT.GE.NKAT) THEN
c    WRITE(10,*), 'FUNCTION EXCEEDED NKAT'
    GOTO 250
    ENDIF
    IF (ABS(F(N)-FBEST).LE.EPSY) THEN
c    WRITE(10,*), 'FUNCTION LESS THAN EPSY'
    GOTO 250
    ENDIF
    IF (KCOUNT.GE.N) GOTO 140
c    WRITE(10,*), '*****PATTERN SEARCH *****'
c    WRITE(10,*), 'VALUES OF X BEFORE PATTERN SEARCH *****',XX
    DO 110 I=1,N
110  XX(I)=2.0*XX(I)-X(I)
c    WRITE(10,*), 'VALUES OF X AFTER PATTERN SEARCH *****',XX
    DO 120 I=1,N
120  X(I)=XXX(I)
    GOTO 25
*****
*    REDUCE STEP SIZE    *
*****
140  KAT=KAT+1
    IF (KFLAG.EQ.1) THEN
c    WRITE(10,*), 'YES KFLAG IS EQUAL TO 1'
    GOTO 160
    ELSE
C    WRITE(10,*), 'KFLAG IS NOT EQUAL TO 1'
    GOTO 190
    ENDIF
160  KFLAG=0
    DO 170 I=1,N
170  XX(I)=X(I)
190  DO 200 I=1,N
200  EPS(I)=EPS(I)*BETA
c    WRITE(10,*), 'STEP SIZE HAS BEEN REDUCED'
c    WRITE(10,*), EPS
    GOTO 25

```

```

250  WRITE(10,*),'FUNCTION VALUE F(X)=' ,OBJ
      WRITE(10,*),'MEAN VALUE:OF THE OBJECTIVE FUNCT. = ',T7
      WRITE(10,*),'STANDARD DEVIATION OF THE :OBJECTIVE FUNCT.= ',T8
      WRITE(10,*),'CONSTRAINTS: G(X) ='
      WRITE(10,251) (G(I),I=1,11)
251  FORMAT(1X,4(D16.10,2X),/,1X,4(D16.10,2X),/,1X,3(D16.10,2X))
C   + /,1X,(D16.10))
      YY(1)=XX(1)*DEG
      YY(2)=XX(2)*DEG
      YY(3)=XX(3)*DEG
      YY(4)=XX(4)
      YY(5)=XX(5)*DEG
      WRITE(10,*),'DESIGN VARIABLE: X'
      DO 260 I=1,N
260  WRITE(10,*) ,KK1,YY(I)
      WRITE(10,*)
      RETURN
      END

```

```

+   SUBROUTINE OBJECT (FUNC,OBJ,X,N,G,M,R,RC,RS,FR,FT,FX,
      FY,PH,T7,T8,DFX,DFY,DRC,DL,PF1,PF2)
      REAL X(N),G(M),RX(3),RY(3),FR(3),FT(3)
      REAL XL(3),XU(3),A1(10),A2(10),AA1(10),AA2(10),ST(10),K1,K2,K3
      REAL K4
      REAL C(3),CL(3),CU(3)
      RAD=(3.1415927/180.0)
      DEG=(180./3.1415927)
      NC=3.0
      CP=1.730
      CQ=1.130
      B2=8.0
      B3=25.4-8.0-X(4)
      Y1=0.8
      Y2=0.65
      S=0.17
      P1=12.0*RAD
      P2=12.0*RAD
      P3=-12.0*RAD
      RO=14.0*RAD
      AMU=TAN(RO)
      B=8.0
      R1=25.4
      SCP=(0.1*CP)/3.
      SCQ=(0.1*CQ)/3.
      SB=0.01*X(4)
      K1=1.
      K2=1.
      K3=1.
      K4=1.

```

```

*****
*   OBJECTIVE FUNCTION *
*****
      FR(1)=CQ*X(4)*(S**Y2)*SIN(P1)

```

```

FR(2)=CQ*B2*(S**Y2)*SIN(P2)
FR(3)=CQ*B3*(S**Y2)*SIN(P3)
FT(1)=CP*X(4)*(S**Y1)
FT(2)=CP*B2*(S**Y1)
FT(3)=CP*B3*(S**Y1)
FP=3.0
DO 2000 I=1,NC
RX(I)=FR(I)*COS(X(I))-FT(I)*SIN(X(I))
RY(I)=FR(I)*SIN(X(I))+FT(I)*COS(X(I))
2000 CONTINUE
FX=0.0
FY=0.0
DO 5000 I=1,NC
FX=FX+RX(I)
FY=FY+RY(I)
5000 CONTINUE
PH=ATAN2(FY,FX)*DEG
RC=SQRT(FX*FX+FY*FY)
RS=2.0*FP*COS(X(5))

Y11=(FX-RS)
Y12=(FY)

A1(1)=-K1*X(4)*(S**Y1)*SIN(X(1))
A1(2)=-K1*B2*(S**Y1)*SIN(X(2))
A1(3)=-K1*B3*(S**Y1)*SIN(X(3))
A1(4)=K1*X(4)*(S**Y2)*SIN(P1)*COS(X(1))
A1(5)=K1*B2*(S**Y2)*SIN(P2)*COS(X(2))
A1(6)=K1*B3*(S**Y2)*SIN(P3)*COS(X(3))
A1(7)=K1*CQ*(S**Y2)*SIN(P1)*COS(X(1))-K1*CP*(S**Y1)*SIN(X(1))

A2(1)= K2*X(4)*(S**Y1)*COS(X(1))
A2(2)=K2* B2*(S**Y1)*COS(X(2))
A2(3)= K2*B3*(S**Y1)*COS(X(3))
A2(4)=K2*X(4)*(S**Y2)*SIN(P1)*SIN(X(1))
A2(5)=K2*B2*(S**Y2)*SIN(P2)*SIN(X(2))
A2(6)=K2*B3*(S**Y2)*SIN(P3)*SIN(X(3))
A2(7)=K2*CQ*(S**Y2)*SIN(P1)*SIN(X(1))+K2*CP*(S**Y1)*COS(X(1))

      IF (Y11.GT.0) THEN
            AY11=Y11
      ELSE
            AY11=-Y11
      ENDIF

      IF (Y12.GT.0) THEN
            AY12=Y12
      ELSE
            AY12=-Y12
      ENDIF

DO 666 I=1,7
      IF (A1(I).LT.0) THEN
            AA1(I)=-A1(I)

```

```

ELSE
AA1(I)=A1(I)
ENDIF

IF (A2(I).LT.0) THEN
AA2(I)=-A2(I)
ELSE
AA2(I)=A2(I)
ENDIF
666 CONTINUE

DO 777 I =1,7
ST(I)=AA1(I)+AA2(I)
777 CONTINUE

T1=(ST(1)**2)*(SCP**2)
T2=(ST(2)**2)*(SCP**2)
T3=(ST(3)**2)*(SCP**2)
T4=(ST(4)**2)*(SCQ**2)
T5=(ST(5)**2)*(SCQ**2)
T6=(ST(6)**2)*(SCQ**2)
T6I=(ST(7)**2)*(SB**2)

T7=K3*(K1*(AY11)+K2*(AY12))
T8=K4*(T1+T2+T3+T4+T5+T6+T6I)**0.5

OBJ= T7+ T8

*****
*   CALCULATION OF VARIATIONS OF CUTTING *
*   FORECES BY LINEAR STATISTICAL APPROACH *
*****
*****
*   VARIATIONS IN CUTTING FORCES *
*   MAGNITUDE IN X AND Y DIRECTIONS *
*****

TX1=(A1(1)**2)*SCP**2
TX2=(A1(2)**2)*SCP**2
TX3=(A1(3)**2)*SCP**2
TX4=(A1(4)**2)*SCQ**2
TX5=(A1(5)**2)*SCQ**2
TX6=(A1(6)**2)*SCQ**2
TX7=(A1(7)**2)*SB**2
DFX=(TX1+TX2+TX3+TX4+TX5+TX6+TX7)**0.5

TY1=(A2(1)**2)*SCP**2
TY2=(A2(2)**2)*SCP**2
TY3=(A2(3)**2)*SCP**2
TY4=(A2(4)**2)*SCQ**2
TY5=(A2(5)**2)*SCQ**2
TY6=(A2(6)**2)*SCQ**2
TY7=(A2(7)**2)*SB**2
DFY=(TY1+TY2+TY3+TY4+TY5+TY6+TY7)**0.5

```

\*\*\*\*\*  
 \* VARIATIONS IN THE RESULTANT CUTING FORCE MAGNITUDE \*  
 \*\*\*\*\*

$$\begin{aligned} \text{DRC1} &= (1/\text{RC}) * (\text{FX} * \text{A1}(1) + \text{FY} * \text{A2}(1)) \\ \text{DRC2} &= (1/\text{RC}) * (\text{FX} * \text{A1}(2) + \text{FY} * \text{A2}(2)) \\ \text{DRC3} &= (1/\text{RC}) * (\text{FX} * \text{A1}(3) + \text{FY} * \text{A2}(3)) \\ \text{DRC4} &= (1/\text{RC}) * (\text{FX} * \text{A1}(4) + \text{FY} * \text{A2}(4)) \\ \text{DRC5} &= (1/\text{RC}) * (\text{FX} * \text{A1}(5) + \text{FY} * \text{A2}(5)) \\ \text{DRC6} &= (1/\text{RC}) * (\text{FX} * \text{A1}(6) + \text{FY} * \text{A2}(6)) \\ \text{DRC7} &= (1/\text{RC}) * (\text{FX} * \text{A1}(7) + \text{FY} * \text{A2}(7)) \end{aligned}$$

$$\begin{aligned} \text{TR1} &= (\text{DRC1} ** 2) * \text{SCP} ** 2 \\ \text{TR2} &= (\text{DRC2} ** 2) * \text{SCP} ** 2 \\ \text{TR3} &= (\text{DRC3} ** 2) * \text{SCP} ** 2 \\ \text{TR4} &= (\text{DRC4} ** 2) * \text{SCQ} ** 2 \\ \text{TR5} &= (\text{DRC5} ** 2) * \text{SCQ} ** 2 \\ \text{TR6} &= (\text{DRC6} ** 2) * \text{SCQ} ** 2 \\ \text{TR7} &= (\text{DRC7} ** 2) * \text{SB} ** 2 \end{aligned}$$

$$\text{DRC} = (\text{TR1} + \text{TR2} + \text{TR3} + \text{TR4} + \text{TR5} + \text{TR6} + \text{TR7}) ** 0.5$$

\*\*\*\*\*  
 \* VARIATIONS IN THE RESULTANT CUTING FORCE DIRECTION \*  
 \*\*\*\*\*

C

$$\begin{aligned} \text{DR1} &= 1. / (\text{FX} * \text{FX} + \text{FY} * \text{FY}) \\ \text{DR2} &= \text{FX} ** 2 \\ \text{DR3} &= \text{SCP} ** 2 \\ \text{DR4} &= \text{SCQ} ** 2 \\ \text{DR5} &= \text{SB} ** 2 \end{aligned}$$

$$\begin{aligned} \text{DL1} &= ((\text{DR1} * (\text{FX} * \text{A2}(1) - \text{FY} * \text{A1}(1))) ** 2) * \text{DR3} \\ \text{DL2} &= ((\text{DR1} * (\text{FX} * \text{A2}(2) - \text{FY} * \text{A1}(2))) ** 2) * \text{DR3} \\ \text{DL3} &= ((\text{DR1} * (\text{FX} * \text{A2}(3) - \text{FY} * \text{A1}(3))) ** 2) * \text{DR3} \\ \text{DL4} &= ((\text{DR1} * (\text{FX} * \text{A2}(4) - \text{FY} * \text{A1}(4))) ** 2) * \text{DR4} \\ \text{DL5} &= ((\text{DR1} * (\text{FX} * \text{A2}(5) - \text{FY} * \text{A1}(5))) ** 2) * \text{DR4} \\ \text{DL6} &= ((\text{DR1} * (\text{FX} * \text{A2}(6) - \text{FY} * \text{A1}(6))) ** 2) * \text{DR4} \\ \text{DL7} &= ((\text{DR1} * (\text{FX} * \text{A2}(7) - \text{FY} * \text{A1}(7))) ** 2) * \text{DR5} \end{aligned}$$

$$\text{DL} = ((\text{DL1} + \text{DL2} + \text{DL3} + \text{DL4} + \text{DL5} + \text{DL6} + \text{DL7}) ** 0.5) * \text{DEG}$$

\*\*\*\*\*  
 \* PFLEGHAR STATIC STABILITY ANALYSIS \*  
 \*\*\*\*\*

$$\begin{aligned} \text{FM}_s &= \text{FT}(1) * ((\text{X}(4)/2) + 8. + \text{B3}) + \text{FT}(2) * (4. + \text{B3}) + \text{FT}(3) * (\text{B3}/2) \\ \text{FM}_b &= \text{FM}_s + (1.45153) * (\text{R1}) \\ \text{T}_h1 &= \text{FM}_s + \text{RC} * (\text{R1}) * \text{SIN}(\text{X}(5) + \text{RO}) \\ \text{PF1} &= \text{T}_h1 / \text{FM}_b \\ \text{T}_h2 &= \text{FM}_b + \text{RC} * (\text{R1}) * \text{SIN}(\text{X}(5) - \text{RO}) \\ \text{PF2} &= \text{T}_h2 / \text{FM}_s \end{aligned}$$

```
*****
*   CONSTRAINTS FOR THE ANGULAR LOCAITON OF CUTTERS   *
*****
```

```
      CALL CHECK(X,XL,XU,N)
      DO 999 I =1,3
      C(I)=X(I)*DEG
      CL(I)=XL(I)*DEG
      CU(I)=XU(I)*DEG
      WRITE(11,*), 'THE CHECK ',CL(I),C(I),CU(I)
999   CONTINUE
```

```
      G(1)= (-X(1)+XL(1))/XU(1)
      G(2)= (X(1)-XU(1))/XU(1)
```

```
      G(3)= (-X(2)+XL(2))/XU(2)
      G(4)= (X(2)-XU(2))/XU(2)
```

```
      G(5)= (-X(3)+XL(3))/XU(3)
      G(6)= (X(3)-XU(3))/XU(3)
```

```
*****
*   CONSTRAINTS FOR WIDTH OF CUT OF THE OUTER CUTTER b1   *
*****
```

```
      G(7) = (-X(4)+5.8252427)/8.2474227
      G(8) = (X(4)-8.2474227)/8.2474227
```

```
*****
*   CONSTRAINTS FOR PADS INCLUDED ANGLE   *
*****
```

```
      G(9) =(-X(5)+45.0*RAD)/55.*RAD
      G(10) =(X(5)-55.0*RAD)/55.*RAD
```

```
*****
*   CONSTRAINTS FOR ' OCATION OF THE OUTER   *
*   CUTTER W.R.T. TO THE GUIDE PADS   *
*****
```

```
      IF ((ABS(X(5)-RO-X(1))).LT.(ABS(X(5)+RO+X(1)))) THEN
          G(11)= (-20.0*RAD+ABS(X(5)-RO-X(1)))/(20.*RAD)
      ELSE
          G(11) = (-20.*RAD+ABS(X(5)+RO+X(1)))/(20.*RAD)
      ENDIF
```

```
          CON=0
          DO 100 I=1,M
          CC=1/G(I)
          CON=CON+CC
100   CONTINUE
          FUNC=OBJ-R*CON
```

```
      RETURN
      END
```



\*\*\*\*\*  
 \* LOWER AND UPPER BOUNDS FOR LOCATION OF CUTTERS \*  
 \*\*\*\*\*

```

SUBROUTINE LIMITS(X,XL,XU,N)
REAL FI(3),X(5),XL(3),XU(3),BT(3),DBT(3),FIL(3),FIU(3)
REAL ZL(3),ZU(3),X1(3),BEETA(3)
NC=3
DEG=(180./3.1415927)
RAD=(3.1415927/180.0)
B2=8.0
B3=25.4-8.-X(4)
RO1=1.1*X(4)-47.8+SQRT((50.8**2)-55.88*X(4))
RC1=25.4-RO1
BT(1)=ASIN(RO1/RC1)
DBT(1)=0.25*BT(1)

DO2=2.*(25.4-X(4))
RO2=1.1*B2-DO2+SQRT((DO2**2)-DO2*8.8)
RC2=(DO2/2.)-RO2
BT(2)=ASIN(RO2/RC2)
DBT(2)=0.25*BT(2)

DO3=2.*(25.4-X(4)-8.)
RO3=1.1*B3-DO3+SQRT((DO3**2)-DO3*1.1*B3)
RC3=(DO3/2.)-RO3
BT(3)=ASIN(RO3/RC3)
DBT(3)=0.25*BT(3)

DO 356 I=1,3
BEETA(I)=BT(I)*DEG
WRITE(11,*),'BEETAS ARE',BEETA(I)
356 CONTINUE
DO 130 I=1,NC
130 FI(I)=X(I)
DO 135 I=1,NC
IM1=I-1
IP1=I+1
IF(IM1.LT.1)IM1=IM1+NC
IF(IP1.GT.NC)IP1=IP1-NC
FIL(I)=FI(IM1)+2.*BT(IM1)+DBT(I)
FIU(I)=FI(IP1)-2.*BT(IP1)-DBT(IP1)
IF (FIU(I).LT.0) FIU(I)=FIU(I)+360.0*RAD
IF (FIU(I)-FIL(I)) 8,18,18
8 IF(FI(I)-FIL(I)) 10,10,15
10 FIL(I)=FIL(I)-360.0*RAD
GOTO 18
15 FIU(I)=FIU(I)+360.0*RAD
18 XL(I)=FIL(I)
XU(I)=FIU(I)
135 CONTINUE
DO 150 I=1,NC
ZL(I)=XL(I)*DEG
ZU(I)=XU(I)*DEG

```

```
      X1(I)=X(I)*DEG
150  CONTINUE
      DO 3333 I=1,NC
3333 CONTINUE
      RETURN
      END

      SUBROUTINE CHECK(X,XL,XU,N)
      REAL FI(3),X(5),XL(3),XU(3),FIL(3),FIU(3)
      NC=3
      DEG=(180./3.1415927)
      RAD=(3.1415927/180.0)
      WRITE(11,*),'THIS IS CHECK'
      CALL LIMITS(X,XL,XU,N)
      DO 10 I=1,NC
      IF (X(I)-XL(I)) 11,10,10
11    X(I)=XL(I)+(XU(I)-XL(I))/10000.0
      CALL LIMITS(X,XL,XU,N)
10    CONTINUE
      DO 15 I=1,NC
      IF (X(I)-XU(I)) 15,15,16
16    X(I)=XU(I)-(XU(I)-XL(I))/10000.0
      CALL LIMITS(X,XL,XU,N)
15    CONTINUE
      RETURN
      END
```

\*\*\*\*\*  
 \* WEIGHTING FACTORS KW1=KW2=1 \*  
 \*\*\*\*\*

FUNCTION VALUE: F(X)= 0.2549576154833945  
 MEAN VALUE OF THE OBJECTIVE FUNCT.: = 9.5665454864501953E-04  
 STANDARD DEVIATION OF THE OBJECTIVE FUNCT.: = 0.2540009609347495  
 CONSTRAINTS: G(X) =  
 -.1273591965D+00 -.7256723642D+00 -.4861705005D+00 -.1383725256D+00  
 -.1077475920D+00 -.6644100696D-01 -.7892525196D-01 -.2147641331D+00  
 -.5538070764D-04 -.4276449417D-08 -.9581324458D+00  
 DESIGN VARIABLE: X  
 333 41.83657  
 333 196.1363  
 333 272.9120  
 333 6.476172  
 333 55.00062

FUNCTION VALUE: F(X)= 0.2541190808548482  
 MEAN VALUE OF THE OBJECTIVE FUNCT. = 1.1122226715087891E-04  
 STANDARD DEVIATION OF THE OBJECTIVE FUNCT. = 0.2540078585876973  
 CONSTRAINTS: G(X) =  
 -.1272984594D+00 -.7257306576D+00 -.4862288237D+00 -.1383471936D+00  
 -.1077310964D+00 -.6641399115D-01 -.7892525196D-01 -.2147641331D+00  
 -.5538490586D-04 -.7743122116D-10 -.9585195184D+00  
 DESIGN VARIABLE: X  
 150 41.82959  
 150 196.1433  
 150 272.9134  
 150 6.476172  
 150 55.00001

FUNCTION VALUE: F(X)= 0.2541201537384542  
 MEAN VALUE OF THE OBJECTIVE FUNCT. = 1.1229515075683594E-04  
 STANDARD DEVIATION OF THE OBJECTIVE FUNCT.: = 0.2540078585876973  
 THE RESULTANT CUTTING FORCE 3.441560268418823  
 CONSTRAINTS: G(X) =  
 -.1272984594D+00 -.7257306576D+00 -.4862288237D+00 -.1383471936D+00  
 -.1077310964D+00 -.6641399115D-01 -.7892525196D-01 -.2147641331D+00  
 -.5538498226D-04 -.1773234012D-11 -.9585202336D+00  
 DESIGN VARIABLE: X  
 22 41.82959  
 22 196.1433  
 22 272.9134  
 22 6.476172  
 22 55.00001

\* FINAL CONVERGENCE ANALYSIS

OBJECTIVE FUNCTION VALUE: F(X) = 0.2541201537384542  
 MEAN VALUE OF THE OBJECTIVE FUNCT. = 1.1229515075683594E-04  
 STANDARD DEVIATION OF THE OBJECTIVE FUNCT.: = 0.2540078585876973

APPROXIMATION OF SOLUTION. X =  
 41.82959  
 196.1433  
 272.9134

6.476172  
55.00001

\*\*\*\*\*

RESULTANT CUTTING FORCE MAGNITUDE RC 3.441560268418823  
DEVIATION IN RC DRC 0.1690059784156910

RESULTANT CUTTING FORCE POSITION ANGLE LDA 1.7861578575021633E-04  
DEVIATION IN LDA DLDA 2.206066433577045

TOTAL RESULTANT PADS SUPPORT REACTION RS 3.441458702087402

CUTTING FORCE MAGINTUDE IN X-DIRECTION FX 3.441560268402100  
DEVIATION IN FX DFX 0.1690060954318920

CUTTING FORCE MAGNITUDE IN Y-DIRECTION FY 1.0728836059570313E-05  
DEVIATION IN FY DFY 0.1325106734467692

RADIAL CUTTING FORCES FR(I) 0.4809141 0.5940720 -0.8111926  
TANGENTIAL CUTTING FORCES FT(I) 2.714711 3.353476 4.579099

STATIC STABILITY COEFFICIENTS 1 259984978103286 1 696777834757663

\*\*\*\*\*

\*\*\*\*\*  
 \*       WEIGHTING FACTORS KW1=1; KW2=0       \*  
 \*\*\*\*\*

FUNCTION VALUE F(X)= 5.8615207672119141E-04  
 MEAN VALUE OF THE OBJECTIVE FUNCT . = 5.8615207672119141E-04  
 STANDARD DEVIATION OF THE OBJECTIVE FUNCT.: = 0.0  
 CONSTRAINTS: G(X) =  
 - 1273224950D+00 - .7257090211D+00 - .4861950874D+00 - .1383725256D+00  
 - 1077496558D+00 - .6642311811D-01 - .7892525196D-01 - .2147641331D+00  
 - 5538068945D-04 - .4295364064D-08 - .9584121704D+00  
 DESIGN VARIABLE: X  
   344 41 83098  
   344 196.1363  
   344 272.9120  
   344 6 476172  
   344 55.00062

FUNCTION VALUE F(X)= 5.2642822265625000E-04  
 MEAN VALUE OF THE OBJECTIVE FUNCT.: = 5.2642822265625000E-04  
 STANDARD DEVIATION OF THE OBJECTIVE FUNCT.: = 0.0  
 CONSTRAINTS: G(X) =  
 - .1273224950D+00 - .7257090211D+00 - .4861950874D+00 - .1383725256D+00  
 - .1077496558D+00 - .6642311811D-01 - .7892525196D-01 - .2147641331D+00  
 - .5538454934D-04 - .4368066464D-09 - .9584469795D+00  
 DESIGN VARIABLE: X  
   22 41.83098  
   22 196.1363  
   22 272.9120  
   22 6 476172  
   22 55 00062

FUNCTION VALUE: F(X)= 6.7234039306640625E-05  
 MEAN VALUE OF THE OBJECTIVE FUNCT.: = 6.7234039306640625E-05  
 STANDARD DEVIATION OF THE OBJECTIVE FUNCT.: = 0.0  
 CONSTRAINTS: G(X) =  
 - .1272924542D+00 - .7257329226D+00 - .4862175286D+00 - .1383660138D+00  
 - 1077461988D+00 - .6640935689D-01 - .7891941071D-01 - .2147699744D+00  
 - .5538488767D-04 - .9634571613D-10 - .9585902095D+00  
 DESIGN VARIABLE: X  
   127 41.82817  
   127 196 1391  
   127 272.9135  
   127 6.476124  
   127 55 00000

FUNCTION VALUE F(X)= 6 6161155700683594E-05  
 MEAN VALUE OF THE OBJECTIVE FUNCT . = 6.6161155700683594E-05  
 STANDARD DEVIATION OF THE OBJECTIVE FUNCT.: = 0.0  
 CONSTRAINTS G(X) =  
 - 1272924542D+00 - .7257329226D+00 - .4862175286D+00 - .1383660138D+00  
 - 1077461988D+00 - .6640935689D-01 - .7891941071D-01 - .2147699744D+00  
 - 5538496407D-04 - 2068773104D-10 - .9585909247D+00  
 DESIGN VARIABLE X  
   22 41 82817

22 196.1391  
 22 272.9135  
 22 6.476124  
 22 55.00000

FUNCTION VALUE:  $F(X) = 6.5803527832031250E-05$   
 MEAN VALUE OF THE OBJECTIVE FUNCT.: =  $6.5803527832031250E-05$   
 STANDARD DEVIATION OF THE OBJECTIVE FUNCT.: = 0.0  
 CONSTRAINTS:  $G(X) =$   
 $-.1272924542D+00 \quad -.7257329226D+00 \quad -.4862175286D+00 \quad -.1383660138D+00$   
 $-.1077461988D+00 \quad -.6640935689D-01 \quad -.7891941071D-01 \quad -.2147699744D+00$   
 $-.5538498226D-04 \quad -.1773234012D-11 \quad -.9585911036D+00$

DESIGN VARIABLE: X

55 41.82817  
 55 196.1391  
 55 272.9135  
 55 6.476124  
 55 55.00000

FUNCTION VALUE:  $F(X) = 6.5445899963378906E-05$   
 MEAN VALUE OF THE OBJECTIVE FUNCT.: =  $6.5445899963378906E-05$   
 STANDARD DEVIATION OF THE OBJECTIVE FUNCT.: = 0.0  
 CONSTRAINTS:  $G(X) =$   
 $-.1272924542D+00 \quad -.7257329226D+00 \quad -.4862175286D+00 \quad -.1383660138D+00$   
 $-.1077461988D+00 \quad -.6640935689D-01 \quad -.7891941071D-01 \quad -.2147699744D+00$   
 $-.5538500045D-04 \quad 0.1714126237D-10 \quad -.9585912824D+00$

DESIGN VARIABLE: X

22 41.82817  
 22 196.1391  
 22 272.9135  
 22 6.476124  
 22 55.00000

FUNCTION VALUE:  $F(X) = 6.5445899963378906E-05$   
 MEAN VALUE OF THE OBJECTIVE FUNCT.: =  $6.5445899963378906E-05$   
 STANDARD DEVIATION OF THE OBJECTIVE FUNCT.: = 0.0  
 CONSTRAINTS:  $G(X) =$   
 $-.1272924542D+00 \quad -.7257329226D+00 \quad -.4862175286D+00 \quad -.1383660138D+00$   
 $-.1077461988D+00 \quad -.6640935689D-01 \quad -.7891941071D-01 \quad -.2147699744D+00$   
 $-.5538500045D-04 \quad 0.1714126237D-10 \quad -.9585912824D+00$

DESIGN VARIABLE: X

22 41.82817  
 22 196.1391  
 22 272.9135  
 22 6.476124  
 22 55.00000

**\* FINAL CONVERGENCE ANALYSIS**

OBJECTIVE FUNCTION VALUE:  $F(X) = 6.5445899963378906E-05$   
 STANDARD DEVIATION OF THE OBJECTIVE FUNCT.: = 0.0  
 MEAN VALUE OF THE OBJECTIVE FUNCT.: =  $6.5445899963378906E-05$   
 APPROXIMATION OF SOLUTION: X =  
 41.82817

196 1391  
272 9135  
6.476124  
55.00000

\*\*\*\*\*

RESULTANT CUTTING FORCE MAGNITUDE RC 3.441402554525570  
DEVIATION IN RC DRC 0.1690044170491020

RESULTANT CUTTING FORCE POSITION ANGLE LDA 1.607615742795361E-04  
DEVIATION IN LDA DLDA 2.206205792675851

TOTAL RESULTANT PADS SUPPORT REACTION RS 3.441458344459534

CUTTING FORCE MAGNITUDE IN X-DIRECTION FX 3.441402554512024  
DEVIATION IN FX DFX 0.1690045209562564

CUTTING FORCE MAGNITUDE IN Y-DIRECTION FY 9.6559524536132813E-06  
DEVIATION IN FY DFY 0.1325129879264676

RADIAL CUTTING FORCES FR(I) 0.4809106 0.5940720 -0.8111962  
TANGENTIAL CUTTING FORCES FT(I) 2.714691 3.353476 4.579120

STATIC STABILITY COEFFICIENTS 1.259963245790955 1.696758390166174

\*\*\*\*\*

```

/      THIS PROGRAM IS FOR MONTE CARLO SIMULATION TO
CALCULATE THE CUTTING FORCES AND PADS' REACTIONS VARIATIONS /

#include <stdio.h>
#include <math.h>
double
# define MAX 30000
# define POINTS    40
# define opt    3
# define rad  3.1415927/180.0
# define deg 180.0/3.1415927
sqr (val)
double val;
{
    return val * val;
}
main ()
{
/***** Declaration of Integers and Reals *****/
int i,k,j;
FILE *fp1,*fp2,*fp3,*fp4,*fp5,*fp6,*fp7,*fp8,*fopen();
float b[opt],kappa[opt],fr[opt][MAX],ft[opt][MAX],f_rl[opt],f_tl[opt],Fp[MAX],
s[opt],phi[opt],mu[MAX],
defr[opt], deft[opt],defrc[opt],rx[MAX],distribu[MAX]
,ry[MAX],rc[MAX],rca[MAX];
float
distribu[MAX],norm1[opt][MAX],norm2[opt][MAX],normalx[MAX],normaly[MAX],
normalrc[MAX],normalrca[MAX],normalfp[MAX],zfx[POINTS],zfy[POINTS],zfp[POI
NTS],
zfrc[POINTS],zfrca[POINTS],cfzx[POINTS],cfzy[POINTS],cfzrc[POINTS],cfzp[POIN
TS],
cfzrca[POINTS],mean2x[POINTS]
,mean2y[POINTS],mean2rc[POINTS],mean2rca[POINTS],mean2fp[POINTS],
float y1,y2,cp,cq,meanmu,meanfp,meanx,meany,meanrc,meanrca,varx=0 0,vary=0 0,
varrc=0.0,varrca=0.0,MX=0,MY=0.0,MRC=0.0,MRCA=0.0,MFP=0.0,
stdmu,varfp,devx,devy,devrc,devrca,devfp,tempx,tempy,temprc,temprca,tempfp,
sigma=-4.0,delta,step,Mx,My,Mrc,Mrca,Mfp,mex,mez;
/***** ` *****/
fp1= fopen("/tmp/ram1.dat","r");
fp2= fopen("/tmp/ram2.dat","r");
fp3= fopen("/tmp/ram3.dat","r");
fp4= fopen("/tmp/ram4.dat","r");
fp5= fopen("/tmp/ram5.dat","r");
fp6= fopen("/tmp/ram6.dat","r");
fp7= fopen("/tmp/ram7.dat","r");

```



```
fp8= fopen("pforcen.dat","w");
```

147

```
for (i=0,i<MAX;i++)
{
fscanf(fp1,"%f",&(norm1[0][i]));
fscanf(fp2,"%f",&(norm1[1][i]));
fscanf(fp3,"%f",&(norm1[2][i]));
fscanf(fp4,"%f",&(norm2[0][i]));
fscanf(fp5,"%f",&(norm2[1][i]));
fscanf(fp6,"%f",&(norm2[2][i]));
fscanf(fp7,"%f",&(distrbu[i]));
}
/*****Data for Simulation *****/
cp=1.730;
cq=1.130;
b[0]=6.476124;
b[1]=8.0;
b[2]= 10.923828;
s[0]=s[1]=s[2]=0.17;
kappa[0]=kappa[1]=12.0*rad;
kappa[2]=-12.0*rad;
phi[0]=41.82959*rad;
phi[1]=196.1433*rad;
phi[2]=272.9134*rad;
y1=0.8;
y2=0.65;
meanmu=0.2;
stdmu=0.0175;
delta=55.*rad;
    for (i=0;i<opt;i++)
    {
        f_r1[i]=cq*b[i]* pow(s[i],(double)y2) *sin(kappa[i]);
        f_t1[i]=cp*b[i]*pow(s[i],(double)y1);
        defr[i]=0.1*f_r1[i];
        deft[i]=0.1*f_t1[i];
    }

for (i=0,i<opt;i++)
    for (j=0;j<MAX;j++)
    {
        fr[i][j]=f_r1[i]+(defr[i]/3.0)*norm1[i][j];
        ft[i][j]=f_t1[i]+(deft[i]/3.0)*norm2[i][j];
    }

for (i=0,i<MAX;i++)
```

```

{
    rx[i]=0.0;
    ry[i]=0.0;
    for (j=0;j<opt;j++)
    {
        rx[i]=rx[i]+fr[j][i]*cos(phi[j])-ft[j][i]*sin(phi[j]);
        ry[i]=ry[i]+fr[j][i]*sin(phi[j])+ft[j][i]*cos(phi[j]);
/*      printf("%f %f\n",rx[i],ry[i]);  */
    }
}

for (i=0;i<MAX;i++)
{
    rc[i]=sqrt(pow(rx[i],(double)2)+pow(ry[i],(double)2));
    rca[i]=atan(ry[i]/rx[i])*deg;
}
/*****Friction Coefficient's Distribution*****/
mex=0;
for (i=0;i<MAX;i++)
{
    mu[i]=meanmu+stdmu*distribu[i];
    mex=mex+mu[i];
}

mez=mex/MAX;
printf("the mean value of the friction is %f\n",mez);

/*****Analysis of Resultant Pad Force *****/

for (i=0;i<MAX;i++)
{
    Fp[i]=(rc[i]*sqrt(1.+sqr(meanmu)))/(2.*cos(delta)*sqrt(1+sqr(mu[i]))),
}

        for (j=0;j<MAX;j++)
        {
            MX=MX+rx[j];
            MY=MY+ry[j];
            MRC=MRC+rc[j];
            MRCA=MRCA+rca[j];
            MFP=MFP+Fp[j];
        }

meanx=MX/MAX;
meany=MY/MAX;
meanrc=MRC/MAX;
meanrca=MRCA/MAX;

```

```
meanfp=MFP/MAX;
```

149

```
    for (j=0;j<MAX;j++)
    {
        varx=varx+sqr(rx[j]-meanx);
        vary=vary+sqr(ry[j]-meany);
        varrc=varrc+sqr(rc[j]-meanrc);
        varrca=varrca+sqr(rca[j]-meanrca);
        varfp=varfp+sqr(Fp[j]-meanfp);
    }
devx=sqrt(varx/(MAX-1.0));
devy=sqrt(vary/(MAX-1.0));
devrc=sqrt(varrc/(MAX-1.0));
devrca=sqrt(varrca/(MAX-1.0));
devfp=sqrt(varfp/(MAX-1.0));

fprintf(fp7,"SIMULATION RESULTS FOR 30000 REPLICAITONS \n");
fprintf(fp7, "\n");
fprintf(fp7, "\n");
fprintf(fp7, "\n");

fprintf(fp7,"Mean value of the cutting force resultant magnitude RC %f\n", meanrc);
fprintf(fp7,"Standard deviation of the cutting force resultant magnitude DRC %f\n",
devrc);
fprintf(fp7, "\n");
fprintf(fp7,"Mean value of the cutting force resultant position angle LDA %f\n",
meanrca);
fprintf(fp7,"Standard deviation of the cutting force resultant position angle DLDA %f\n",
devrca);
fprintf(fp7, "\n");
fprintf(fp7,"Mean value of the cutting force magnitude in X-direction FX %f\n", meanx);
fprintf(fp7,"Standard deviation of the cutting force magnitude in X-direction DFX %f\n",
devx);
fprintf(fp7, "\n");
fprintf(fp7,"Mean value of the cutting force magnitude in Y-direction FY %f\n", meany);
fprintf(fp7,"Standard deviation of the cutting force magnitude in Y-direction DFY %f\n",
devy);
fprintf(fp7, "\n");
fprintf(fp7,"Mean value of the resultant pads force magnitude FP %f\n", meanfp);
fprintf(fp7,"Standard deviation resultant pads force magnitude DFP %f\n",devfp);
fprintf(fp7, "\n");
/***** Normal Variate *****/
    for (j=0;j<MAX;j++)
    {
        normalx[j]=(rx[j]-meanx)/devx;
```

```

normaly[j]=(ry[j]-meany)/devy;
normalrc[j]= (rc[j]-meanrc)/devrc;
normalrca[j]=(rca[j]-meanrca)/devrca;
normalfp[j]=(Fp[j]-meanfp)/devfp;
}

```

```

for (j=0;j<MAX-1;j++)
  for (k=j+1;k<MAX;k++)
    if (normalx[k] < normalx[j])
      {
        tempx=normalx[j];
        normalx[j]=normalx[k];
        normalx[k]=tempx;
      }

for (j=0;j<MAX-1;j++)
  for (k=j+1;k<MAX;k++)
    if (normaly[k] < normaly[j])
      {
        tempy=normaly[j];
        normaly[j]=normaly[k];
        normaly[k]=tempy;
      }

for (j=0;j<MAX-1;j++)
  for (k=j+1;k<MAX;k++)
    if (normalrc[k] < normalrc[j])
      {
        temprc=normalrc[j];
        normalrc[j]=normalrc[k];
        normalrc[k]=temprc;
      }

for (j=0;j<MAX-1;j++)
  for (k=j+1;k<MAX;k++)
    if (normalrca[k] < normalrca[j])
      {
        temprca=normalrca[j];
        normalrca[j]=normalrca[k];
        normalrca[k]=temprca;
      }

for (j =0;j<MAX-1;j++)
  for(k=j+1;k<MAX;k++)

```

```

        if (normalfp[k] < normalfp[j])
            {
                tempfp=normalfp[j];
                normalfp[j]=normalfp[k];
                normalfp[k]=tempfp;
            }

/***** Frequency Distribution *****/
step=8 0/POINTS;
for (i=0;i<POINTS;i++)
    {
        Mx=0.0;
        My=0.0;
        Mrc=0.0;
        Mrca=0.0;
        Mfp=0.0;
        sigma=sigma+step;
        for (j=0;j<MAX;j++)
            {
                if (normalx[j] < sigma)
                    Mx++;
                if (normaly[j] < sigma)
                    My++;
                if (normalrc[j] < sigma)
                    Mrc++;
                if (normalrca[j] < sigma)
                    Mrca++;
                if (normalfp[j] < sigma)
                    Mfp++;
            }
        cfzx[i]=Mx/(MAX*step);
        zfx[i]=sigma-step/2.0;
        zfx[i]=zfx[i]*devx+meanx;

        cfzy[i]=My/(MAX*step);
        zfy[i]=sigma-step/2.0;
        zfy[i]=zfy[i]*devy+meany;

        cfzrc[i]=Mrc/(MAX*step);
        zfrc[i]=sigma-step/2.0;
        zfrc[i]=zfrc[i]*devrc+meanrc;

        cfzrca[i]=Mrca/(MAX*step);
        zfrca[i]=sigma-step/2.0;
        zfrca[i]=zfrca[i]*devrca+meanrca,

```

```

        cfzp[i]=Mfp/(MAX*step);
        zfp[i]=sigma-step/2.0;
        zfp[i]=zfp[i]*devfp+meanfp;
    }
    mean2x[0]=cfzx[0];
    mean2y[0]=cfzy[0];
    mean2rc[0]=cfzrc[0];
    mean2rca[0]=cfzrca[0];
    mean2fp[0]=cfzp[0];

    for (i=1;i<POINTS;i++)
    {
        mean2x[i]=cfzx[i]-cfzx[i-1];
        mean2y[i]=cfzy[i]-cfzy[i-1];
        mean2rc[i]=cfzrc[i] -cfzrc[i-1];
        mean2rca[i]=cfzrca[i] -cfzrca[i-1];
        mean2fp[i]=cfzp[i]-cfzp[i-1];
    }

```

/\*\*\*\*\*\*Final Results for PDF'S\*\*\*\*\*\*/

```

    for (i=0;i<POINTS,i++)
    {
        fprintf(fp7,"%f%f%f%f%f%f%f%f%f\n",zfx[i],mean2x[i],zfy[i],
        mean2y[i],zfrc[i],mean2rc[i],zfrca[i],mean2rca[i],zfp[i],mean2fp[i]);
    }
}

```

Mean value of the cutting force resultant magnitude RC	3.444192
Standard deviation of the cutting force resultant magnitude DRC	0.168005
Mean value of the cutting force resultant position angle LDA	0.014294
Standard deviation of the cutting force resultant position angle DLDA	2.169659
Mean value of the cutting force magnitude in X-direction FX	3.441731
Standard deviation of the cutting force magnitude in X-direction DFX	0.168116
Mean value of the cutting force magnitude in Y-direction FY	-0.000923
Standard deviation of the cutting force magnitude in Ydirection DFY	0.129958
Mean value of the pad force resultant magnitude FP	3.002007
Standard deviation of the pad force magnitude DFP	0.146641

**APPENDIX - B**

**PDF OF RESULTANT CUTTING FORCE MAGNITUDE FOR DIFFERENT  
REPLICATIONS**



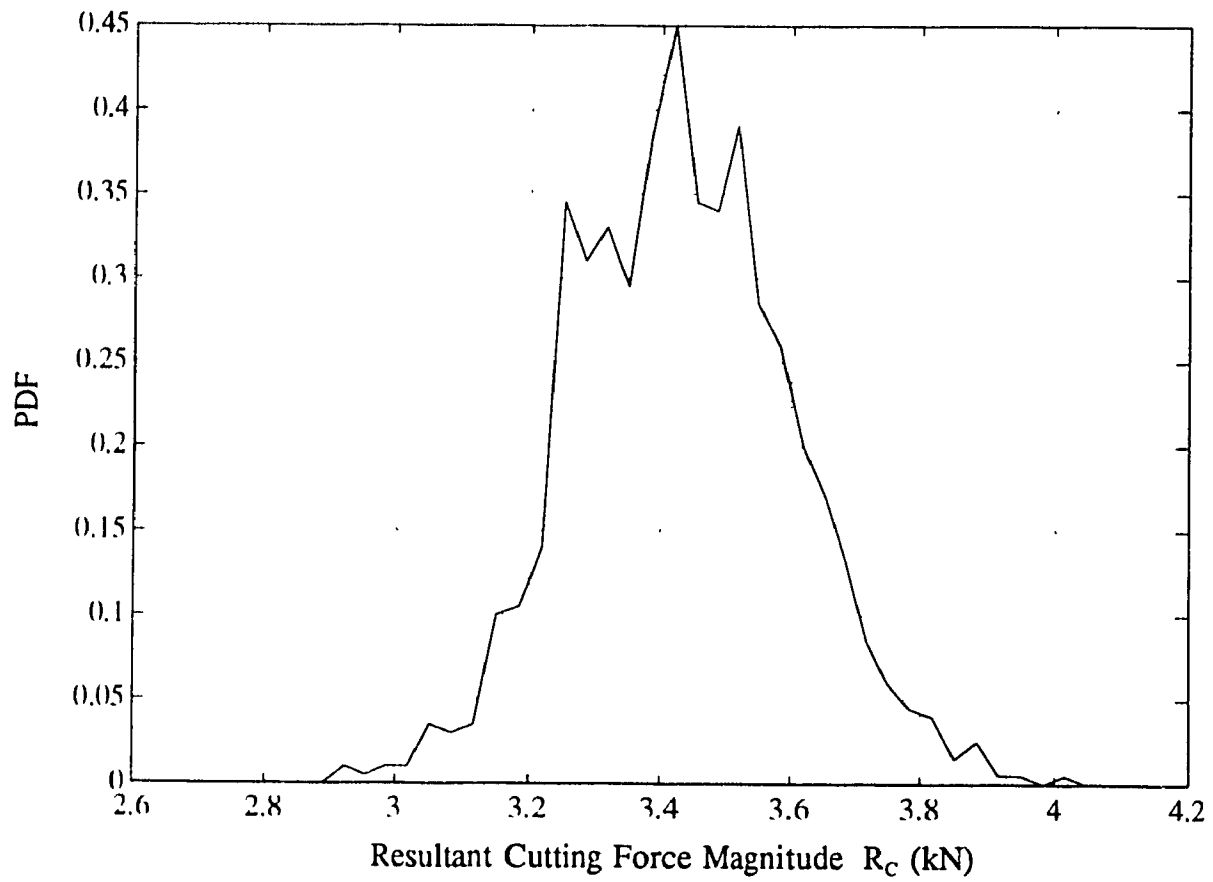


Fig. B1 PDF of Resultant Cutting Force Magnitude for 1000 Replications

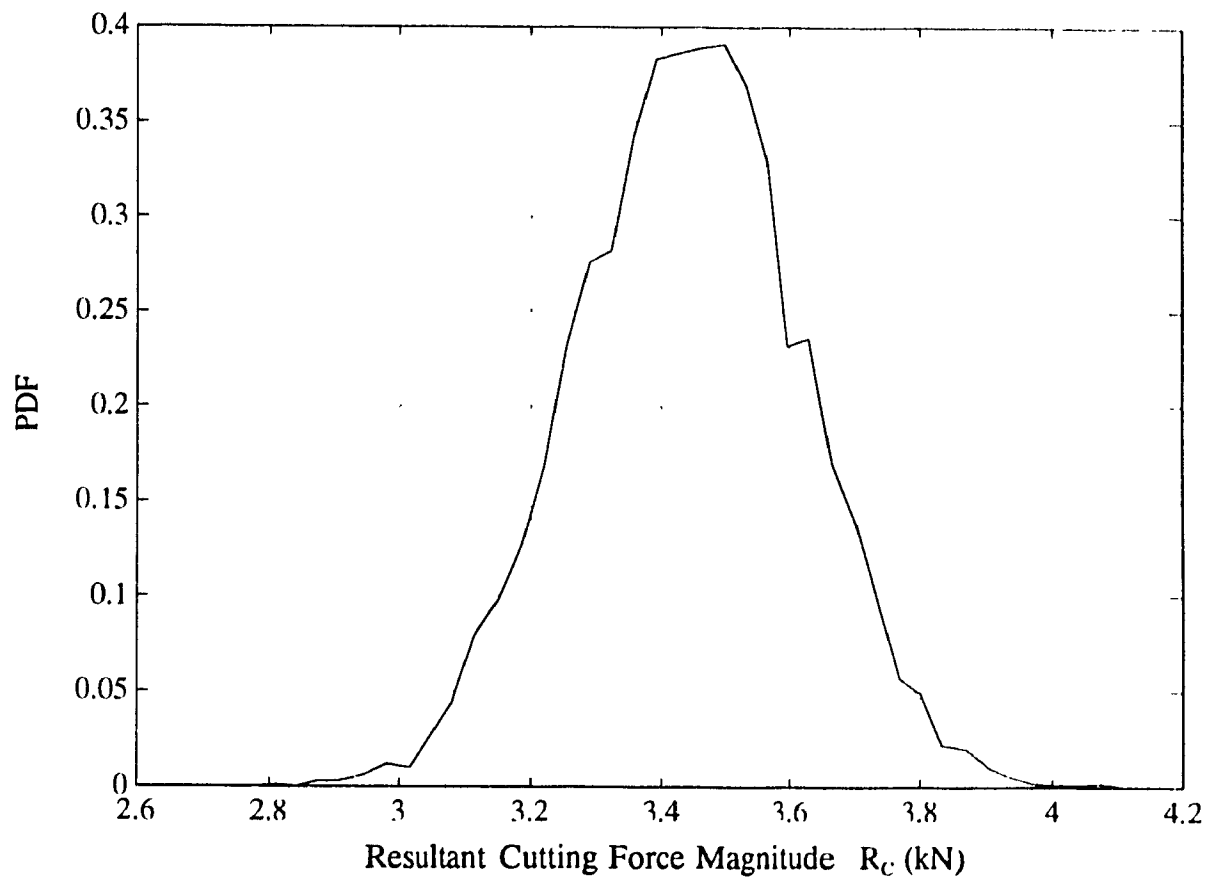


Fig. B2 PDF of Resultant Cutting Force Magnitude for 5000 Replications

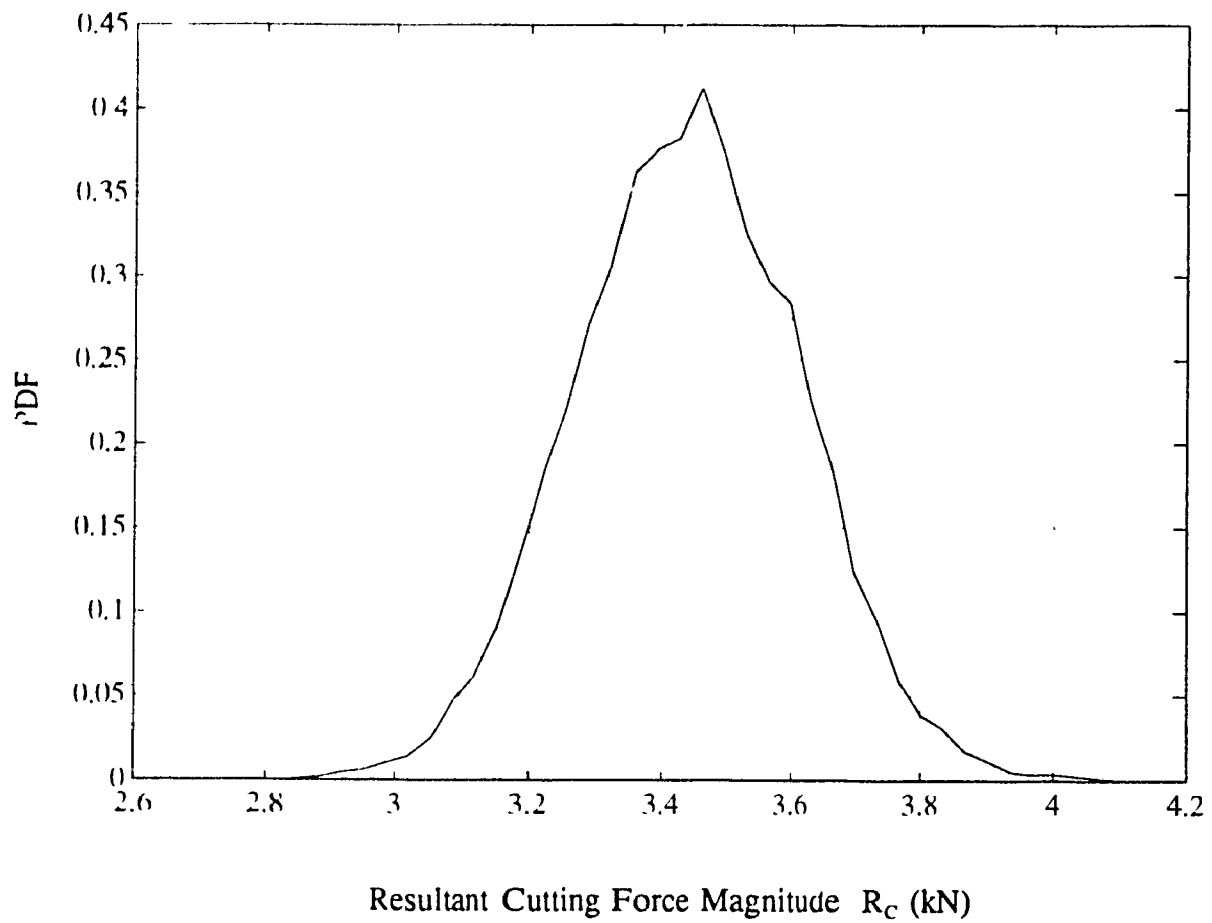


Fig. B3 PDF of Resultant Cutting Force Magnitude for 10000 Replications

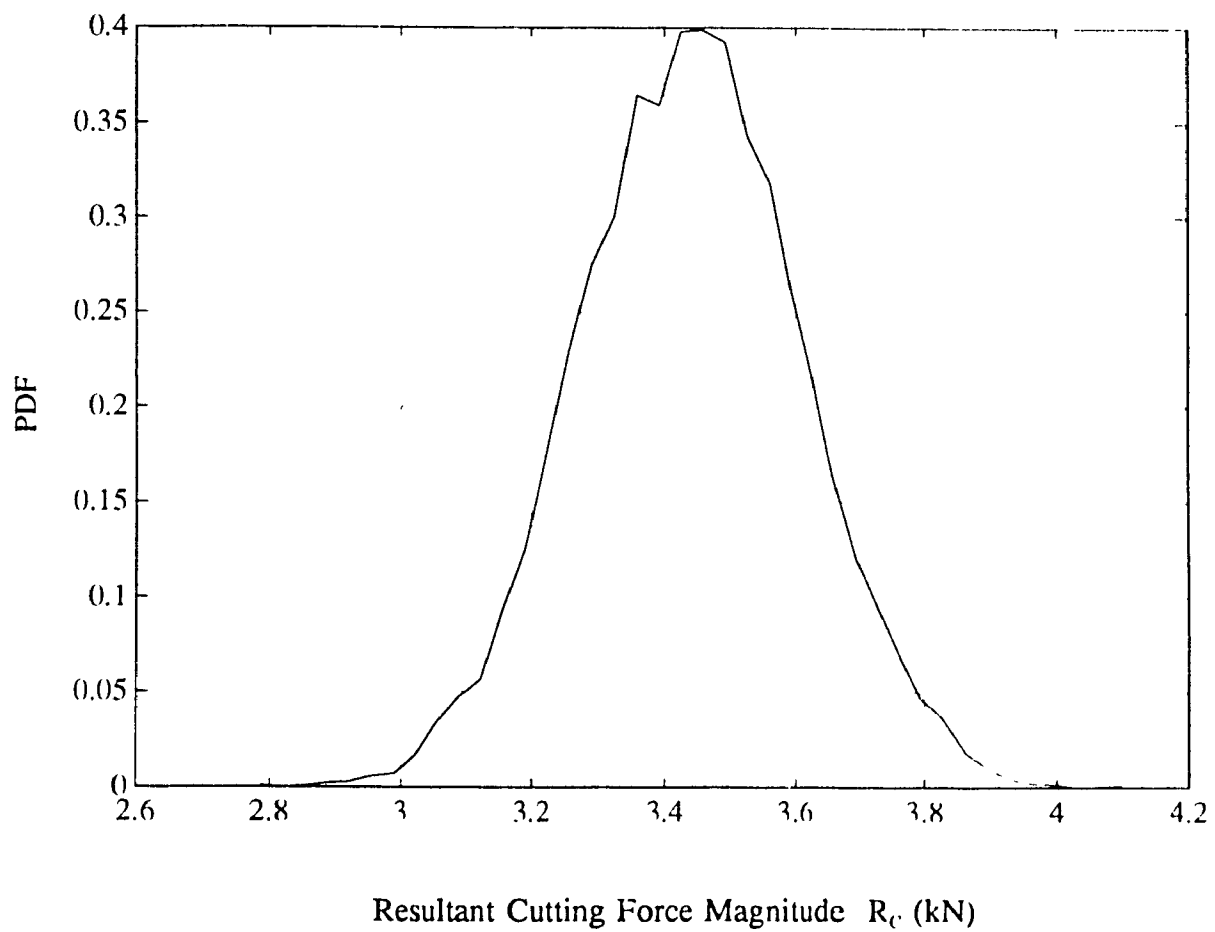


Fig. B4 PDF of Resultant Cutting Force Magnitude for 15000 Replications

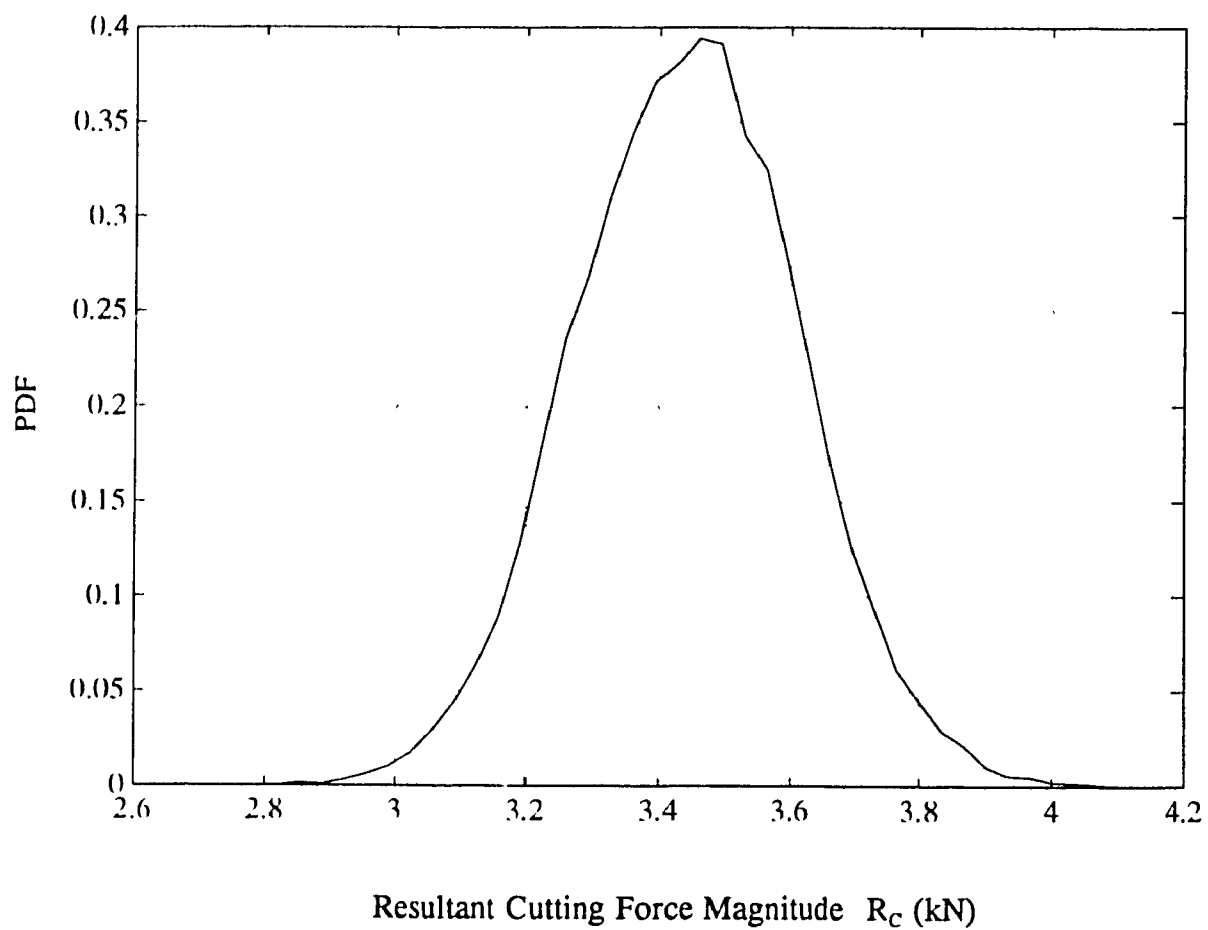


Fig. B5 PDF of Resultant Cutting Force Magnitude for 20000 Replications

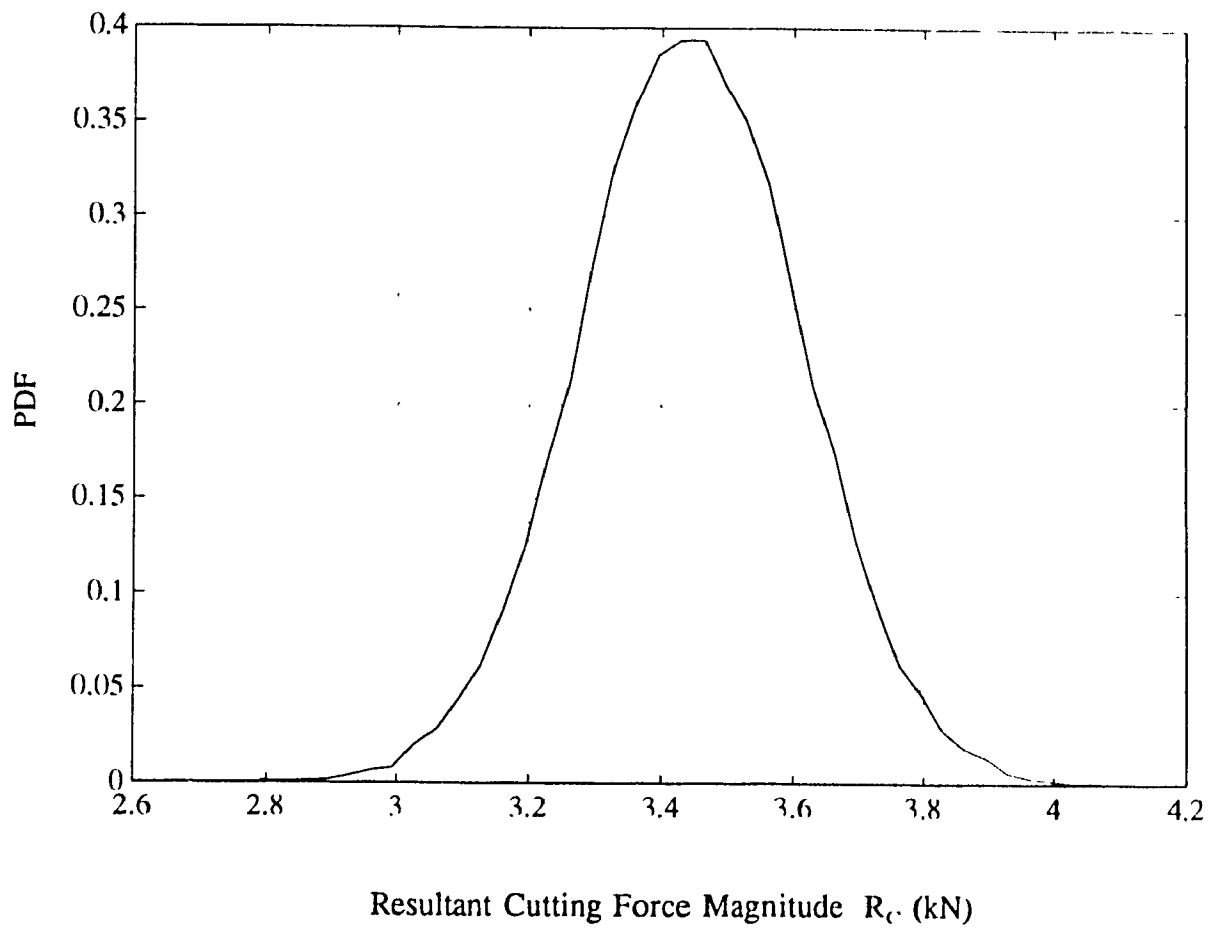


Fig. B6 PDF of Resultant Cutting Force Magnitude for 25000 Replications